

Light Water Reactor Sustainability Program

Loss of Coolant Accident / Emergency Core Coolant System Evaluation of Risk-Informed Margins Management Strategies for a Representative Pressurized Water Reactor

Ronaldo Szilard
Hongbin Zhang
Aaron Epiney
Carlo Parisi
Paul Talbot



September 2016

U.S. Department of Energy Office of Nuclear Energy

DISCLAIMER

This information was prepared as an account of work sponsored by an agency of the U.S. Government. Neither the U.S. Government nor any agency thereof, nor any of their employees, makes any warranty, expressed or implied, or assumes any legal liability or responsibility for the accuracy, completeness, or usefulness, of any information, apparatus, product, or process disclosed, or represents that its use would not infringe privately owned rights. References herein to any specific commercial product, process, or service by trade name, trade mark, manufacturer, or otherwise, does not necessarily constitute or imply its endorsement, recommendation, or favoring by the U.S. Government or any agency thereof. The views and opinions of authors expressed herein do not necessarily state or reflect those of the U.S. Government or any agency thereof.

Light Water Reactor Sustainability Program

Loss of Coolant Accident / Emergency Core Coolant System Evaluation of Risk-Informed Margins Management Strategies for a Representative Pressurized Water Reactor

Ronaldo Szilard
Hongin Zhang
Aaron Epiney
Carlo Parisi
Paul Talbot

September 2016

**Idaho National Laboratory
Idaho Falls, Idaho 83415**

<http://www.inl.gov>

**Prepared for the
U.S. Department of Energy
Office of Nuclear Energy
Under DOE Idaho Operations Office
Contract DE-AC07-05ID14517**

EXECUTIVE SUMMARY

A Risk Informed Safety Margin Characterization (RISMC) toolkit and methodology are proposed for investigating nuclear power plant core, fuels design and safety analysis, including postulated Loss-of-Coolant Accident (LOCA) analysis. This toolkit, under an integrated evaluation model framework, is named LOCA Toolkit for the U.S. (LOTUS).

A LOTUS demonstration for a generic plant, similar to an operating four-loop pressurized water reactor, for large break LOCA events is performed to assess safety margins for the proposed NRC 50.46c rule, Emergency Core Cooling System (ECCS) performance during LOCA.

This demonstration includes coupled analysis of core design, fuel design, thermal-hydraulics and systems analysis, using advanced risk analysis tools and methods to investigate a wide range of results.

Different core loading strategies, fuel design options, and range of operating conditions are analyzed. The set of modeled results indicate that peak clad temperature and fuel cladding oxidation responses are well characterized by performance based modeling under large break LOCA conditions. Furthermore, these demonstration calculations indicate the importance of safety margin management and planning for future operating cycles. Since nuclear fuel stays in a reactor for multiple operating cycles, planning of loading and operating strategies needs to be well thought of.

In the future, the development of core design optimization capabilities within the LOTUS framework can provide a complete toolkit to perform Risk-Informed Safety Margin Management for the existing fleet. Core design optimization is essential for fuel cycle economics, hence a robust optimization capability would play an essential role to keep the current fleet operating economically.

The intrinsic value of a successful research and development activity in this area is expected to be significant. LOTUS has the potential of becoming a powerful safety margin management toolkit for industry stakeholders to address the challenges imposed by the proposed 10 CFR 50.46c rulemaking by relying on a more rigorous mathematical apparatus to address the important issue of uncertainties in safety analyses.

Once LOTUS achieves its objectives, it can potentially outweigh some of the costs associated with the proposed rule rollout, hence keeping the U.S. fleet competitive with other sources of energy. A more informed analysis with respect to the actual margin available in each plant also can potentially reduce extensive (and costly) iterations between licensees and regulators when dealing with rule compliance and operational issues. Ultimately, studying and understanding the available data in a risk-informed manner will yield a higher degree of safety and cost efficiency.

CONTENTS

EXECUTIVE SUMMARY	iii
FIGURES	vii
TABLES	x
ACRONYMS	xi
1. INTRODUCTION	1
1.1 The NRC Proposed 10 CFR 50.46c Rule and its Implications	2
2. RISMIC INDUSTRY APPLICATIONS	4
2.1 The RISMIC Approach for IA1	5
2.2 RISMIC Margin Characterization Approach: Full Monte Carlo versus the Wilks’ Approach	7
3. INDUSTRY APPLICATION 1: INTEGRATED CLADDING/ECCS PERFORMANCE ANALYSIS	9
3.1 The IA1 Problem Description	11
3.1.1 Margin Characterization	11
3.1.2 Margin Optimization	12
3.2 Proposed Solution Method (LOTUS)	13
4. LOTUS DEMONSTRATION	15
4.1 Reference System	15
4.1.1 Reactor Vessel	15
4.1.2 Reactor Coolant System	15
4.1.3 Emergency Core Cooling System (ECCS)	18
4.2 Reference Transient	18
4.3 LOTUS-B and LOTUS-A	24
4.3.1 Phase I – LOTUS-B (Baseline)	24
4.3.2 Phase II – LOTUS-A (Advanced)	25
4.3.3 Planned Activities	25
4.4 LOTUS Computational Tools	27
4.4.1 PHYSICS	27
4.4.2 NESTLE	28
4.4.3 MAMMOTH	29
4.4.4 VERA-CS	29
4.4.5 MPACT	30
4.4.6 HELIOS-2	31
4.4.7 COBRA-TF	31
4.4.8 FRAPCON/FRAPTRAN	32
4.4.9 BISON	33
4.4.10 RELAP5-3D	33
4.4.11 RELAP-7	34
4.4.12 RAVEN	35
4.4.13 LWROPT	35

4.5	Core Design Automation.....	36
4.5.1	Lattice Code Interface Tools for PHISICS/RELAP5-3D and HELIOS-2.....	36
4.5.2	Equilibrium Cycle Strategy.....	42
4.5.3	Cross Section Library Calculations	43
4.5.4	Coupled PHISICS/RELAP5-3D Calculation.....	45
4.5.5	Transient Power Maneuvers	46
4.6	Fuels Performance.....	49
4.7	Systems Analysis.....	50
4.8	Risk Assessment.....	54
4.8.1	Uncertainty Propagation	54
4.8.2	Limit Surface Search.....	55
4.8.3	Reduced-Order Models and Surrogate Models.....	55
4.8.4	Sensitivity Screening	56
5.	LOTUS DEMONSTRATION RESULTS.....	57
5.1	Core Design Automation.....	57
5.1.1	Common Core Geometry for HE-LL and HE-LL-O Core Designs	57
5.1.2	Option 1: HE-LL Core	57
5.1.3	Option 2: HE-LL-Optimized Core (HE-LL-O)	63
5.1.4	Transient Power Maneuvers for HE-LL and HE-LL-O Core Designs	69
5.2	Fuels Performance.....	72
5.2.1	HE-LL Core Design.....	73
5.2.2	HE-LL-Optimized Core Design.....	74
5.3	Systems Analysis.....	75
5.3.1	HE-LL Core Design.....	75
5.3.2	HE-LL-Optimized (HE-LL-O) Core Design	79
5.4	Risk Assessment.....	81
6.	CONCLUSIONS, FUTURE WORK AND THE PATH FORWARD.....	83
6.1	Results Conclusions	83
6.2	IA1 Future Work	84
6.3	Path Forward	85
7.	REFERENCES	88
	APPENDIX.....	91

FIGURES

Figure 1. Analytical Generic Limit Proposed by the NRC for Existing Fuel, ECR & PCT versus Hydrogen Content. [1].....	3
Figure 2. Overview of a Notional Process for Optimizing Core Configuration and Demonstrating Acceptable Safety Performance.....	3
Figure 3. Schematic of the RISMIC Toolkit.....	4
Figure 4. Industry Applications within the LWRS-RISMIC Program.....	5
Figure 5. Flow Chart of the RIMM Integrated Evaluation Model. [4].....	7
Figure 6. RISMIC Margin Quantification and Risk Assessment Paradigm.....	8
Figure 7. Schematic Illustration of LOTUS.....	10
Figure 8. Characterization of a Hypothetical Core (The Points and Curves Displayed Are Notional Values, i.e., They Are Not Actual Calculations, They Are Representations of a Certain Outcome for Illustration Purposes).	12
Figure 9. Optimization of a Characterized Core (The Curves Displayed Do Not Represent Actual Calculations; They Represent a Desired Pattern for Demonstration Purposes Only).	13
Figure 10. LOTUS Data Stream.	14
Figure 11. RELAP5-3D Nodalization Diagram for the Reactor Vessel.	16
Figure 12. RELAP5-3D Nodalization of a Typical Four-Loop PWR Primary System.	17
Figure 13. Illustration of Simulations of ECCS for LB-LOCA Transients.	18
Figure 14. Schematic of Double Ended Guillotine Break.....	19
Figure 15. Start of the LB-LOCA.	20
Figure 16. Sketch of ECCS Bypass.	20
Figure 17. Refill Phase.....	21
Figure 18. Beginning of Reflood.	21
Figure 19. Nitrogen Injection at the End of Accumulator Discharge.	22
Figure 20. Reflood Phenomena.....	23
Figure 21. Depressurization during a LB-LOCA.....	23
Figure 22. PCT Trace during a LB-LOCA.	24
Figure 23. Schematic Illustration of LOTUS-A and LOTUS-B.....	25

Figure 24. LOTUS Demonstration: Core Simulation Strategy.....	37
Figure 25. For Core Design: XS Generation and Core Calculation Iteration Scheme.....	38
Figure 26. "On the Fly" Cross Section Generation Scheme.	39
Figure 27. Material Density Feedback to the Lattice Code Tool Scheme.	40
Figure 28. Library Assembly Tool Scheme.	41
Figure 29. SPH Iteration Scheme.....	42
Figure 30. IA1 Demonstration of a PWR Design Strategy.....	43
Figure 31. HELIOS-2 Model for an IA1 PWR Demonstration (An Assembly for Option 1 with WABA Pins Is Shown).....	44
Figure 32. Left) Cross Section Library Locations Generated with HELIOS-2, Right) 8 Group Energy Structure Generated with HELIOS-2.	44
Figure 33. RELAP5-3D Core Nodalisation Used for the Core Simulation.	46
Figure 34. Load Following Maneuver Power History.	47
Figure 35. Control Rod Positions and Insertion Sequence.	48
Figure 36. RAVEN Samples the LOCA Start Times and Runs RELAP5 in Multi-Deck Mode.	48
Figure 37. Schematic Illustration of the Mapping between the Core Design Analysis and the RELAP5-3D Analysis Core Model for a typical Four-Loop PWR.....	51
Figure 38. Schematic Illustration of the Heat Structure Mapping for the Hot Assembly and Its Hot Rod with the Hot Channel (One for Each Group of Assemblies).....	52
Figure 39. Schematic Illustration of the Heat Structure Mapping for Average Assemblies and their Respective Hot Rods with the Average Flow Channel.	52
Figure 40. Left) BEAVRS Core Layout Indicating Enrichment and Burnable Absorber Positions in Cycle 1. Right) BEAVRS Key Parameters.....	58
Figure 41. Option 1 (HE-LL): 17x17 Pin BEAVRS Assembly. In this Example with 12 WABA Rods (B), 12 Guide Tubes (G) and One Instrument Tube (I) in the Center.	58
Figure 42. Option 1 (HE-LL): Equilibrium Cycle Reloading Pattern, Fresh Fuel Enrichment and Number of Burnable Absorber (BA) Pins in the Fresh Fuel Assemblies.....	60
Figure 43. Option 1 (HE-LL): Pbar, Fdh, Fq and Burnup for Each Assembly at BOC (Top) and EOC (Bottom).	61
Figure 44. Option 1 (HE-LL): Core Averaged Axial Power Distribution for Fresh (0B), Once Burned (1B) and Twice Burned (2B) Fuel Assemblies at BOC, MOC and EOC.....	62
Figure 45. Option 1 (HE-LL): Maximum Pin Peaking Factors for Each Assembly at BOC and EOC.....	62

Figure 46. Option 2 (HE-LL-O): Left) Current 17x17 Pin Assembly. In this Example Shown with 128 IFBA Rods (Circles) and 25 Guide Tubes (Black); Right) Axial Fuel Pin Design: High Enriched Center Part with Top and Bottom Blankets 2.6% Enriched.	64
Figure 47. Option 2 (HE-LL-O): Equilibrium Cycle Reloading Pattern, Fresh Fuel Enrichment and Number of Burnable Absorber (BA) Pins in the Fresh Fuel Assemblies.	66
Figure 48. Option 2 (HE-LL-O): Pbar, Fdh, Fq and Burnup for each Assembly at BOC (Top) and EOC (Bottom).	67
Figure 49. Option 2 (HE-LL-O): Core Average Axial Power Distribution for Fresh (0B), Once Burned (1B) and Twice Burned (2B) Fuel Assemblies at BOC, MOC and EOC.....	68
Figure 50. Option 2 (HE-LL-O): Maximum Pin Peaking Factors for each Assembly at BOC and EOC. 68	
Figure 51. Option 1 (HE-LL): Skewed Power Shapes at the End of the Maneuver at BOC (Top), at 300 Days (Middle) and at EOC (Bottom). Shown Are Core Average Axial Power Distributions for Fresh (0B), Once Burned (1B) and Twice Burned (2B) Fuel Assemblies.	70
Figure 52. Option 2 (HE-LL-O): Skewed Power Shapes at the End of the Maneuver at BOC (Top), at 300 Days (Middle) and at EOC (Bottom). Shown Are Core Average Axial Power Distributions for Fresh (0B), Once Burned (1B) and Twice Burned (2B) Fuel Assemblies.	72
Figure 53. Power History for the Hot Rod in a Twice Burned Fuel Assembly.	73
Figure 54. Cladding Hydrogen Content versus Rod Average Burnup.....	73
Figure 55. Power History for the Hot Rod in a Twice Burned Fuel Assembly.	74
Figure 56. Cladding Hydrogen Content versus Fuel Rod Average Burnup.....	74
Figure 57. PDF and CDF for PCTR at EOC.....	76
Figure 58. PDF and CDF for ECRR at EOC.	76
Figure 59. PCT versus Pre-Transient Cladding Hydrogen Content.....	77
Figure 60. ECR versus Pre-Transient Cladding Hydrogen Content.	78
Figure 61. ECR versus PCT for the Limiting Cases.	78
Figure 62. PCT versus Pre-Transient Cladding Hydrogen Content for the Liming Cases.	80
Figure 63. ECR versus Pre-Transient Cladding Hydrogen Content for the Limiting Cases.....	80
Figure 64. PCT (Top) and ECR (Bottom) ROM Uncertainty Quantification by Region: (Left) Monte Carlo Samples; (Right) Mean with 5-95 Percentiles; (Red) Proposed Limit.	82
Figure 65. PCT (Left) and ECR (Right) Results by Fuel Type (Burnup) for a HE-LL Core Reload and Design Strategy.	83
Figure 66. PCT (Left) and ECR (Right) Results by Fuel Type (Burnup) for a HE-LL-Optimized Core Reload and Design Strategy.	83

TABLES

Table 1. LOTUS-A/B Timeline of Activities and Resources for each Area of Development..... 26

Table 2. Common Data from Fuel Rod Design for Different Physics in LOCA Analysis. 49

Table 3. Distribution of Parameter Uncertainties. 53

Table 4. Summary of the 95/95 Estimators for PCT and ECR for the HE-LL Core Design. 77

Table 5. Summary of the 95/95 Estimators for PCT and ECR for the HE-LL-Optimized Core Design. .. 79

ACRONYMS

10 CFR	Title 10, Code of Federal Regulations
1D	One Dimensional
2D	Two Dimensional
3D	Three Dimensional
ANS	American National Standard
AOR	Analysis of Record
API	Application Programming Interfaces
ARO	All Rods Out
ATF	Accident Tolerant Fuel
ATWS	Anticipated Transients without Scram
BA	Burnable Absorber
BEAVRS	Benchmark for Evaluation And Validation of Reactor Simulations
BEPU	Best Estimate Plus Uncertainty
BOC	Begin of Cycle
BOL	Beginning of Life
CASL	Consortium for the Advanced Simulation of Light Water Reactors
CCFL	Counter Current Flow Limitation
CD-A	Core Design Automation
CD-O	Core Design Optimization
CDF	Cumulative Distribution Function
CFR	Code of Federal Regulation
CHF	Critical Heat Flux
CMFD	Coarse Mesh Finite Difference
COBRA-TF	Coolant Boiling in Rod Arrays – Two Fluid
CR	Control Rod
CRAM	Chebyshev Rational Approximation Method
CRGT	Control Rod Guide Tubes
CTF	COBRA-TF
CVCS	Chemical and Volume Control System
CWO	Core Wide Oxidation
DNB	Departure from Nucleate Boiling
DOE	U.S. Department of Energy

ECC	Emergency Core Cooling
ECCS	Emergency Core Cooling System
ECR	Equivalent Cladding Reacted
ECRR	ECR ratio
EOC	End of Cycle
EOL	End of Life
EPRI	Electric Power Research Institute
FA	Fuel Assembly
FOM	Figure of Merit
FP	Fuel Performance
FTE	Full-Time-Equivalent
FY	Fiscal Year
GEH	General Electric-Hitachi
GWd	Gigawatt-day
HE-LL	High Energy-Low Leakage
HE-LL-O	HE-LL-Optimized
HFP	Hot Full Power
HPC	High Performance Computing
HPI	High Pressure Injection
HZP	Hot Zero Power
ID	Inner Diameter
IA1	Industry Application #1
IAPWS	International Association for the Properties of Water and Steam
IEM	Integrated Evaluation Model
IFBA	Integral Fuel Burnable Absorber
IFM	Intermediate Flow Mixer grids
INL	Idaho National Laboratory
INSTANT	Intelligent Nodal and Semi-structured Treatment for Advanced Neutron Transport
KW	Kilowatt
LB-LOCA	Large Break LOCA
LOCA	Loss of Coolant Accident
LOTUS	LOCA Analysis Toolkit for the U.S.
LOTUS-A	LOTUS Advanced
LOTUS-B	LOTUS Baseline

LPD	Low-Pressure Drop
LPI	Low Pressure Injection
LWR	Light Water Reactor
LWROPT	LWR Optimization
LWRS	Light Water Reactor Sustainability
MLO	Maximum Local Oxidation
MOC	Method of Characteristics
MOC	Middle of Cycle
MOL	Middle of Life
MOOSE	Multi-Physics Object-Oriented Simulation Environment
MPACT	Michigan Parallel Characteristics based Transport
MRTAU	Multi-Reactor Transmutation Analysis Utility
MSIV	Main Steam Line Isolation Valve
MUR	Measurement Uncertainty Recapture
MWd	Megawatt-day
MWth	Megawatt thermal
NEM	Nodal Expansion Method
NPP	Nuclear Power Plant
NRC	U.S. Nuclear Regulatory Commission
OD	Outside Diameter
ODE	Ordinary Differential Equation
PCT	Peak Clad Temperature
PCTR	PCT ratio
PDE	Partial Differential Equation
PDF	Probability Density Function
PHISICS	Parallel and Highly Innovative Simulation for INL Code System
PIRT	Phenomena Identification and Ranking Table
PORV	Power-operated Relief Valves
PPM	Parts per Million
PWR	Pressurized Water Reactor
R&D	Research and Development
RA	Risk Assessment
RAVEN	Risk Analysis Virtual Environment
RCCA	Rod Cluster Control Assemblies

RCP	Reactor Coolant Pumps
RCS	Reactor Coolant System
RELAP5	Reactor Excursion and Leak Analysis Program 5
RELAP-7	Reactor Excursion and Leak Analysis Program 7
RFA	Robust Fuel Assembly
RIMM	Risk Informed Margin Management
RISMC	Risk Informed Safety Margin Characterization
ROM	Reduced Order Model
RPAC	RISMC Pathway Advisory Committee
RTP	Rated Thermal Power
SA	Simulated Annealing
SA	System Analysis
SPH	Super Homogenization
STP	South Texas Project
TAMU	Texas A&M University
TH	Thermal Hydraulics
tHM	(metric) ton of Heavy Metal
TRD	Thermal Reaction Accumulated Duty
TRISO	Tristructural-Isotropic
UO ₂	Uranium Dioxide
UQ	Uncertainty Quantification
VERA	Virtual Environment for Reactor Applications
VERA-CS	VERA Core Simulator
WABA	Wet Annular Burnable Absorbers
WEC	Westinghouse Electric Company
WPPM	Weight Parts Per Million
XML	Extensible Markup Language
ZrB ₂	Zirconium Diboride

Loss of Coolant Accident / Emergency Core Coolant System Evaluation of Risk-Informed Margins Management Strategies for a Representative Pressurized Water Reactor

1. INTRODUCTION

The U.S. Nuclear Regulatory Commission (NRC) is currently proposing rulemaking 10 CFR 50.46c to revise the loss-of-coolant-accident (LOCA) and emergency core cooling system (ECCS) acceptance criteria to include the effects of higher burnup on cladding performance. The key implications of this proposition are that the core, fuels, and cladding performance cannot be evaluated in isolation anymore. Both cladding and ECCS performance need to be considered in a coupled manner. This may also suggest that models for cladding performance as well as LOCA methodologies need to be updated. Given the acceptance criteria levied by the proposed rule, a question is raised: How can we best configure the core and operate the plant while still satisfying the proposed regulatory acceptance criteria?

In 2015, the Risk-Informed Safety Margin Characterization (RISMC) Pathway, as part of the DOE Light Water Reactor Sustainability (LWRS) research and development program initiated a set of demonstration activities to support the industry in the transition to the proposed 50.46c rule and to offer potential solutions to LOCA/ECCS analysis. This is the subject of this report, the Industry Application #1 (IA1). Its purpose is to provide the plant owner/operator a vehicle to inform decisions to manage margins related to compliance with the proposed 10 CFR 50.46c rule. In this project, margin is measured relative to the 10 CFR 50.46c proposed rule. The industry will need to comply with the proposed rule within seven years of the proposed change (the timeline for implementation is still being discussed among the NRC, fuel vendors, and licensees, and will depend on many factors, such as methodology changes, amount of work to be submitted for regulatory approval, and regulatory reviews).

The RISMC toolkit is now sufficiently mature to provide a set of LOCA analysis tools that provide the plant owner/operator a vehicle to manage margins and inform decisions if compliance with the proposed 10 CFR 50.46 is challenged by changes in the operational envelope. IA1's goal is to develop an Integrated Evaluation Model (IEM) to understand how uncertainties are propagated across the physical disciplines and data involved, as well as how risks are evaluated in postulated LOCA events under 10 CFR 50.46c. This IEM is called LOCA Toolkit for the U.S. (LOTUS) and it couples five technical disciplines that are important in LOCA analysis, namely core design, fuels performance, system analysis, risk assessment and core design optimization. A focus of LOTUS is to establish the automation interfaces among the five disciplines. LOTUS will utilize, in a first step, current state-of-the-art computer codes. The risk-informed margins management approach for IA1 will provide a means of quantifying the impact of key

LOCA analysis figures-of-merit like peak cladding temperature (PCT), and equivalent cladding reacted (ECR), and other fuel specific characteristics. The information that risk tools and analysis provide can then be used for decision-making and margin management. This development is one of several “industry applications” being addressed within the RISMC Pathway, as part of the DOE LWRs research and development Program.

An Industry Application #1 initial report in 2015 [2] focused on the proposed RISMC methodology and showing an early demonstration using reduced order models. The current work expands to LOTUS demonstrations including coupled disciplines in core design, fuels performance, system analysis and risk assessment. The core optimization discipline is left for future work. This report presents a first step towards developing a margins management toolkit for core, fuel design, and safety analysis coupling various physics disciplines and multiple levels of fidelity.

1.1 The NRC Proposed 10 CFR 50.46c Rule and its Implications

As mentioned, the U.S. NRC is considering rulemaking that would revise the requirements in 10 CFR 50.46. In the proposed rulemaking, designated as 50.46c, the NRC proposed performance-based equivalent cladding reacted (ECR) criteria as a function of cladding hydrogen content before a postulated LOCA (pre-transient) in order to include the effects of higher burnup on cladding performance as well as to address other technical issues. The pre-transient cladding hydrogen content, in turn, is a function of fuel burnup and cladding materials. The proposed rule would apply to all light water reactors and to all zirconium based cladding types. Key aspects of the proposed rule are as follows:

- Cladding performance cannot be evaluated in isolation. Cladding performance and ECCS performance need to be considered in a coupled way, which examines the interactions across the disciplines involved.
- Models for cladding performance even within the design basis will need to be updated for regulatory purposes.
- Effort needs to be expended in searching regulatory issue space for the limiting case (“ECCS performance must be demonstrated for a range of postulated loss-of-coolant accidents of different sizes, locations, and other properties, sufficient to provide assurance that the most severe postulated loss-of-coolant accidents have been identified. ECCS performance must be demonstrated for the accident, and the post-accident recovery and recirculation period”.)

A characteristic of the proposed rulemaking, as illustrated in Figure 1, imposes more restrictive and fuel rod-dependent cladding embrittlement criteria. Therefore, a thorough characterization of the reactor core is required in large break LOCA (LB-LOCA) analyses in order to identify the limiting case and limiting rods.

The rule implementation process is expected to take approximately seven years following the rule effective date. A loss of operational margin may result due to the more restrictive cladding embrittlement criteria. Initial and future compliance with the rule may

significantly increase vendor workload and licensee costs, as a spectrum of fuel rod initial burnup states may need to be analyzed to demonstrate compliance.

The total costs for the industry to accommodate the proposed rule can be in excess of \$500 million. If plants have to operate at more restrictive conditions than currently allowed, the indirect cost could be even larger. Consequently, there will be an increased focus on licensee decision making related to LOCA analysis to minimize cost and impact, and to manage margin. Figure 2 shows a high-level concept of one way to address the needs created by the proposed rule.

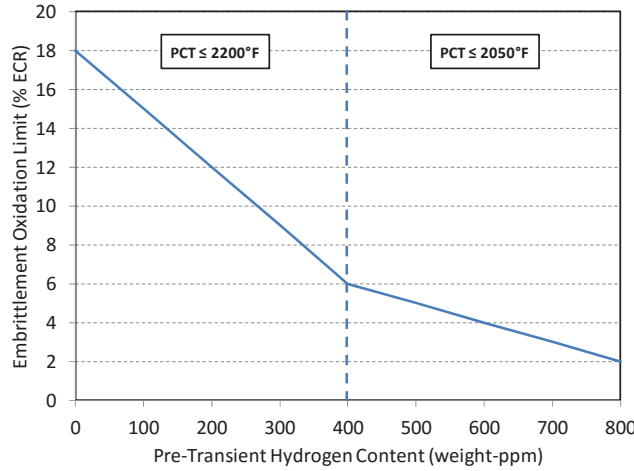


Figure 1. Analytical Generic Limit Proposed by the NRC for Existing Fuel, ECR & PCT versus Hydrogen Content. [1]

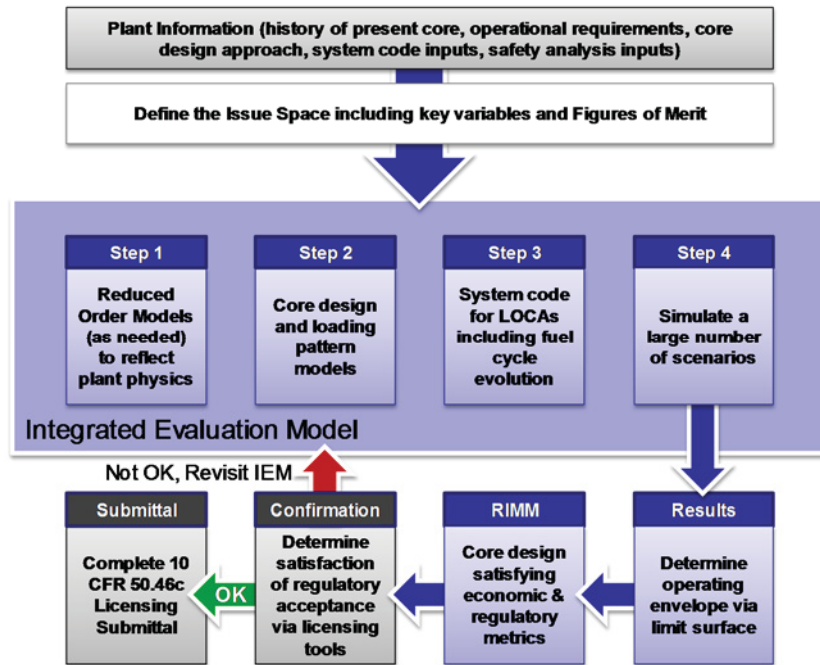


Figure 2. Overview of a Notional Process for Optimizing Core Configuration and Demonstrating Acceptable Safety Performance.

2. RISMC INDUSTRY APPLICATIONS

As mentioned in the introduction, in 2015, as part of the DOE LWRS, INL initiated a program to develop analytical capabilities to support the industry in the transition to the proposed LOCA acceptance rule. One of these programs is the Industry Application #1 (IA1) within the Risk-Informed Safety Margin Characterization (RISMC) Pathway of LWRS [2,3].

RISMC will develop and provide methodologies and tools to plant operators/owners to support plant decisions for risk-informed margins management. These include improved economics, reliability and sustain safety of current nuclear power plants. With RISMC, we estimate how close we are (or not) to an event, not just the frequency of an event, providing information on how safety margins can be improved. Goals of the RISMC pathway are to:

- .. develop and demonstrate a risk-assessment method coupled to safety margin quantification. Nuclear plant owners and decision makers could then use the developed methods to help with their margin recovery strategy.
- .. create an advanced RISMC toolkit. This should help the nuclear plant owner to represent safety margins more accurately. The toolkit will be based on the MOOSE solver framework and is being created to avoid issues and limitations with legacy tools (see Figure 3).

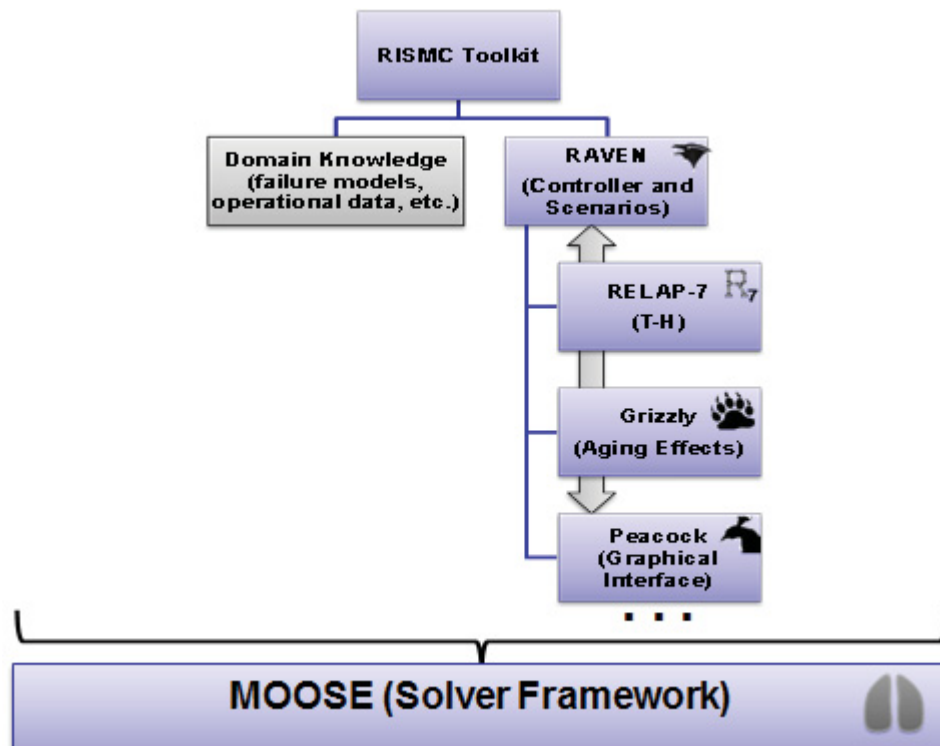


Figure 3. Schematic of the RISMC Toolkit.

As mentioned, the RISMIC R&D Pathway within the DOE LWRs program includes the RISMIC Toolkit development and the Risk-Informed Margin Management (RIMM) Applications (see Figure 4). The corresponding R&D activities are separated in “Tools”, “Data” and “Methods”. The “Tools” development focuses on MOOSE and its attached advanced codes. The “Data” part includes the Verification, Validation and Uncertainty part for all levels of the analysis, i.e. from the component to the facility scale. Finally, the Industry Applications form the “Methods” part of RISMIC. As one can see from Figure 4, the Industry Applications seek a close collaboration with the industry either through EPRI or directly with a plant owner, operator or vendor. The safety analysis guidelines resulting from the Industry Applications will be made available to the industry.

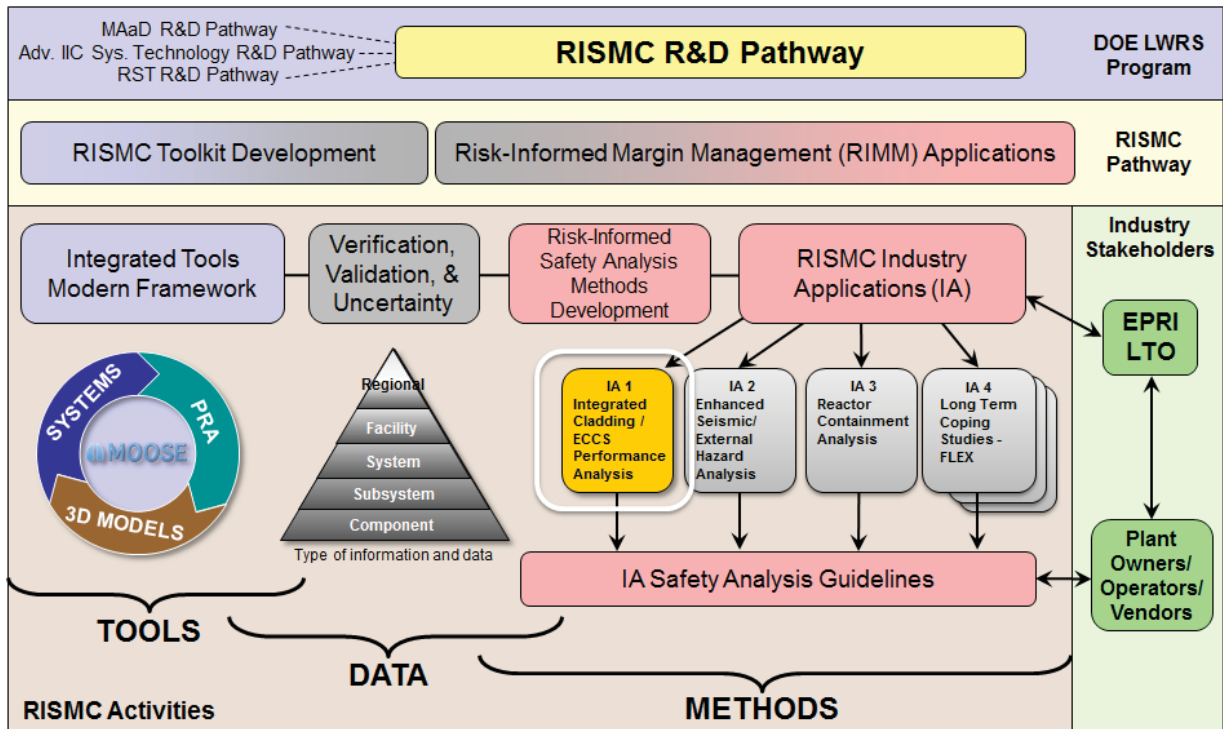


Figure 4. Industry Applications within the LWRs-RISMIC Program.

2.1 The RISMIC Approach for IA1

Nuclear installation designers, vendors and licensees (plant owner/operators) operate in a regulated environment. Traditionally, the economics of the industry prevent large deviations from well-established procedures within the licensing basis of the evaluation models, which are already in place. For example, the complex multi-physics LOCA problem is solved via operator splitting where various engineering disciplines are interfaced with well-set rules, which have been developed over the years consistently with specific acceptance criteria and regulatory requirements. Further, the propagation of uncertainties across the various functional groups is addressed by defining bounding assumptions at the interfaces which limit the possibility that the impact of an issue in a

specific discipline (error discovered, design change or other) to cross-over to other physics in an efficient fashion.

Such traditional processes and interfaces do not easily adapt to new integrated methods and cannot fully leverage the progress that has been made in computation and numerical algorithms. Also there is a difficulty in absorbing new knowledge in the processes, which is now recognized by regulators and the industry as a whole. In other words the methods are limited in their responsiveness. Even state-of-the-art, best estimate plus uncertainty methods provide little information on the actual margin available in the plants. Most margins reside in engineering judgment and conservative assumptions, which were built to deal with the imperfect knowledge.

Moving forward, the industry is expected to develop better-standardized databases and improved interfaces across the various engineering disciplines as more automation is implemented in the processes. This will enable consideration of new paradigms to manage the uncertainties across the various disciplines with a truly multi-physics approach to the LOCA problem.

The proposed RIMM IA1 methodology and tool will provide a means of quantifying the impact on the key LOCA analysis figures of merit PCT, ECR, and core-wide oxidation (CWO) of a change in LOCA analysis inputs. This information would be obtained without the resource requirement, cost, and schedule, of an actual LOCA reanalysis using the integrated LOCA evaluation model LOTUS. The information that the tool provides can then be used for decision-making and margin management. The project is expected to create value by anticipating the trends towards integrated multi-physics models and focusing on developing a methodology that effectively addresses the limitations of traditional LOCA methods as presented above. The primary goal is to explore an integrated approach for knowledge and uncertainty management, as illustrated in Figure 5.

The global vision for the RIMM IEM LOTUS is summarized in the following propositions:

- Provide a responsive toolkit for the plant operator, which enables rapid decisions on considered changes within the LOCA issue space (as regulated under the proposed 10 CFR 50.46c). The goal is to greatly reduce the response cycle.
- Enable current knowledge to be factored into the process to enhance safety and operation optimization.
- Quantify currently not quantified uncertainties (to the extent practical) and trends to a realistic representation of the LOCA, which provides insights on the design. This includes the combination of risk and physics simulations as illustrated in Figure 6.
- Foster an approach that can lead to new knowledge and understanding of the LOCA scenarios, which could be “locked” in the engineering assumption of licensing calculations. Enable a more effective “exploration” of the issue space in order to improve core design.

- Eliminate issues associated with the Wilks’ approach (including variability in the estimator, risk of under-prediction of or over-prediction of FOM, lack of knowledge in what is limiting in the design, incapacity to perform sensitivity studies, etc.)
- A “plug-and-play” design of the multi-physics tool, which enables plant owner/operators and vendors to consider and further develop the RIMM Framework for use with their established codes and methods

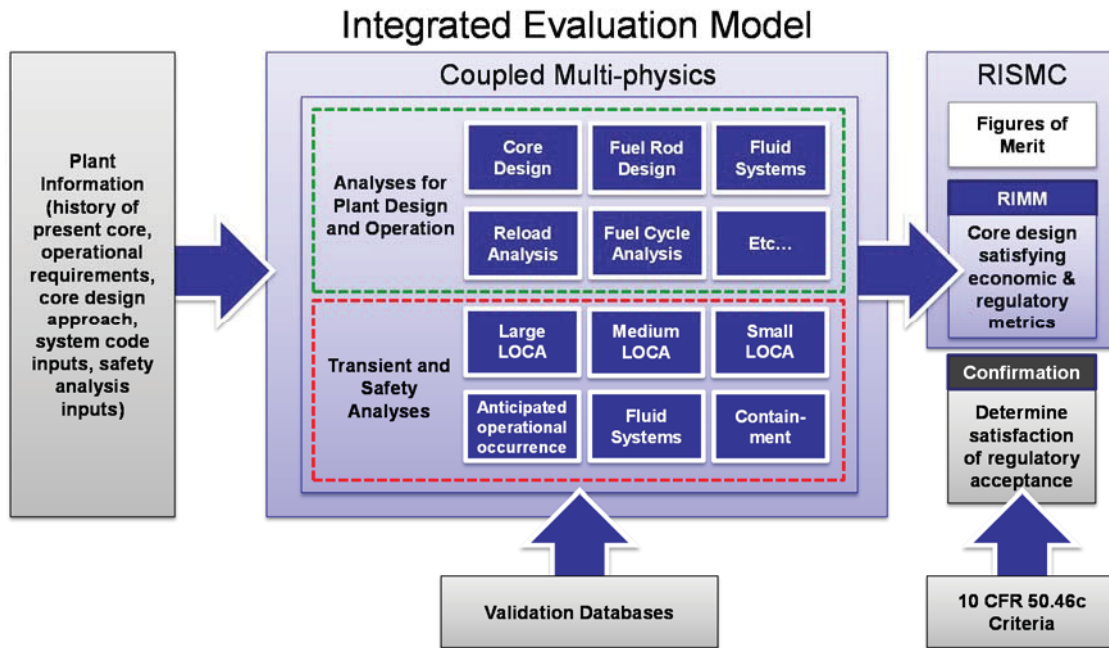


Figure 5. Flow Chart of the RIMM Integrated Evaluation Model. [4]

Note that LOTUS is not intended to replace licensing Analyses of Record (AORs) but rather to replace or aid the engineering judgment applied in managing those AORs. In other words, LOTUS is a margin management and optimization tool. This objective is achieved by representing the plant realistically, but in a way that makes it feasible to explore the issue space thoroughly, with all the uncertainties included and by considering and managing the entire body of knowledge.

2.2 RISMC Margin Characterization Approach: Full Monte Carlo versus the Wilks’ Approach

An important driver for developing LOTUS is the elimination of issues associated with the Wilks’ approach [5] (variability in the estimator, i.e. risk of under-prediction of or over-prediction of figures of merit, lack of knowledge in what’s truly limiting in the design, incapacity to perform sensitivity studies, impact assessment etc.). Despite its widespread adoption by the industry (AREVA, GEH and Westinghouse), the use of small sample sizes to infer statement of compliance to the 10 CFR 50.46 rule, has been a cause of unrealized operational margin in today’s best estimate plus uncertainty methods. Moreover, the debate on the proper interpretation of the Wilks’ theorem in the context of safety analyses is not

fully resolved yet more than a decade after its introduction in the frame of safety analyses in the nuclear industry. This represents both a regulatory and applicant risk in rolling out new methods.

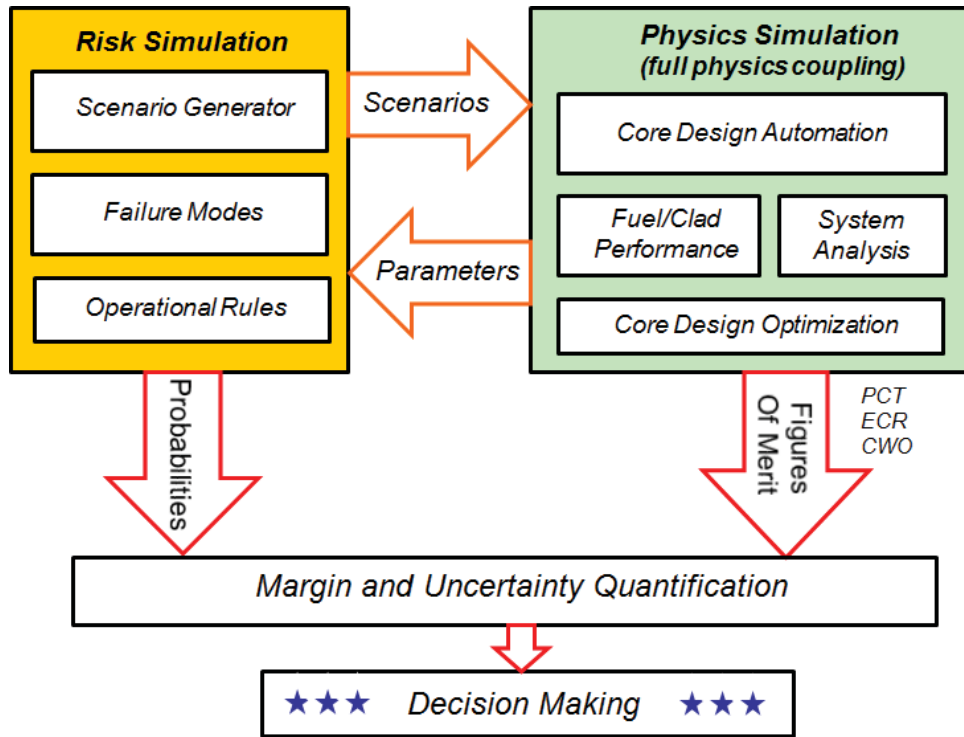


Figure 6. RISMC Margin Quantification and Risk Assessment Paradigm.

The proposed rule added another layer of complexity for the demonstration of compliance. Under the current rule PCT, Maximum Local Oxidation (MLO) and Core Wide Oxidation limits are set to specific values (2200 F, 17% and 1% respectively). Using Wilks compliance is easily demonstrated by ranking the corresponding values obtained from the simulations in the sample and ensuring the rank representing the 95/95 estimates from a small sample is below those limits. Considering there are three outcomes (PCT, MLO and CWO), the highest ranked set from a sample of 124 can be chosen.

With the proposed rule, the limit is a curve, more specifically both PCT and MLO (maximum Equivalent Clad Reacted (ECR) in this case) limits are functions of cladding hydrogen content, which varies from rod to rod in the core. Applying Wilks' method would require to define new figures of merit that synthesize this relationship. Additionally, if the analyst is ultimately interested in tracking the margin in each core region that would not be possible unless a much larger sample size is used. With LOTUS, the answer is to move toward full Monte Carlo simulations when it comes to managing uncertainties. It has to be acknowledged that the sample size needed to reduce the confidence interval on the estimate (standard error) to the magnitude desired may require sample sizes in excess of 1,000-10,000 cases. However the benefit is that full Monte Carlo simulations enables to assess the impact of input parameter changes to distributions and determine the significance of the changes.

3. INDUSTRY APPLICATION 1: INTEGRATED CLADDING/ECCS PERFORMANCE ANALYSIS

As mentioned, the general idea behind the Industry Application #1 is the development of an Integrated Evaluation Model (IEM). The motivation is to revisit how uncertainties are propagated across the stream of physical disciplines and data involved, as well as how risks are evaluated in a LOCA safety analysis as regulated under 10 CFR 50.46c. The use of an integrated approach in managing the data stream is probably the most important aspect of what is proposed here. This also is well suited with current trends in industry to enhance automation and develop integrated databases across their organizations. As mentioned in the introduction, this IEM is called LOTUS, which stands for LOCA Toolkit for the U.S., and it represents the LWRS Program's response to the stated problem.

A LOCA safety analysis involves several disciplines, which are computationally loosely (externally) coupled to facilitate the process and maintenance of legacy codes and methods. A review of a few examples of analyses performed by vendors such as AREVA and Westinghouse Electric Company (WEC) is instructive to define the state-of-the-art in the industry. The key disciplines involved in a LOCA analysis are:

- Core physics;
- Fuel rod thermo-mechanics;
- Clad corrosion;
- LOCA thermal-hydraulics;
- Containment behavior.

The focus of LOTUS is to establish the automation interfaces among the five disciplines as depicted in Figure 7. These five disciplines include:

1. Core Design Automation, which focuses on automating the cross section generation, core design and power maneuvering process.
2. Fuel Performance, which focuses on automating the interface between core design and fuel performance calculations and the interface between fuel performance and system analysis.
3. System Analysis, which focuses on automating the process required to setup large number of system analysis codes runs needed to facilitate RISMC applications on LOCA.
4. Uncertainty Quantification and Risk Assessment, which focus on establishing the interfaces to enable combined deterministic and probabilistic analysis.
5. Core Design Optimization which focuses on developing core design optimization tool that can perform in-core and out-of-core design optimization.

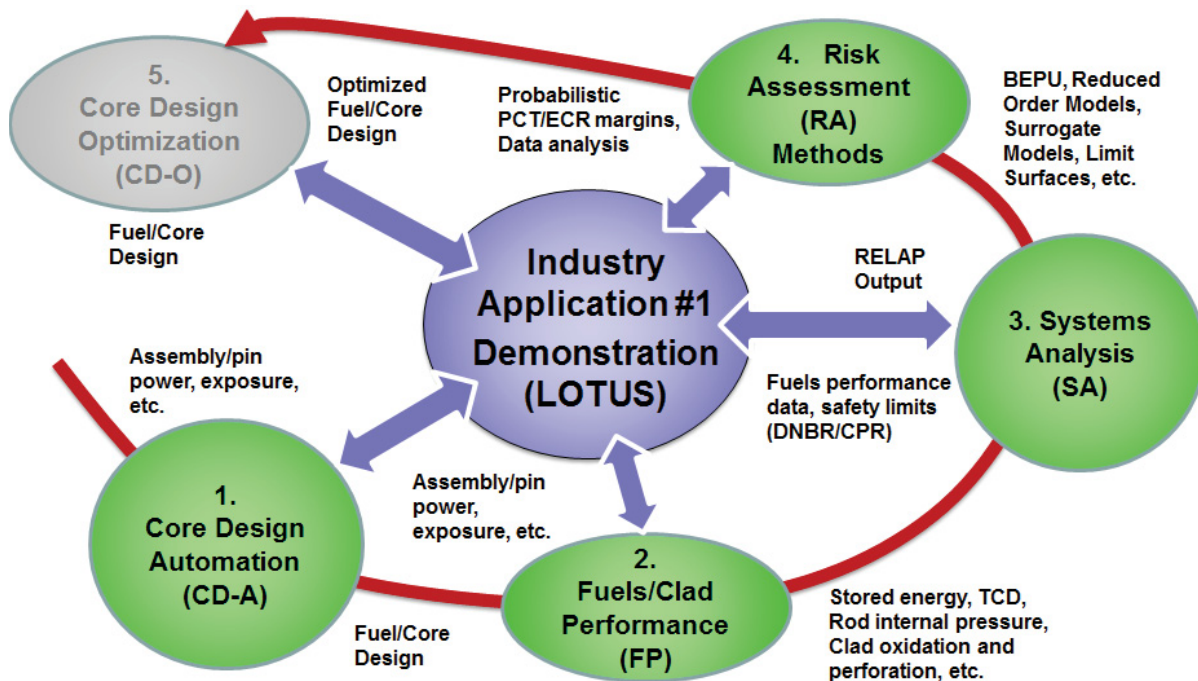


Figure 7. Schematic Illustration of LOTUS.

LOTUS utilizes existing computer codes as well as advanced computer codes still being developed under various DOE programs to provide feedback and guide development of advanced tools. Regardless of the specific codes used to model the physics involved, the methodology proposed here is a paradigm shift in managing the uncertainties and assessing risks. The primary characteristic of LOTUS is to be an integrated multi-physics tool. This is a model in sharp contrast with the “operator split” or “divide-and-conquer” approach currently adopted in the industry, where every physics is resolved independently and coupling is addressed by complex interface procedures. There are significant assumptions and engineering judgment in setting up these procedures which make the propagation of uncertainties across the disciplines complex, prone to errors, and more importantly, current methods retain analytical margin which cannot be exploited.

The value proposition of LOTUS for industry stakeholders can be summarized in the following objectives:

- Provide quantitative estimates of design or operational margin loss or gain associated with various combinations of changes in LOCA analysis inputs.
- Allow/inform marketing strategies related to LOCA analysis by better informing licensees in their decision process.
- Provide LOCA inputs related studies in response to customer inquiries and requests.
- Respond to LOCA-related regulatory inquiries and requests for additional information.

Currently there are no nuclear plant owner-operators in the U.S. that perform LOCA analysis for determining compliance with 10 CFR 50.46. In the U.S., Analysis of Records (AORs) is generated by nuclear vendors under contract by the plant operators. The vendor is responsible of the development of codes and methods while seeking generic approval of the methodology over a target class of plants. The vendor then performs the plant specific analysis for the licensee to demonstrate compliance with the 10 CFR 50.46 criteria. The plant operator manages the analysis inputs and maintains the AORs. The vendor is responsible of managing the analysis process and assessing impact of input errors, which may be found after the AOR is in place.

A limited number of owner-operators perform LOCA analysis for other purposes such as pipe break mass and energy release or training simulator validation. For an owner/operator, the LOTUS methodology and tool has two distinct types of potential applications. The more likely type of potential applications is for LOCA analysis related work contracted to the fuel vendor, which could include the following potential uses:

- Obtain quantitative estimates of design or operational margin loss or gain associated with various combinations of changes in LOCA analysis inputs.
- Obtain quantitative estimates of impact on the LOCA analysis figures-of-merit due to changes in LOCA analysis inputs (including reporting of LOCA analysis Δ PCT and Δ ECR due to LOCA analysis input changes that are required by 10 CFR 50.46).

Another possible type of potential application is to use the LOTUS methodology and tools as an independent owner-operator LOCA analysis capability; especially LOTUS requires minimum infrastructure and training for its usage. This capability could be used to perform vendor-independent LOCA scoping or audit calculations that would facilitate decision making related to the impact of plant and fuel design changes, as well as provide an enhanced vendor oversight capability. An owner-operator could develop this capability with in-house staff or by outsourcing to an engineering services or consulting entity.

The 5th area shown in Figure 7, the core design optimization focuses on developing core design optimization tool that can perform in-core and out-of-core design optimization. This area is a possibility to be investigated in the future.

3.1 The IA1 Problem Description

Following the discussion in Section 2.1, the problem of the Industry Application #1 can be separated in two: First, the plant owner/operator will determine how much margin the plant has compared to 10 CFR 50.46. This is called the margin characterization of the plant. In second step, to recover some of the margin, the owner/operator might want to do a core/plant optimization.

3.1.1 Margin Characterization

As an analysis result, the owner/operator will use LOTUS to “characterize” the core designed for operation. Figure 8 illustrates this process, where LOTUS maps an envelope of maximum ECR as a function of cycle exposure. This allows the operator to have a

realistic assessment of an operating core, and conceivably be more prepared for a quick response re-analysis in case a problem might occur.

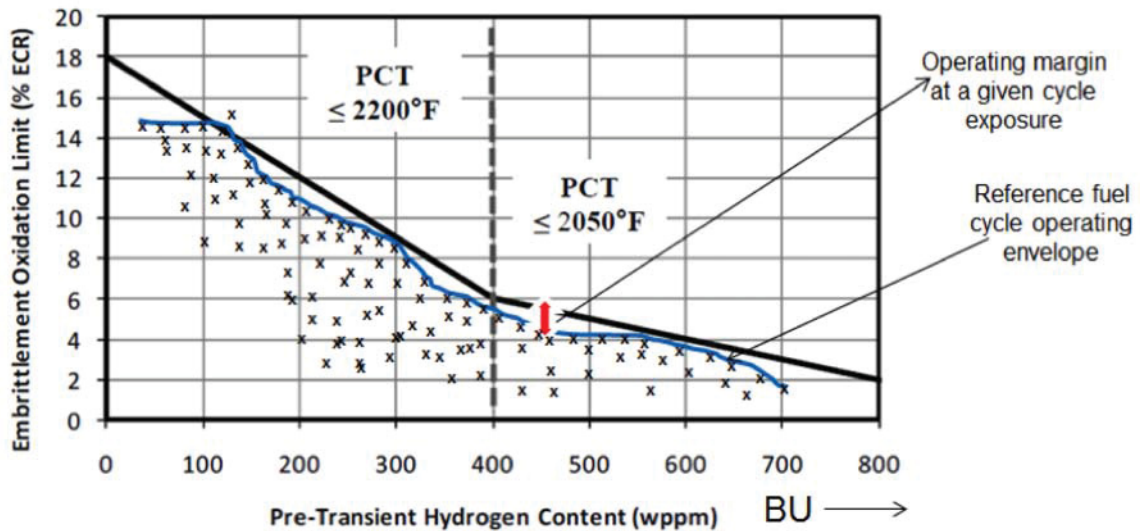


Figure 8. Characterization of a Hypothetical Core (The Points and Curves Displayed Are Notional Values, i.e., They Are Not Actual Calculations, They Are Representations of a Certain Outcome for Illustration Purposes).

3.1.2 Margin Optimization

The characterization of a reference core with LOTUS is intended to simplify the existing reload analysis process, although not intended to replace the existing licensing process. In principle, a reload engineer that has trained LOTUS to analyze a given core design can re-analyze such reference design in much faster time than using a traditional reload design analysis process.

Eventually, we will be able to incorporate optimization schemes into LOTUS that can quickly reshape a desired parameter envelope (in this case ECR) as an optimization feature of a core design process, as illustrated in Figure 9. In practice, such a step will require additional changes of today's design process, in order to incorporate LOCA analysis as an integrated element of the reload analysis process.

Note that the concept described above is simplified, and it serves the purpose of only illustrating the approach proposed. In practice, LOTUS will need to evaluate a multi-dimensional problem not easily visualized as points on a burnup-oxidation plot.

Computational constraints to analyzing highly complex systems with many variables to be considered have kept us in the past from executing these types of schemes. Today, with the development of the RISMIC Toolkit built in a state-of-the-art computational environment we are able to implement complex multi-physics approaches solving fully coupled systems problems in acceptable time.

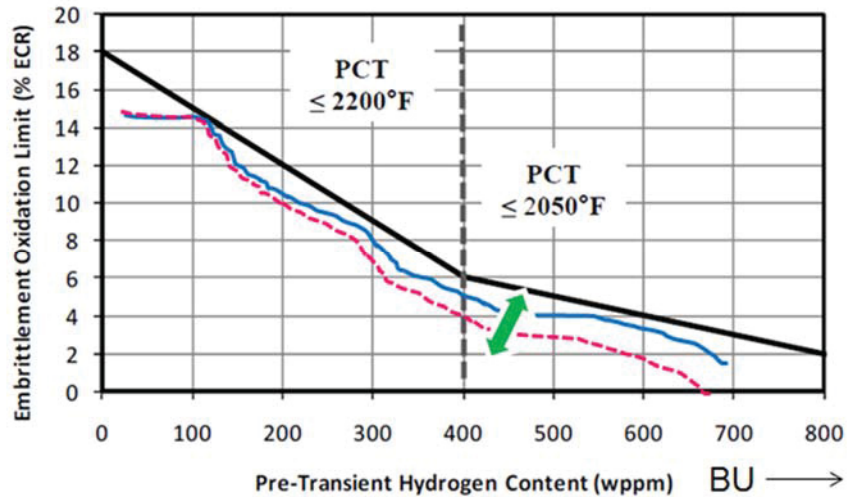


Figure 9. Optimization of a Characterized Core (The Curves Displayed Do Not Represent Actual Calculations; They Represent a Desired Pattern for Demonstration Purposes Only).

3.2 Proposed Solution Method (LOTUS)

The first step in obtaining the desired technical capability to perform the type of analyses that address the challenges presented earlier is to revisit how uncertainties are propagated across the stream of physical disciplines involved. Regardless the specific codes used to model the physics involved, the methodology presented here is really a different strategy in managing the uncertainties. As mentioned earlier, the primary objective of LOTUS is to be an integrated multi-physics tool. In the LOTUS framework uncertainties are propagated directly from all the uncertain design and model parameters. The interactions between the various model parameters are directly solved within the LOTUS framework.

This interaction not only facilitates the automation of the process, but it is also mathematically more robust because the advanced procedure considered to propagate uncertainties and/or perform global sensitivity and risk studies requires inputs sampled to be independent. This requirement is hard to achieve following the traditional “divide-and-conquer” approach.

Conventional methods are strongly “code-oriented.” The analyst has to be familiar with the details of the codes utilized, in particular with respect to their input and output structures. This represents a significant barrier for widespread use beside the small pool of experts within the specific organization or even groups within the organization that develops such codes. It becomes apparent how difficult is to make changes and accelerate progress under such paradigm, especially in heavily regulated environment where even a minor line changes in a code carries a heavy cost of bookkeeping and regulatory actions.

The LOTUS vision is to move toward to a “plug and play” or “task oriented” approach where the codes are simply modules ‘under the hood’ that provides the input-output relationship for a specific discipline. The focus shifts on managing the data stream

at a system level, as depicted in Figure 10. LOTUS is essentially a workflow engine with capability to drive physics simulators, model complex systems and provide risk assessment.

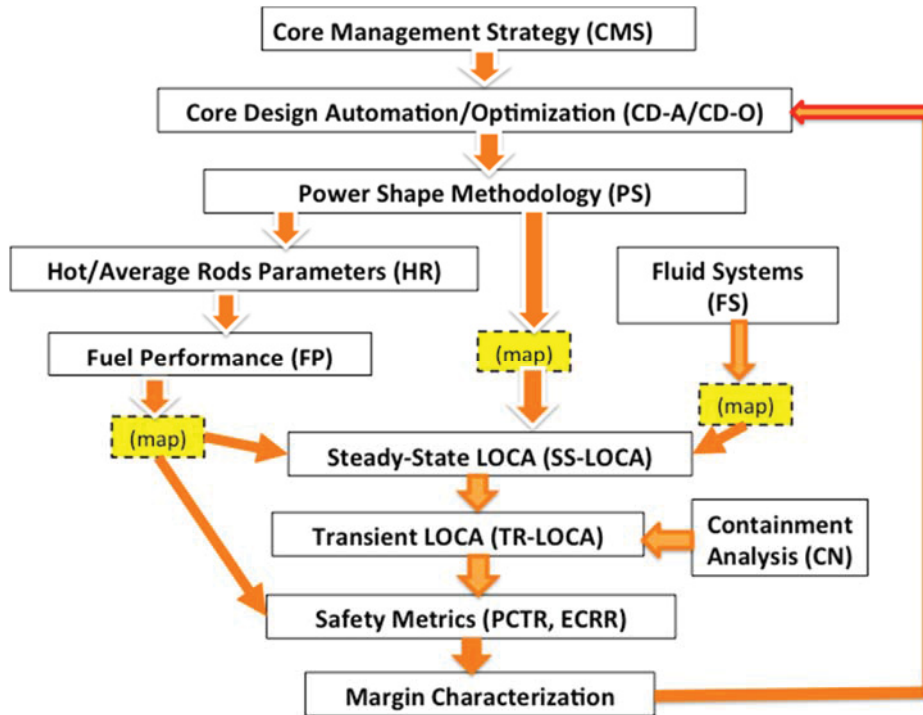


Figure 10. LOTUS Data Stream.

As a multi-physics analytical framework, LOTUS is not intended to replace licensing Analysis of Records (AORs), but rather to replace or aid the “engineering judgment” which is typically applied in the management and maintenance of those AORs. The goal is an analytical and computational device that can represent a power plant realistically with all the uncertainties included and that considers all physical disciplines involved in an integrated fashion.

A “plug-and-play” approach will enable plant owners and vendors to consider and further customize the LOTUS framework for use within their established codes and methods. Therefore, it could potentially become the engine for license-grade methodologies. In other words, it is possible that LOTUS technology could be advanced in the future to a level of fidelity and maturity that it could be used for some licensing or regulatory situations. An example would be the reporting of LOCA analysis Δ PCT and Δ ECR related to LOCA analysis input changes that are required by 10 CFR 50.46c.

As mentioned earlier, the ultimate goal is then to incorporate optimization schemes in LOTUS that can quickly reshape a desired parameter envelope (for example ECR) as an optimization feature of a core design process. This step will require additional changes to today’s design process, in order to incorporate LOCA analysis as an integrated element of the reload analysis process.

4. LOTUS DEMONSTRATION

This Chapter presents a demonstration of the above-presented LOTUS methodology. The demonstration includes all aspects of LOTUS except the core optimization part, which is planned to be added in the future. The demonstration is carried out for a generic reference PWR and a reference LOCA transient presented in the subsequent sections. Furthermore, the presented demonstration uses existing computer codes. This is called LOTUS-B, “B” for baseline. It is planned to replace these existing computer codes as the new, advanced codes currently under development become available. This will be called LOTUS-A, where “A” stands for advanced. A timeline for the transition from LOTUS-B to LOTUS-A is shown later in this Chapter.

4.1 Reference System

The reference system to be simulated in this work is a typical four loop PWR power plant with a rated thermal power of 3411 MW. All the major flow paths for both primary and secondary systems are described, including the main steam and feed systems. Also modeled are primary and secondary power-operated relief valves (PORVs) and safety valves. The emergency core cooling system (ECCS) was included in the modeling of the primary side, and the auxiliary feedwater system was included in the secondary side modeling. A description of the primary and the secondary systems is presented in the following sections.

4.1.1 Reactor Vessel

The reactor vessel model, as schematically shown in Figure 11, includes the downcomer, downcomer bypass, lower plenum, core, upper plenum, and upper head. The following leakage paths are represented in the vessel model: downcomer to upper plenum, cold leg inlet annulus to upper plenum, and upper plenum to the upper head by way of the guide tubes. Heat structures represent both external and internal metal mass of the vessel as well as the core rods. Decay heat was assumed to be at the ANS-5.1 standard rate.

4.1.2 Reactor Coolant System

The four primary coolant loops in the typical PWR model, as shown in Figure 12, are designated as loops A, B, C and D. Each modeled loop contained a hot leg, U-tube steam generator, pump suction leg, pump and cold leg. The pressurizer was attached to the C loop and the pressurizer spray lines were attached to the B and C loop cold leg. Heat structures were added to each volume in the primary loops to represent the metal mass of the piping and steam generator tubes.

The secondary system of the plant is also modeled. The steam generator secondary side model represents the major flow paths in the secondary and includes the downcomer, boiler region, separator and dryer region, and the steam dome. The major flow paths of the steam line out to the turbine governor valves are modeled. Each line from the steam generator secondary out to the common steam header is modeled individually, and included a main steam line isolation valve (MSIV), a check valve, safety relief valves, and PORVs.

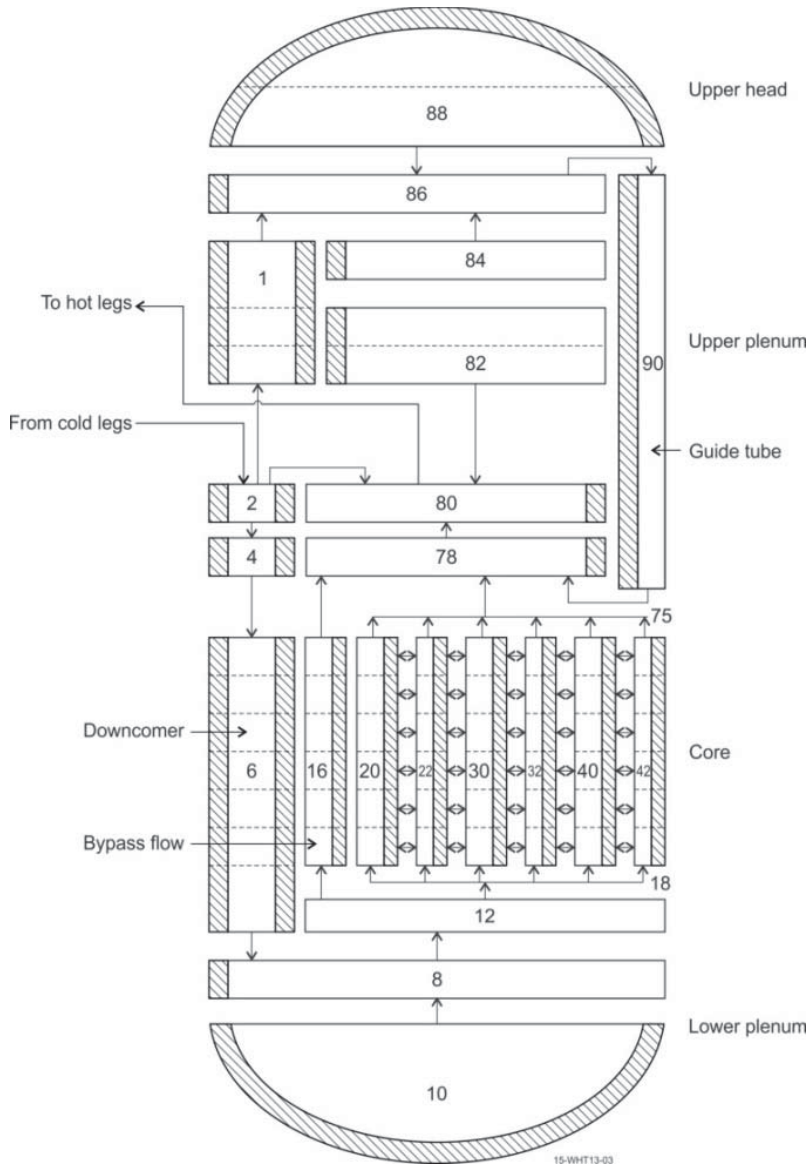


Figure 11. RELAP5-3D Nodalization Diagram for the Reactor Vessel.

The major flow paths of the feedwater system are modeled. The feedwater system consisted of the main feedwater system and the auxiliary feedwater system. The control system models include a steam dump control system, steam generator level control, pressurizer pressure control system, and pressurizer level control systems, etc. Heat structures for the secondary system included the internal and external metal mass for each of the steam generators.

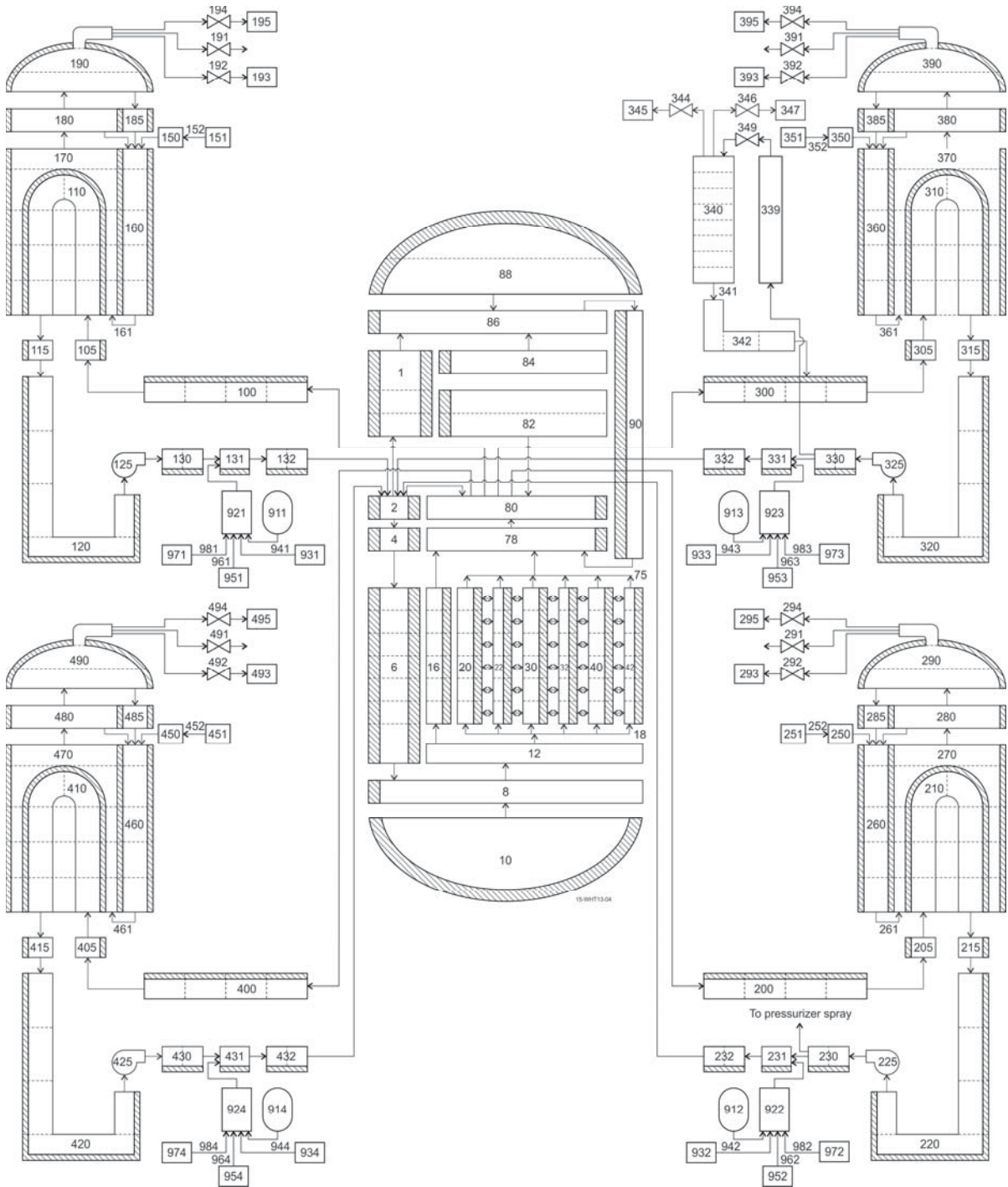


Figure 12. RELAP5-3D Nodalization of a Typical Four-Loop PWR Primary System.

4.1.3 Emergency Core Cooling System (ECCS)

Attached to each cold leg is a low pressure injection (LPI) connection port and an accumulator with its associated piping. A high-pressure injection (HPI) connection is also attached to each cold leg. The LPI and HPI models were set up to inject one-fourth of the total HPI and LPI flow into each loop. The RELAP5-3D model developed here can be used to perform simulations of various accident scenarios including large break loss-of-coolant accident (LB-LOCA), which is the primary interest of this work. For the LB-LOCA scenario, the break is located at cold leg A of the PWR, as shown in Figure 13.

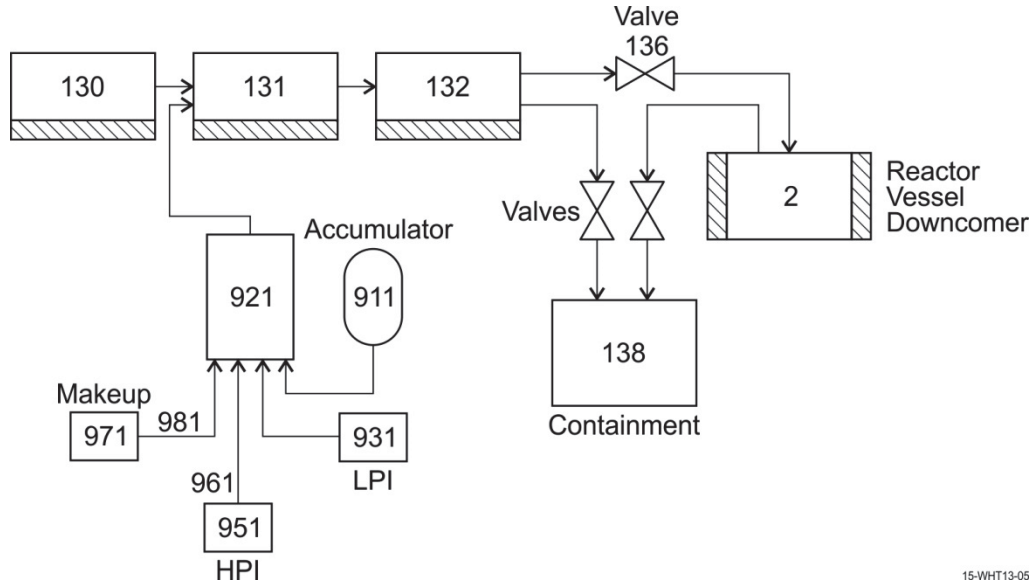


Figure 13. Illustration of Simulations of ECCS for LB-LOCA Transients.

4.2 Reference Transient

The Large Break LOCA scenario considered in this analysis is initiated by a large break of one of the cold legs (Figure 14). The cold leg is typically considered as the most limiting location as it limits the ECCS injection in the cold leg, it promotes flow stagnation in the core, and it cause ECCS injection bypass. The transient is characterized by three distinct periods: blow-down, refill, and reflood. The scenario is described for PWRs equipped with U-tube steam generators. The analysis was originally presented in the “LOCA Compendium”.

The blow-down period extends from the initiation of the break until the primary side depressurizes sufficiently that emergency core cooling (ECC) water can start to penetrate the downcomer (20-30 seconds into the transient). The flow out of the break is large, but limited by critical flow phenomena. No control rod insertion is credited in the event. The boiling and flashing, which occurs in the core as result of the rapid depressurization, is sufficient to shut down the fission process due to negative reactivity feedbacks.

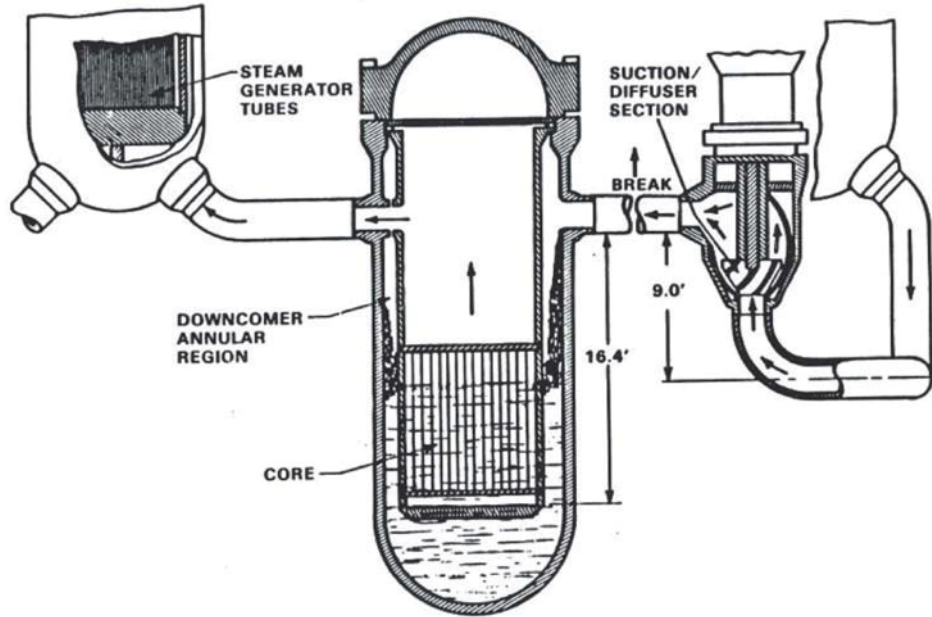


Figure 14. Schematic of Double Ended Guillotine Break.

The reactor coolant pumps (RCPs) are assumed to be either functioning or coasting down depending on the off-site power availability assumption. Even if the RCPs are running, the performance will be degraded by the void. The break flow will eventually reverse the flow in the core and a stagnation situation can be reached in the core (Figure 15). The hot fuel rods quickly exceed the critical heat flux, as the core flow reverses, resulting in a sharp reduction in heat transfer to the coolant. As the pressure decreases, the reversed flow induced by the break diminishes and positive core flow can be reestablished.

During the blow-down phase, the cladding temperature first rises rapidly as the initial stored energy in the fuel pellets is transferred to the cladding. After the initial heat-up, the cladding temperature will decrease due to the down flow of high velocity steam through the core. The lower power regions in the core may even quench during this blow-down cooling phase.

Between 10 to 20 seconds after the break, the RCS pressure decreases below the accumulator pressure. The accumulators begin injecting cold water into the cold legs, but the initial injection is swept out of the vessel and into the broken cold leg by the continuing high flow of steam from the core (Figure 16). This is called ECCS bypass.

Approximately 20 to 30 seconds after the break, the RCS pressure approaches the containment pressure and break flow becomes un-choked. This initiates the refill phase. The ECCS water from the accumulators and the pumped safety injection refill the lower plenum and establishes a water level in the downcomer (Figure 17). As the coolant enters the core, the reflooding process begins.

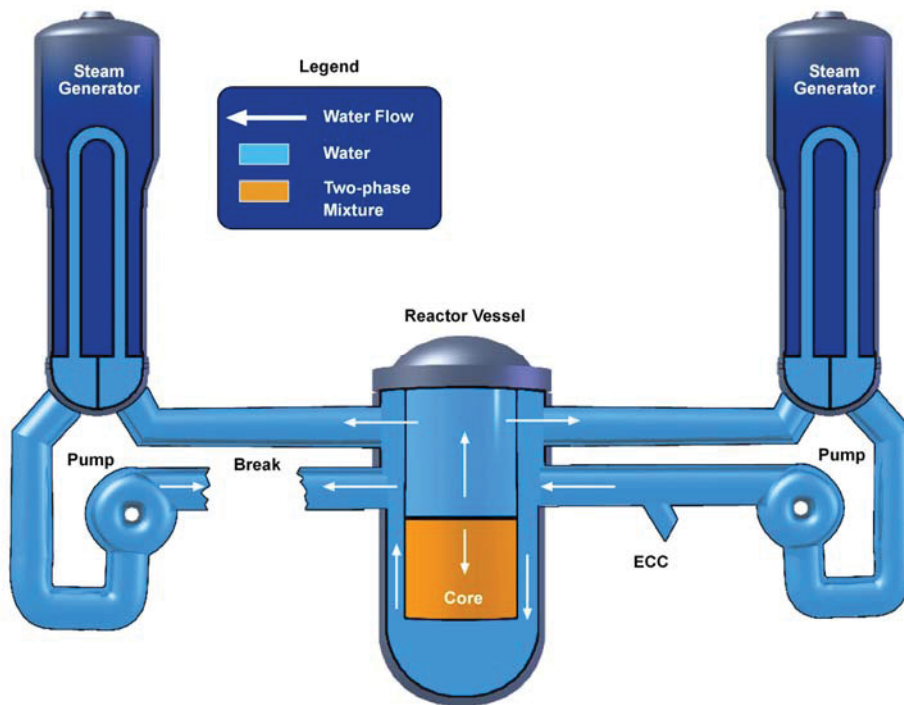


Figure 15. Start of the LB-LOCA.

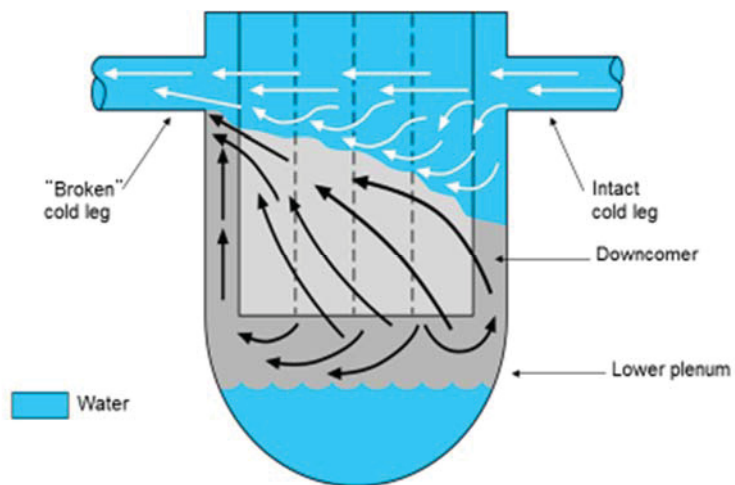


Figure 16. Sketch of ECCS Bypass.

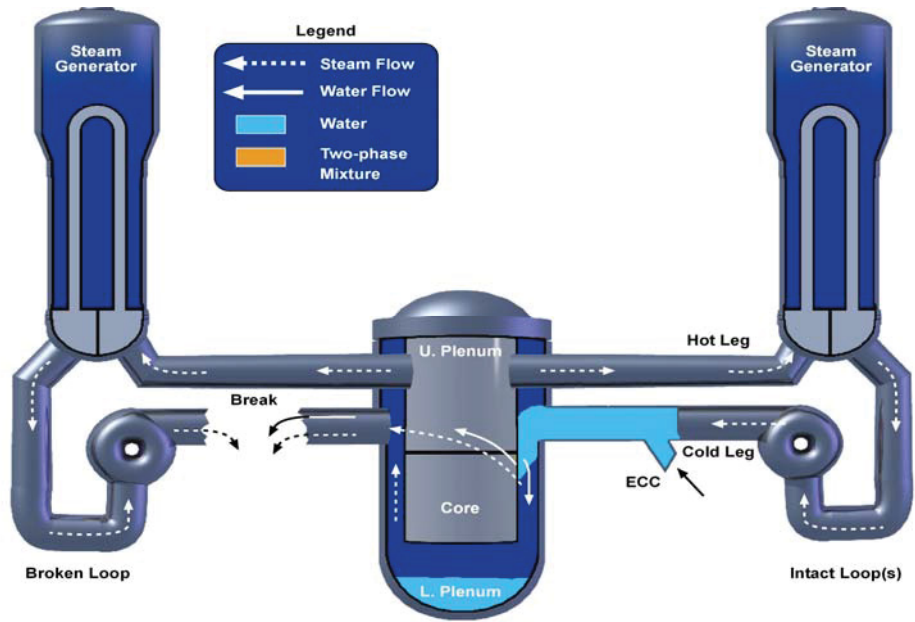


Figure 17. Refill Phase.

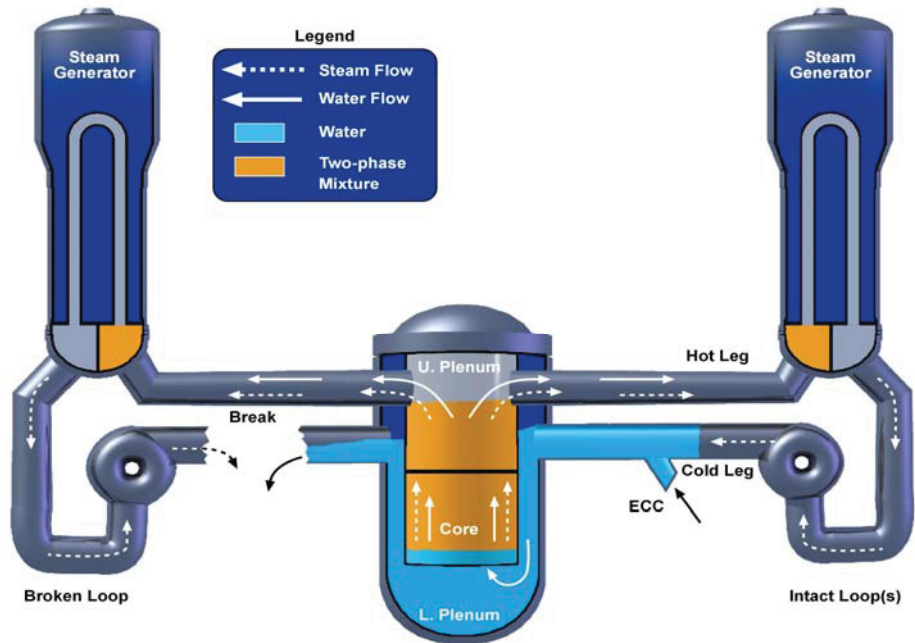


Figure 18. Beginning of Reflood.

The reflood of the core is gravity driven. The water head in the downcomer and the backpressure in the upper plenum determine the core-flooding rate. The flow into the core is initially oscillatory, as cold water rewets the hot fuel rods, generating steam, which in turn creates a local pressurization in the core. This, in turn creates a feedback mechanism and a manometric effect between the level in the downcomer and the level in the core.

As the core gradually quenches, steam is generated as the fuel rod dump their stored energy in the liquid and droplets entrained in the steam. This steam, and the water it entrains flows through the vessel upper plenum, the broken loop hot leg, the steam generator, and the pump before it can be vented out the break (Figure 18). Water that condensed in the steam generators cannot flow back into the core due to the counter current flow limitation (CCFL) that exist in different places in the system, especially the top of the core and the entrance to the steam generators.

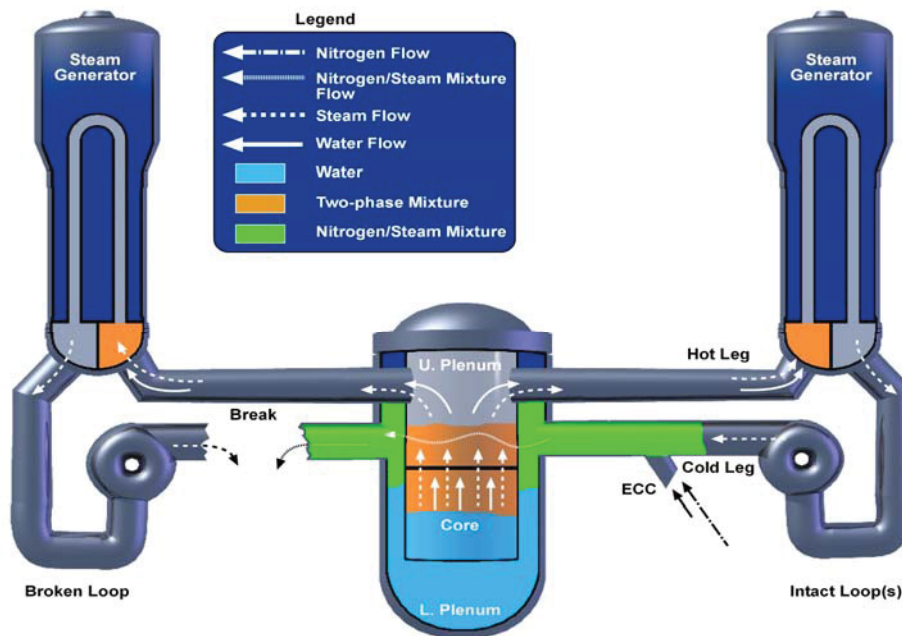


Figure 19. Nitrogen Injection at the End of Accumulator Discharge.

As the accumulators empty nitrogen gas is discharged in the system (Figure 19). As nitrogen enters the loop and the downcomer steam condensation is suppressed which creates a temporary pressurization in the downcomer and core liquid in-surge during reflood.

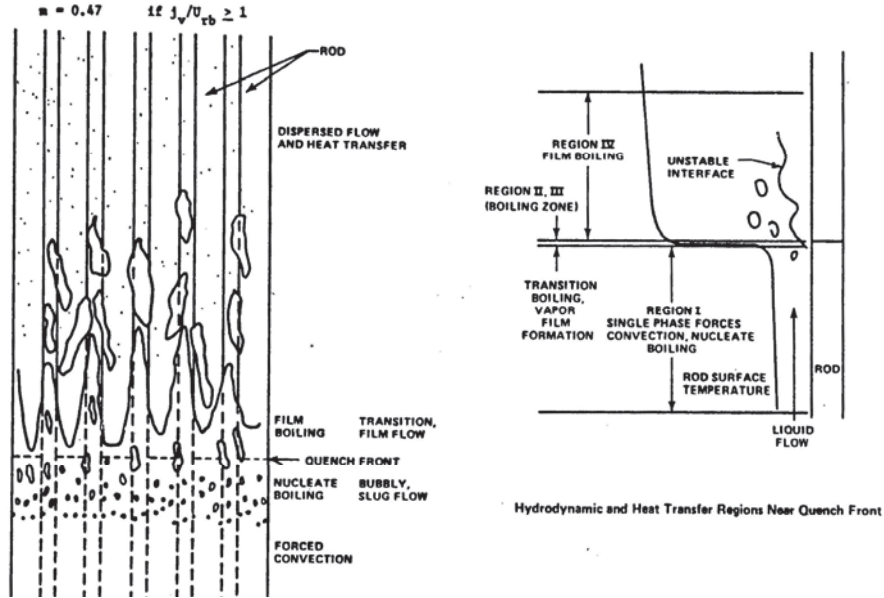


Figure 20. Reflood Phenomena.

Core reflood is a relatively slow process. As the bottom elevations are quenched, the top elevations continue to gradually heat up and eventually turnaround once the cooling rate exceeds the decay heat rate. The cooling mechanism is controlled by dispersed flow film boiling where droplets act as the ultimate heat sink to de-superheat steam at higher elevation (Figure 20). The reflood transient may last for several minutes. Figure 21 and Figure 22 show the typical transient for the primary pressure and PCT transient.

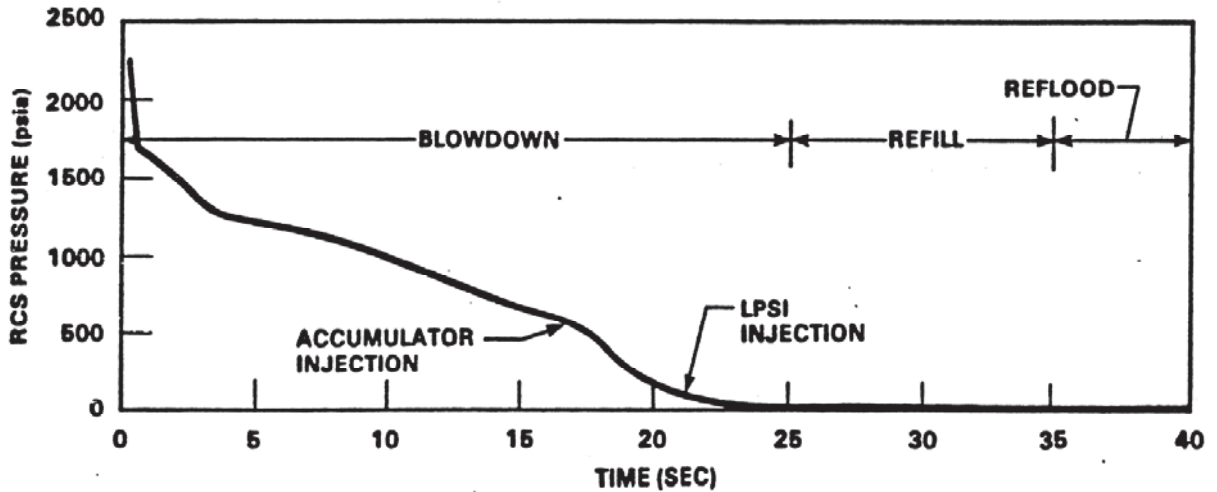


Figure 21. Depressurization during a LB-LOCA.

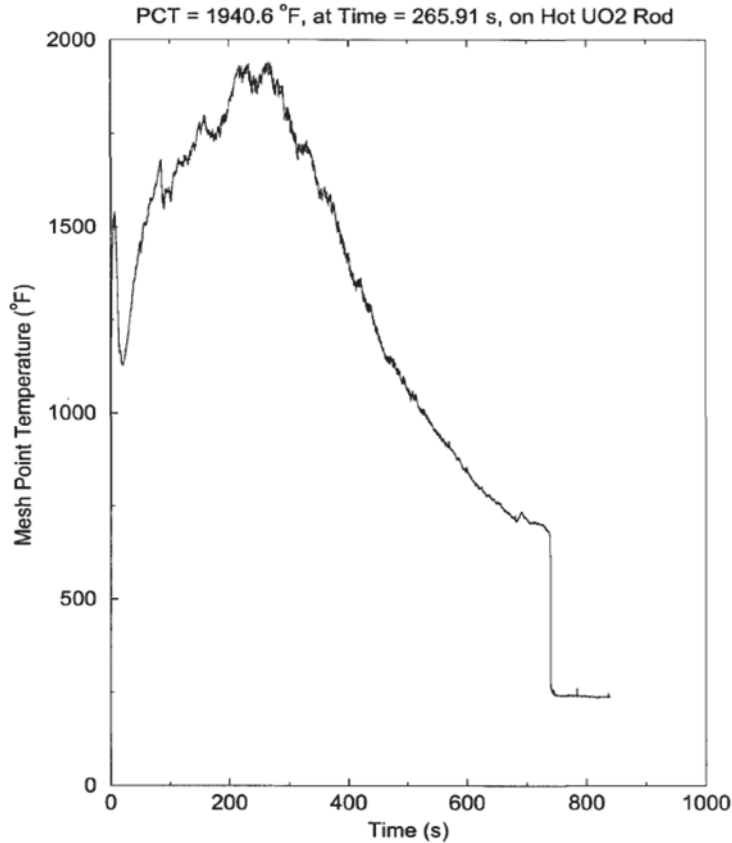


Figure 22. PCT Trace during a LB-LOCA.

4.3 LOTUS-B and LOTUS-A

The LOTUS project will be developed in two phases. First, for fiscal years 2016-17 LOTUS-B will be demonstrated using ‘Baseline’ (already existing) RISMC tools and methods to demonstrate the first four elements (1-4) of Figure 23, core design automation (CD-A), fuels/clad performance (FP), systems analysis (SA), and UQ and risk assessment (RA) methods. Second, for fiscal years 2017-19, all five elements (1-5) of LOTUS-A (Figure 23,) will be demonstrated, which will include ‘Advanced’ (in development by LWRS and other DOE R&D Programs) RISMC tools and methods, including core design optimization (CD-O) advanced schemes.

4.3.1 Phase I – LOTUS-B (Baseline)

For the first two years, four elements (1 through 4 in Figure 23) of the LOTUS-B toolkit are exercised. Each element implements a set of existing, well-established code(s) into the LOTUS-B toolkit, as illustrated in Figure 23 by (B). A set of all activities to be executed within this timeline is outlined in Table 1.

4.3.2 Phase II – LOTUS-A (Advanced)

In conjunction with the Baseline development, for a period of about three years, the advanced phase of the LOTUS project will be executed (fiscal years 2017-19). The duration and timeline associated with the LOTUS-A phase is in part dependent on the execution and lessons learned of the Baseline phase, and availability and maturity of the advanced tools in development today. An example of tools and methods to be implemented during the advanced phase is shown in Figure 23 by the (A) symbol. Also, a set of all activities to be executed during Phase II is outlined in Table 1.

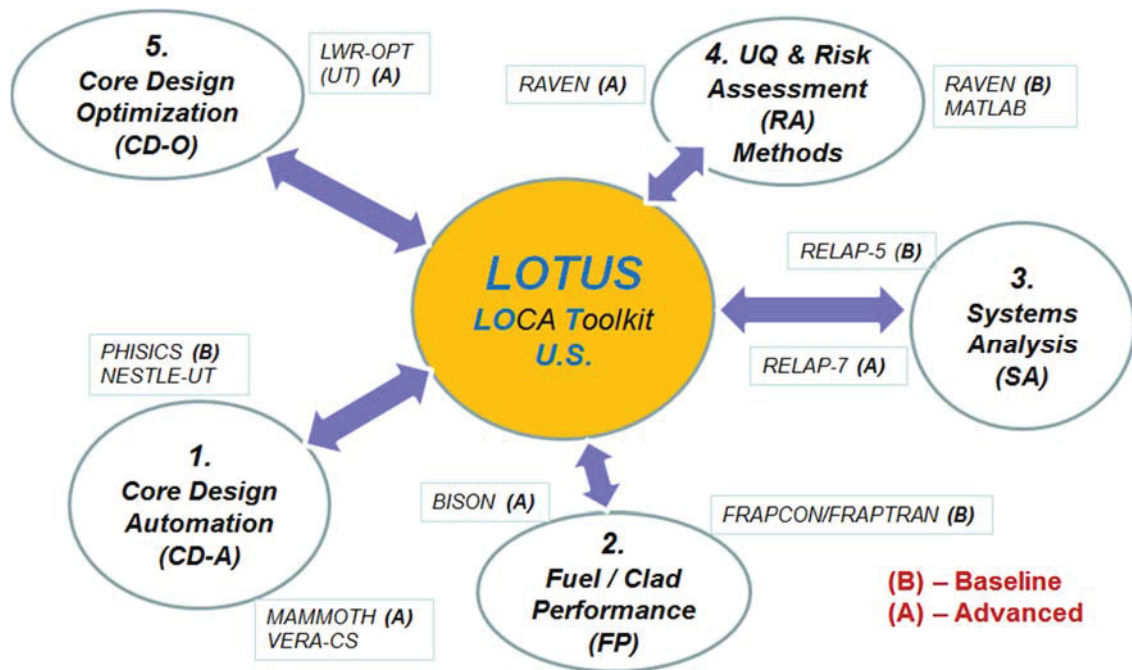


Figure 23. Schematic Illustration of LOTUS-A and LOTUS-B.

4.3.3 Planned Activities

The anticipated time for completion of LOTUS-B and LOTUS-A are two years and three years, respectively. The time for completion of the LOTUS tools may however vary depending on actual funding levels per fiscal year. The activities and resources per task shown in Table 1 are estimates at this time, and may vary as well for the same reasons.

Table 1. LOTUS-A/B Timeline of Activities and Resources for each Area of Development.

Technical Areas	Phase I: LOTUS-B		Phase II: LOTUS-A		
	FY-2016	FY-2017	FY-2017	FY-2018	FY-2019
Core Design Automation (CD-A)	Automate cross section generation 0.3 FTE	Adapt the NESTLE code into core design process 0.3 FTE	Initial assessment of CASL-LWRS collaboration – VERA-CS/BISON-CASL analysis of LB-LOCA 0.3 FTE	Adapt CASL’s VERA-CS code into the core design process 0.3 FTE	Demonstrate core design automation with advanced codes 0.4 FTE
	Improve HE-LL reference core design 0.2 FTE	Improve core design automation process 0.2 FTE		Adapt INL’s MAMMOTH code into the core design process 0.3 FTE	
	Automate power maneuvering process 0.2 FTE	Improve power maneuvering process 0.2 FTE		Power maneuvering for MAMMOTH and for VERA-CS 0.3 FTE	
	Data request for an operating plant demonstration 0.2 FTE	Execute operating plant demonstration 0.3 FTE			
Fuel/Clad Performance (FP)	Automate data transfer from CD-A to FRAPCON 0.3 FTE	Enable large number of FRAPCON runs to perform UQ 0.3 FTE	Automate data transfer from CD-A to BISON 0.2 FTE	Perform BISON runs with UQ for hot/average rods in each assembly 0.3 FTE	Demonstrate coupled RELAP-7/ BISON runs under LOCA conditions 0.5 FTE
	Perform FRAPCON runs for hot rod/average rods in each assembly 0.2 FTE	Demonstrate coupled RELAP5/FRAPTRAN runs under LOCA conditions 0.3 FTE	Investigate physics needed from FRAPCON/FRAPTRAN to BISON 0.3 FTE	Automate data transfer from BISON to RELAP-7 0.3 FTE	
	Automate data transfer from FRAPCON to RELAP5 0.3 FTE				
	Demonstrate coupled RELAP5/FRAPCON steady-state initialization condition for HE-LL reference design 0.3 FTE				
Systems Analysis (SA)	Automate data transfer from CD-A power maneuvering to RELAP5 0.2 FTE	Refine BEPU process with CD-A/FP automation 0.2 FTE		Adapt RELAP-7 into system analysis 0.4 FTE	Demonstrate BEPU analysis capability with RELAP-7 0.5 FTE
	Demonstrate LOTUS driven LB-LOCA analysis capability 0.2 FTE	Extend the RELAP-5 model to include long term cooling 0.3 FTE			
	Data request for an operating plant demonstration (summer) (pilot candidate: TAMU/STP) 0.3 FTE	Execute operating plant demonstration 0.3 FTE			

Uncertainty Quantification and Risk Assessment (RA)	Enhance BEPU analysis capability to expand uncertain parameter table 0.2 FTE	Demonstrate fuel performance surrogate models with RAVEN 0.3 FTE	Demonstrate UQ using reduced order methods (ROM) and limit surfaces with RAVEN 0.3 FTE	Develop dynamic PRA model for LOCA analysis 0.4 FTE	Demonstrate combined PRA and deterministic analysis for LOCA 0.3 FTE
	Assessment of RAVEN capabilities vs MATLAB 0.2 FTE				
	Initiate RAVEN implementation 0.1 FTE				
Core Design Optimization (CD-O)			Develop the core design optimization algorithm for LWROPT 0.5 FTE	Implement core design optimization algorithm into LOTUS 0.3 FTE	Demonstrate optimized core design with LWROPT 0.5 FTE
Overall LOTUS Project	Establish the LOTUS framework (Software and data structure) 0.1 FTE	Refine LOTUS framework to improve the automation process 0.1 FTE		Integration of advanced simulation tools into the LOTUS framework 0.4 FTE	Demonstration of LOTUS-A using HE-LL reference design 0.4 FTE
	Demonstrate steady-state automated data transfer among CD-A/FP/SA/RA 0.2 FTE	Demonstrate automated data transfer among CD-A/FP/SA/RA under transient conditions 0.1 FTE			LOTUS-A operating plant demonstration 0.4 FTE
	Demonstrate BEPU analysis with LOTUS 0.2 FTE	LOTUS-B operating plant demonstration 0.2 FTE			
TOTAL	3.7 FTEs	3.1 FTEs	1.6 FTEs	3.0 FTEs	3.0 FTEs

4.4 LOTUS Computational Tools

4.4.1 PHISICS

PHISICS is a neutronics code system in development at INL. [6] The different modules for PHISICS are a nodal and semi-structured spherical harmonics-based transport core solver [Intelligent Nodal and Semi-structured Treatment for Advanced Neutron Transport (INSTANT)] [7] for steady-state and time-dependent problems, a depletion module [Multi-Reactor Transmutation Analysis Utility (MRTAU)], [8] and a cross-section mixer-interpolator (MIXER) module. [9] Each different module of PHISICS contains a kernel (module) that solves a basic problem. A local driver is assigned to each kernel that is able to run it in stand-alone mode. Communication between the kernels is managed by the use of global data types that hold global information (cross-section data, mesh, fluxes, etc.) that are needed by more than one kernel to perform complex calculations involving different kernels. Global drivers solving a complex problem calling different kernels can be developed easily with this flexible software structure. The PHISICS code is still in development to extend its capabilities.

The transport core solver INSTANT is the key kernel of the PHISICS framework. INSTANT is parallelized and is designed to take full advantage of medium to large clusters (10 to 1000 processors). It is based on the second-order formulation of the transport equation discretized in angle by spherical harmonics while in space it uses orthonormal polynomials of an arbitrary order. In addition to steady-state solutions, INSTANT is able to solve time-dependent problems. For that, a scheme based on a second-order backward Euler scheme with explicit delayed neutron treatment has been implemented as a new module for the PHISICS suite.

MRTAU is a generic depletion code developed at INL. [8] In addition to core depletion, the code can be utilized for stand-alone decay heat calculations. It tracks the time evolution of the isotopic concentration of a given material accounting for nuclear reactions occurring in the presence of neutron flux and also due to natural decay (Bateman equation). The code uses a Taylor series expansion-based algorithm at arbitrary order and the Chebyshev Rational Approximation Method (CRAM) for computation of the exponential matrix.

The MIXER module does all the cross-section handling for the different kernels. MIXER can handle macroscopic, microscopic, and “mixed” cross sections. A macroscopic cross-section library contains macroscopic cross sections for each type of material used in the calculation (fuel, reflector, etc.) tabulated for the state parameters (temperature, burnup, CR position, etc.). MIXER interpolates these cross sections at the requested state parameters, and no limits in tabulation dimensions or neutron energy groups exist. A microscopic or mixed cross-section library contains the tabulated cross sections for each isotope considered in the calculation. MIXER reads a description containing a list of isotopes and corresponding densities for each material and interpolates the microscopic cross sections at the requested state parameters. Macroscopic cross sections for each material are generated with the corresponding number densities. With this capability, mixed macroscopic and microscopic cross sections are also possible. For example, it is possible to provide macroscopic absorption cross sections without xenon for a material and the microscopic xenon absorption cross section together with a xenon density. MIXER will calculate the xenon absorption contribution and add it to the macroscopic cross section. MIXER can read different cross-section library formats. Among them is an original simple XML-based format, but also AMPX, ISOTXS, and ECCO library formats that allow cross-section libraries to be prepared with SCALE, ERANOS, or MC2. More library types are planned to be supported in the future.

PHISICS is currently used in LOTUS-B as a core design tool.

4.4.2 NESTLE

NESTLE [10] is a few-group multi-dimensional nodal core simulator. It employs the nodal expansion method (NEM) to solve the few-group neutron diffusion equations. The NESTLE reactor core simulator was developed originally in the late 1980s at North Carolina State University and has been used widely over the last twenty years. NESTLE utilizes the nodal expansion method for eigenvalue, adjoint, fixed source steady-state and transient problems. A collaboration among the University of Tennessee, Oak Ridge

National Laboratory, and North Carolina State University during the last five years has led to a new and improved version of NESTLE written in modern Fortran and developed with modern software engineering practices. New features include a simplified input format, a drift-flux model for high slip two-phase thermal hydraulics, advanced depletion and isotope tracking using ORIGEN, output files compatible with VISIT visualization software, and compatibility with SCALE, SERPENT, and CASMO lattice physics. The new features have expanded NESTLE's versatility from large pressurized water reactors to new core models including boiling water reactors, small modular reactors, and fluoride salt cooled high temperature reactors. NESTLE has unique capabilities like advanced isotope tracking.

NESTLE is considered as an alternative to PHISICS.

4.4.3 MAMMOTH

MAMMOTH [11] is the reactor physics application for the MOOSE framework and combines the capabilities of the Rattlesnake solver (steady state and transient neutron transport), BISON (fuels performance) and RELAP-7 (thermal/hydraulics). MAMMOTH contains cross section interpolation and depletion capabilities required for cycle analysis with Rattlesnake, using temperature data provided by BISON. Individually, these packages provide little to no advantage over existing methods, but combined within MAMMOTH provide a powerful and tightly coupled multi-physics capability not available elsewhere. This provides the ability to better quantify multiple performance aspects of the core design concept under normal and off-normal conditions. MAMMOTH can prepare cross section libraries from DRAGON-5 and Serpent lattice physics calculations. In addition, MAMMOTH includes an SPH equivalence methodology, which enables the preservation of the lattice physics reaction rates and, thus, provide highly accurate calculations. MAMMOTH does not currently support pin power reconstruction but most of the LWR models in place are pin-cell models, which directly resolve accurate pin powers.

MAMMOTH is an advanced core design code still being developed at INL. Certain features required for LWR analysis such as core shuffling and fuel burnup calculations are not available yet and may be developed in FY-2016 and FY-2017.

4.4.4 VERA-CS

VERA-CS [12] includes coupled neutronics, thermal-hydraulics, and fuel temperature components with an isotopic depletion capability. The neutronics capability employed is based on MPACT, [13] a three-dimensional (3D) whole core transport code. The thermal-hydraulics and fuel temperature models are provided by the COBRA-TF (CTF) subchannel code. [15] The isotopic depletion is performed using the ORIGEN code system.

VERA-CS is developed by CASL, a DOE Energy Innovation Hub.

4.4.5 MPACT

MPACT [13] is a 3D whole core transport code that is capable of generating subpin level power distributions. This is accomplished by solving an integral form of the Boltzmann transport equation for the heterogeneous reactor problem in which the detailed geometrical configuration of fuel components, such as the pellet and cladding, are explicitly retained. The cross section data needed for the neutron transport calculation are obtained directly from a multigroup cross section library, which has traditionally been used by lattice physics codes to generate few-group homogenized cross sections for nodal core simulators. Hence, MPACT involves neither a priori homogenization nor group condensation for the full core spatial solution.

The integral transport solution is obtained using the method of characteristics (MOC), and employs discrete ray tracing within each fuel pin. MPACT provides a 3D MOC solution; however, for practical reactor applications, the direct application of MOC to 3D core configuration requires considerable amounts of memory and computing time associated with the large number of rays. Therefore, an alternative approximate 3D solution method is implemented in MPACT for practical full core calculations, based on a "2D/1D" method in which MOC solutions are performed for each radial plane and the axial solution is performed using a lower-order one-dimensional (1D) diffusion or SP3 approximation. The core is divided into several planes, each on the order of 5-10 cm thick, and the planar solution is obtained for each plane using 2D MOC. The axial solution is obtained for each pin, and the planar and axial problems are coupled through a transverse leakage. The use of a lower order 1D solution, which is most often the nodal expansion method (NEM) with the diffusion or P3 approximation, is justified by the fact that most heterogeneity in the core occurs in the radial direction rather than the axial direction. Alternatively, a full 3D MOC solution can be performed, if the computational resources are available.

The Coarse Mesh Finite Difference (CMFD) acceleration method, which was originally introduced to improve the efficiency of the nodal diffusion method, is used in MPACT for the acceleration of the whole core transport calculation. The basic mesh in the CMFD formulation is a pin cell, which is much coarser than the flat source regions defined for MOC calculations (typically there are on the order of fifty (50) flat source regions in each fuel pin). The concept of dynamic homogenization of group constants for the pin cell is the basis for the effectiveness of the CMFD formulation to accelerate whole core transport calculations. The intra-cell flux distribution determined from the MOC calculation is used to generate the homogenized cell constants, while the MOC cell surface-averaged currents are used to determine the radial nodal coupling coefficients. The equivalence formalism makes it possible to generate the same transport solution with CMFD as the one obtained with the MOC calculation. In addition to the acceleration aspect of the CMFD formulation, it provides the framework for the 3D calculation in which the global 3D neutron balance is performed through the use of the MOC generated cell constants, radial coupling coefficients, and the NEM generated axial coupling coefficients.

In the simulation of depletion, MPACT can call the ORIGEN code, which is included in the SCALE package. However, MPACT has its own internal depletion model, which is

based closely on ORIGEN, with a reduced isotope library and number of isotopes. The internal depletion model has been used for this study.

4.4.6 HELIOS-2

The software HELIOS-2 (Studsvik ScandPower) is known to be one of the most popular lattice codes [14]. Lattice codes are used to calculate the neutron flux distribution over a user-defined 2D region of the reactor. This region can range from a fraction of an assembly to the full core. The lattice geometry can be input with great detail, i.e. fuel pins including gaps and cladding, control rods, burnable absorbers, etc. can be modeled explicitly. The resulting 2D transport solution of the flux is usually used to generate cross section libraries for the use in subsequent 3D core calculations. These cross section libraries can be generated with the desired number of energy groups, as well as for different combination of reactor state variables (e.g. fuel temperature, moderator density, control rod insertion, burnup, etc.) in which the subsequent 3D core simulator can interpolate.

HELIOS-2 currently employs two different methodologies for the solution of the transport equation, the method of characteristics and the collision probability solver. Resonance self-shielding is calculated via the subgroup method, with a transport-based Dancoff calculation. The predictor-corrector method is used for depletion, and the depletion path allows arbitrary state changes, generalized decay capabilities, and branch-off calculations at any point in the solution path (in order to compute the flux solution for different combination of state variables). HELIOS-2 has been extensively validated against measured critical experiments, continuous-energy Monte Carlo calculations, and international isotopic benchmarks. It delivers exceptional accuracy for traditional, non-traditional, and experimental fuel designs.

HELIOS-2 is currently used to generate cross section libraries in LOTUS-B.

4.4.7 COBRA-TF

COBRA-TF (Coolant Boiling in Rod Arrays – Two Fluid) [15] is a transient subchannel code based on two-fluid formulation that separates the conservation equations of mass, energy, and momentum to three fields of vapor, continuous liquid, and entrained liquid droplets. The conservation equations for the three fields and for heat transfer from and within fuel rods are solved using a semi-implicit and finite-difference numerical scheme, using closure equations to account for inter-phase mass and heat transfer and drag, mechanical losses, inter-channel mixing, and fluid properties. The code is applicable to flow and heat transfer regimes beyond CHF, and is capable of calculating reverse flow, counter flow and crossflow with either three-dimensional (3D) Cartesian or subchannel coordinates for TH or heat transfer solutions. It allows for full 3D LWR core modeling and has been used extensively for LWR Loss-Of-Coolant Accident (LOCA) and non-LOCA analyses including the DNB analysis.

The COBRA-TF (CTF) code was originally developed by the Pacific Northwest Laboratory and has been updated over several decades by several organizations. CTF is being further improved as part of the VERA multi-physics software package, including:

- Improvements to user-friendliness of the code through creation of a PWR preprocessor utility.
- Code maintenance, including source version tracking, bug fixes, and transition to modern Fortran.
- Incorporation of an automated build and testing system using CMake/CTest/Tribits.
- Addition of new code outputs for better data accessibility and simulation visualization.
- Extensive source code optimizations and full parallelization of the code, enabling fast simulation of full core subchannel models.
- Improvements to closure models, including Thom boiling heat transfer model and Yao-Hochreiter-Leech grid-heat-transfer enhancement model, and Tong factor for the W-3 CHF correlation.
- Addition of consistent set of steam tables from IAPWS-97 standard.
- Application of extensive automated code regression test suite to prevent code regression during development activities.
- Code validation study with experimental data.

In a steady-state or transient CTF simulation, subchannel data, such as flow rate, temperature, enthalpy, and pressure and fuel rod temperatures are projected onto a user-specified or pre-processor generated mesh and written to files in a format suitable for visualization. The freely available Paraview software is used for visualizing three-dimensional data resulting from large full core models and calculations.

The steady-state analysis capability for VERA-CS is available. However VERA-CS is computationally prohibitive and requires HPCs with several thousand cores. Therefore, it will be adapted in LOTUS in FY-2017 as a benchmark tool to check the final designs obtained from the baseline tools.

4.4.8 FRAPCON/FRAPTRAN

FRAPCON [19] is a computer code that calculates the steady-state response of light-water reactor fuel rods. The code calculates the temperature, pressure, and deformation of a fuel rod as functions of time-dependent fuel rod power and coolant boundary conditions. The phenomena modeled by the code include: 1) heat conduction through the fuel and cladding to the coolant; 2) cladding elastic and plastic deformation; 3) fuel-cladding mechanical interaction; 4) fission gas release from the fuel and rod internal pressure; and 5) cladding oxidation. The code contains necessary material properties, water properties, and heat-transfer correlations. Other input parameters to the RELAP5 model required from FRAPCON include the gap closure and cladding roughness. The internal pressure is required from FRAPCON calculations in order for RELAP5 to perform clad ballooning and rupture calculations. The FRAPCON results are needed to initialize the fuel heat structure models as a part of calculating the steady-state solution that initializes the LOCA transient simulations.

The Fuel Rod Analysis Program Transient (FRAPTRAN) [20] is a FORTRAN language computer code that calculates the transient performance of light-water reactor fuel rods during reactor transients and hypothetical accidents such as loss-of-coolant accidents, anticipated transients without scram, and reactivity-initiated accidents. FRAPTRAN calculates the temperature and deformation history of a fuel rod as a function of time-dependent fuel rod power and coolant boundary conditions. Although FRAPTRAN can be used in “standalone” mode, it is often used in conjunction with, or with input from, other codes. The phenomena modeled by FRAPTRAN include a) heat conduction, b) heat transfer from cladding to coolant, c) elastic-plastic fuel and cladding deformation, d) cladding oxidation, e) fission gas release, and f) fuel rod gas pressure.

FRAPCON/FRAPTRAN are mature codes and are used in LOTUS-B for fuel performance simulations.

4.4.9 BISON

BISON [21] is a finite element-based nuclear fuel performance code applicable to a variety of fuel forms including light water reactor fuel rods, TRISO particle fuel, and metallic rod and plate fuel. It solves the fully-coupled equations of thermo-mechanics and species diffusion, for either 1D spherical, 2D axisymmetric or 3D geometries. Fuel models are included to describe temperature and burnup dependent thermal properties, fission product swelling, densification, thermal and irradiation creep, fracture, and fission gas production and release. Plasticity, irradiation growth, and thermal and irradiation creep models are implemented for clad materials. Models are also available to simulate gap heat transfer, mechanical contact, and the evolution of the gap/plenum pressure with plenum volume, gas temperature, and fission gas addition. BISON has been coupled to the mesoscale fuel performance code MARMOT, demonstrating fully-coupled multiscale fuel performance capability. BISON is based on the MOOSE framework and can therefore efficiently solve problems using standard workstations or very large high-performance computers. BISON is currently being validated against a wide variety of integral light water reactor fuel rod experiments.

BISON is an advanced fuel performance code being developed at INL and offers distinctive advantages over FRAPCON/FRAPTRAN such as 3D simulation capability, etc. However, for LWR LOCA analyses, certain models such as cladding hydrogen uptake, cladding oxidation, etc. are not yet fully developed. As those models become well developed, BISON will be incorporated into LOTUS starting in FY-2017.

4.4.10 RELAP5-3D

The RELAP5-3D [22] code has been developed for best-estimate transient simulation of light water reactor coolant systems during postulated accidents. Specific applications of the code have included simulations of transients in light water reactor (LWR) systems such as loss of coolant, anticipated transients without scram (ATWS), and operational transients such as loss of feedwater, loss of offsite power, station blackout, and turbine trip. RELAP5-3D, the latest in the series of RELAP5 codes, is a highly generic code that, in addition to calculating the behavior of a reactor coolant system during a

transient, can be used for simulation of a wide variety of hydraulic and thermal transients in both nuclear and nonnuclear systems involving mixtures of vapor, liquid, non-condensable gases, and nonvolatile solute.

RELAP5-3D is suitable for the analysis of all transients and postulated accidents in LWR systems, including both large- and small-break loss-of-coolant accidents (LOCAs) as well as the full range of operational and fusion reactor transient applications. Additional capabilities include space reactor simulations, gas cooled reactor applications, fast breeder reactor modeling, and cardiovascular blood flow simulations.

The RELAP5-3D code is based on a non-homogeneous and non-equilibrium model for the two-phase system that is solved by a fast, partially implicit numerical scheme to permit economical calculation of system transients. The objective of the RELAP5-3D development effort from the outset was to produce a code that included important first-order effects necessary for accurate prediction of system transients but that was sufficiently simple and cost effective so that parametric or sensitivity studies were possible.

The code includes many generic component models from which general systems can be simulated. The component models include pumps, valves, pipes, heat releasing or absorbing structures, reactor kinetics, electric heaters, jet pumps, turbines, compressors, separators, annuli, pressurizers, feedwater heaters, ECC mixers, accumulators, and control system components. In addition, special process models are included for effects such as form loss, flow at an abrupt area change, branching, choked flow, boron tracking, and non-condensable gas transport.

The system mathematical models are coupled into an efficient code structure. The code includes extensive input checking capability to help the user discover input errors and inconsistencies. Also included are free-format input, restart, renodalization, and variable output edit features. These user conveniences were developed in recognition that generally the major cost associated with the use of a system transient code is in the engineering labor and time involved in accumulating system data and developing system models, while the computer cost associated with generation of the final result is usually small.

RELAP5-3D is a mature code for LOCA analysis and is used in LOTUS-B.

4.4.11 RELAP-7

The RELAP-7 [23] (Reactor Excursion and Leak Analysis Program) code is the next generation nuclear reactor system safety analysis code being developed at Idaho National Laboratory (INL). The code is based on the INL's modern scientific software development framework MOOSE (Multi-Physics Object Oriented Simulation Environment). The overall design goal of RELAP-7 is to take advantage of the previous thirty years of advancements in computer architecture, software design, numerical integration methods, and physical models. The end result will be a reactor systems analysis capability that retains and improves upon RELAP5-3D's capability and extends the analysis capability for all reactor system simulation scenarios.

The RELAP-7 project, which began in Fiscal Year 2012, will become the main reactor systems simulation toolkit for LWRS (Light Water Reactor Sustainability) program's RISMIC (Risk Informed Safety Margin Characterization) effort and the next generation tool in the RELAP reactor safety/systems analysis application series. The key to the success of RELAP-7 is the simultaneous advancement of physical models, numerical methods, and software design while maintaining a solid user perspective. Physical models include both PDEs (Partial Differential Equations) and ODEs (Ordinary Differential Equations) and experimental based closure models. RELAP-7 will utilize well-posed governing equations for two-phase flow, which can be strictly verified in a modern verification and validation effort. Closure models used in RELAP5 and other newly developed models will be reviewed and selected to reflect the progress made during the past three decades and provide a basis for the closure relations that will be required in RELAP-7. RELAP-7 uses modern numerical methods, which allow implicit time integration, second-order schemes in both time and space, and strongly coupled multi-physics.

RELAP-7's analysis capabilities need further development to be able to be used to perform LOCA analysis. Based on the current development schedule for RELAP-7, it will be ready to be incorporated into LOTUS in FY-2018 to perform LOCA analysis.

4.4.12 RAVEN

RAVEN [24] is a software framework able to perform parametric and stochastic analysis based on the response of complex system codes. The initial development was aimed at providing dynamic risk analysis capabilities to the thermal-hydraulic code RELAP-7, currently under development at Idaho National Laboratory (INL). Although the initial goal has been fully accomplished, RAVEN is now a multi-purpose stochastic and uncertainty quantification platform, capable of communicating with any system code. In fact, the provided Application Programming Interfaces (APIs) allow RAVEN to interact with any code as long as all the parameters that need to be perturbed are accessible by input files or via python interfaces. RAVEN is capable of investigating system response and explore input space using various sampling schemes such as Monte Carlo, grid, or Latin hypercube. However, RAVEN's strength lies in its system feature discovery capabilities such as: constructing limit surfaces, separating regions of the input space leading to system failure, and using dynamic supervised learning techniques.

RAVEN is used to perform risk analysis for the baseline simulation tools as well as for the advanced simulation tools.

4.4.13 LWROPT

A new computer software for performing LWR (with the emphasis of PWR) in-core and out-of-core fuel cycle optimization for multiple cycles simultaneously may be developed within the LOTUS framework. The computer code is called LWROPT. Simulated annealing (SA) is used to optimize the new fuel inventory and loading pattern for each cycle considered. 3D core simulators such as PHISICS and NESTLE are used to perform loading pattern calculations in conjunction with simulated annealing. LWROPT

will have features including: 1) User controlled depletion schedule; 2) Spent fuel pool simulation which allows fuel assemblies to be reinserted into the reactor core; 3) Multi-cycle optimization capability; 4) User defined coastdown option; 5) Automated equilibrium cycle design; 6) Loading pattern design optimization using simulated annealing.

LWROPT can give utilities the power to perform their own fuel design analyses. These include: design of the core loading pattern and control rod pattern for future cycles, assess a fuel vendor proposed core design to confirm that it meets requirements or to achieve a more efficient design, perform fuel bid evaluations to compare fuel design proposals from multiple fuel vendors using the same point of reference, explore various fuel designs with respect to batch feed size (impact on cycle length, thermal margins), the ability to quickly explore a wide range of core designs that can lead to a better core design still meeting safety margins.

LWROPT does not yet exist. The development effort is envisioned according to the plan presented in the next section.

4.5 Core Design Automation

The modular approach for LOTUS will enable plant owners/vendors to further customize the LOTUS framework for use within their established codes and methods. One of the LOTUS modules deals with the core design automation (see Figure 23). The purpose of this module is to supply the LOCA analysis with initial conditions, i.e. assembly/pin power histories, power shapes, etc. to be employed by the Fuels/Clad Performance (FP) and System Analysis (SA) modules.

In the CD-A module, the plant owner/operator will characterize his core design with the tools he has. He will then integrate his tools/methods into the LOTUS framework for the downstream analysis. For the current LOTUS demonstration, the tools used are the already coupled codes PHISICS [6,9] and RELAP5-3D [22]. Cross section generation will be done using the Studsvik lattice code HELIOS-2 [14]. The coupling tools of the PHISICS/RELAP5-3D and HELIOS-2 code as well as the resulting possible calculation methodologies are described in the following sections.

4.5.1 Lattice Code Interface Tools for PHISICS/RELAP5-3D and HELIOS-2

The core simulation strategy employed to generate the data needed by the subsequent LOCA analysis is schematically shown in Figure 24. The first step of the strategy is to generate homogenized neutron cross sections. HELIOS-2 computes the cross sections for different geometrical conditions and different reactor states in the core. In this manner, a cross section library can be generated that captures effects like control rods, burnable poisons, etc. as well as different fuel temperatures, moderator densities, boron concentrations and burnup levels. The PHISICS reactor physics package coupled to the thermal-hydraulic system code RELAP5-3D is used in the second step, in order to compute 3D assembly power distributions, burnups, etc. needed as initial conditions for the subsequent LOCA analysis. Depending on the available data base to initiate the calculation,

(core and fuel geometry description, burnup maps, reloading pattern, power distributions, etc.), the PHISICS package can, in addition to solve the 3D core, also burn the core to the desired burnup level, shuffle and reload the core and search for critical control rod positions or boron concentrations.

The HELIOS-2, PHISICS/RELAP5-3D coupling shown in Figure 24 allows for different core calculation strategies. The two most common applications, the “core design” and the “On the fly cross section generation” are described here, but other computation schemes could be imagined.

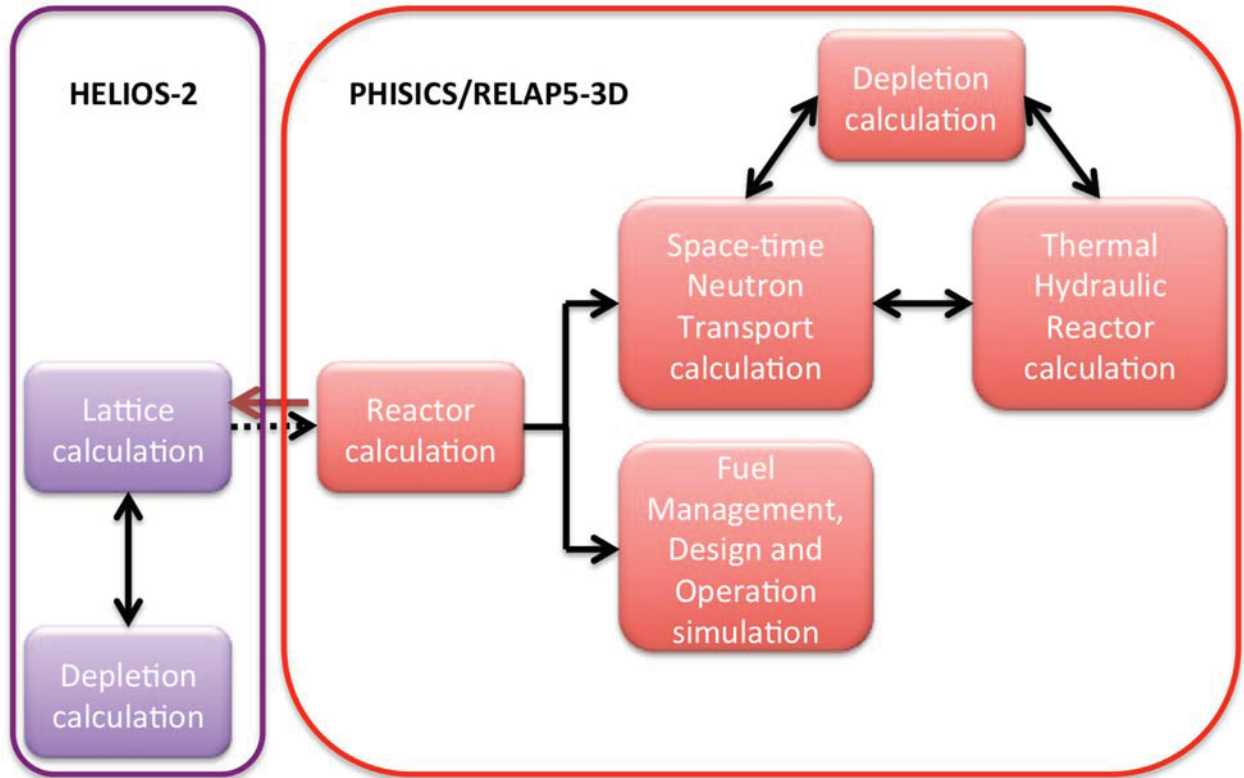


Figure 24. LOTUS Demonstration: Core Simulation Strategy.

Core design: Traditionally, the two above mentioned steps in the core analysis, i.e. cross section generation and 3D core calculation are performed independently. This means that cross sections for an a-priori known core design are calculated and then passed to the reactor calculation. During the reactor calculation studies, the cross section libraries are not changed anymore, because the geometry and fuel compositions normally do not change anymore. In the case of core design studies, where the core design is not known a-priori, cross section generation and core calculation need to be iterated, i.e. every time during the design process when the core/assembly geometry or fuel are changed, a new cross section library needs to be calculated. Figure 25 shows the schema of this core design process. As an example, assume that the core designer wants to find the fuel enrichment needed to obtain a certain cycle length. The cycle length is his design goal and the fuel enrichment is the parameter he can change in his core design. The designer has to iterate the schema in

Figure 25 until convergence, i.e. he will search for the fuel enrichment (leading to the desired cycle length) using a certain cross section library. Once he finds the fuel enrichment that gives him the desired cycle length, he will recompute the cross sections for this fuel enrichment and redo the core calculation. Using the new cross sections, he adjusts the enrichment again until he finds the desired cycle length. When the core calculations with the new computed cross sections and the cross section from the previous iteration lead to the same cycle length, the iteration process ends. The final cross section library including all dependencies like fuel temperature, moderator density, boron concentration, control rod insertion, burnup etc. can then be used in subsequent core analyses for the particular design.

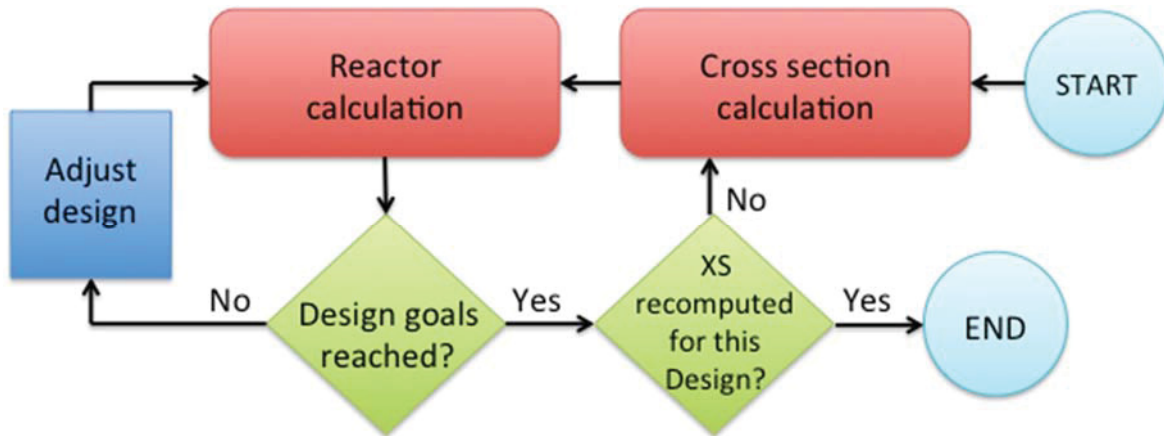


Figure 25. For Core Design: XS Generation and Core Calculation Iteration Scheme.

“On the fly” cross section generation: In the previous cross section generation strategy, the cross section library is pre-computed for different reactor states like fuel temperatures, moderator densities and burnups. PHISICS/RELAP5-3D will then look up and interpolate the cross sections depending on the state variables in each computational node. Instead of pre-computing cross section libraries tabulated for fuel temperature, moderator density, burnup etc, it is possible to compute the cross sections “on the fly”, i.e. when they are needed. Figure 26 shows this iteration scheme. Let us assume the user wants to compute a steady state core power distribution for a given reactor design, reactor power and burnup. He will compute the power distribution with his reactor tool using an initial guess for the cross sections. In addition, PHISICS/RELAP5-3D will provide the fuel temperature distributions and isotopic compositions for the burned materials. Once these or other user specified variables change more than a tolerance decided by the user, the cross sections are recomputed with the lattice code for that particular reactor state. The reactor calculation resumes and this scheme is repeated until convergence is reached for the desired reactor state. The same scheme can be applied to a transient calculation instead of a steady state search.

A suite of tools has been developed to assist the user to automatize the generation of cross sections to be used with PHISICS/RELAP5-3D as well as to pre- and post-process results. In order to automatically re-compute cross sections when needed according to the above mentioned schemes, for example after a fuel reloading simulated by PHISICS, a

generic interface for lattice codes has been developed for the PHISICS code package. The tools included in the interface are:

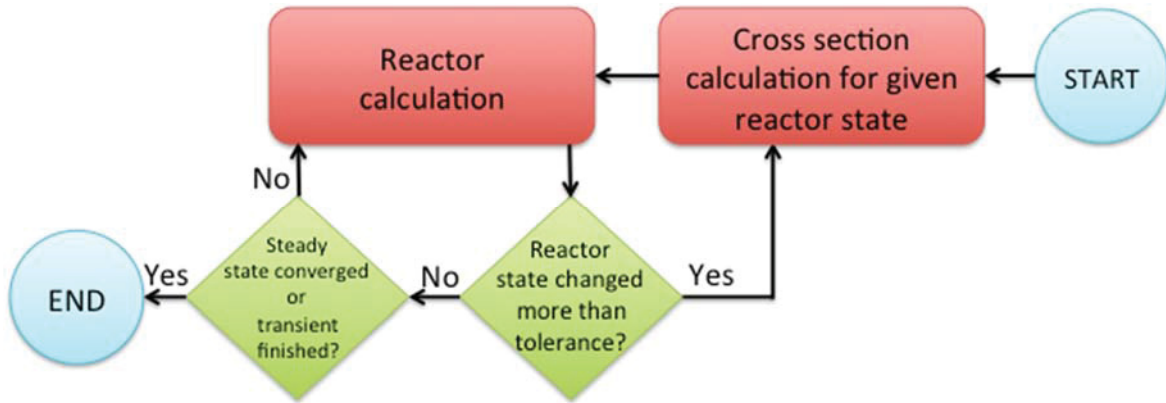


Figure 26. "On the Fly" Cross Section Generation Scheme.

- Material density feedback to the lattice code tool:* This tool provides to the lattice code material densities from the PHISICS/RELAP5-3D calculation at any point in the calculation when a cross section recalculation is desired, for example after the core has been shuffled. For each cross section library used by PHISICS/RELAP5-3D, the interface volume-averages the isotopic densities for the materials associated to this library in the core calculation. The interface reads a dedicated XML input file, in which the user establishes the connection between the cross section library (used by PHISICS) and the lattice code material identifiers. In addition, for each material, the user can specify which isotopes are going to be transferred into the lattice code input and which not. This allows simulating assembly reprocessing or cooling before the new cross sections are calculated. The user can also specify a scaling factor for each isotope to account for the homogenization of the materials in the core calculation. In addition, isotopes can be scaled proportionally to a set of other isotopes to account for stoichiometry. This is useful for example for oxygen with needs to be scaled for example according to the all the uranium isotopes. Figure 27 illustrates how the material density feedback tool works. The homogenized isotope densities from the PHISICS/RELAP5-3D core calculation are first read and averaged by the tool and then distributed (de-homogenized) into the detailed geometry used by the lattice code. Isotopes that are part of the fuel, cladding, etc. are distributed into the corresponding regions according to the scaling factors and stoichiometry specified by the user in the input file for the tool. One can see that the tool can cope with any level of accuracy the user would like to have. It is possible to associate only one cross section library to the whole core, in which case the densities passed by the tool will be the core average. It is also possible to associate a different cross section library to every node in the core calculation, in which case the actual isotopic densities without any averaging will be passed to the lattice code for each node. This would require that the lattice code input has one

material defined for each node in the reactor calculation. The tool has been developed with a modular design, i.e. the subroutines dealing with the core calculation and lattice code calculation are separated. This makes it easy to integrate other lattice or core solvers in the future.

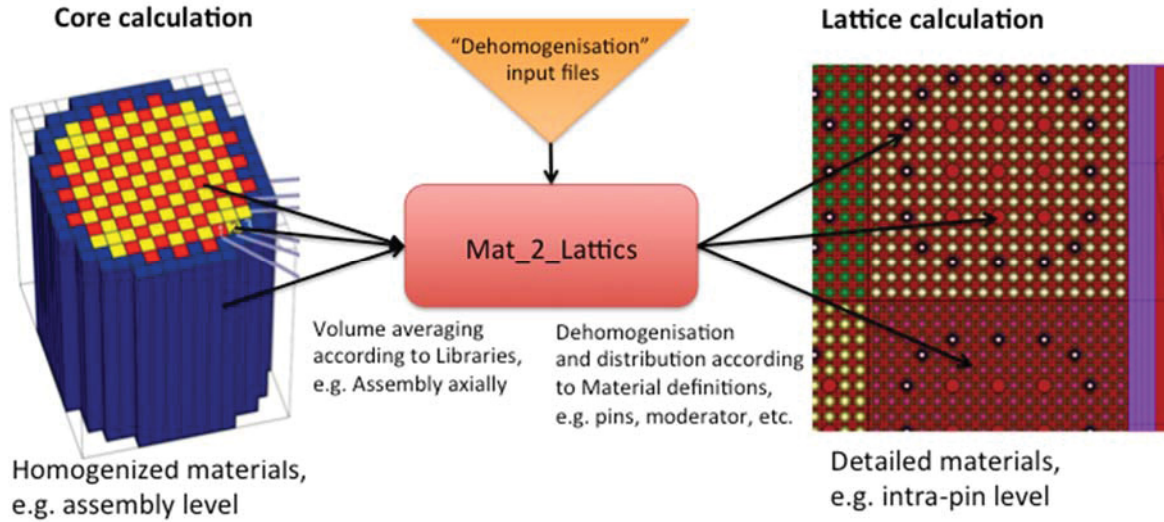


Figure 27. Material Density Feedback to the Lattice Code Tool Scheme.

- Library assembly tool:* The cross-section libraries generated by the lattice calculation might be needed to be post-processed before use with PHISICS/RELAP5-3D depending on the chosen calculation scheme. A library assembly tool has been developed that combines the generated cross section libraries according to user specifications. The tool also updates the library definition input file for PHISICS (lib.xml), accordingly. An example use of the library assembly tool is illustrated in Figure 28. Let's assume that the lattice code generates a library for a fresh assembly, a once burned assembly and a twice-burned assembly as a function of burnup. For the lattice calculation, these 3 libraries all start from zero burnup, since the lattice code does not know to which burnup level the provided initial compositions for once and twice burned assemblies correspond. For the PHISICS calculation on the other hand, these 3 libraries are only one library for the whole lifecycle of one assembly through the three cycles. The tool combines the 3 separate libraries into one and adjusts (shifts) the burnup tabulation values for the once and twice burned assemblies according to the burnup values from the source where the material compositions have been taken to run the lattice calculation that generated the 3 separate libraries. The library assembly input file specifies how the libraries have to be combined. It could for example contain the shuffling scheme of the core.

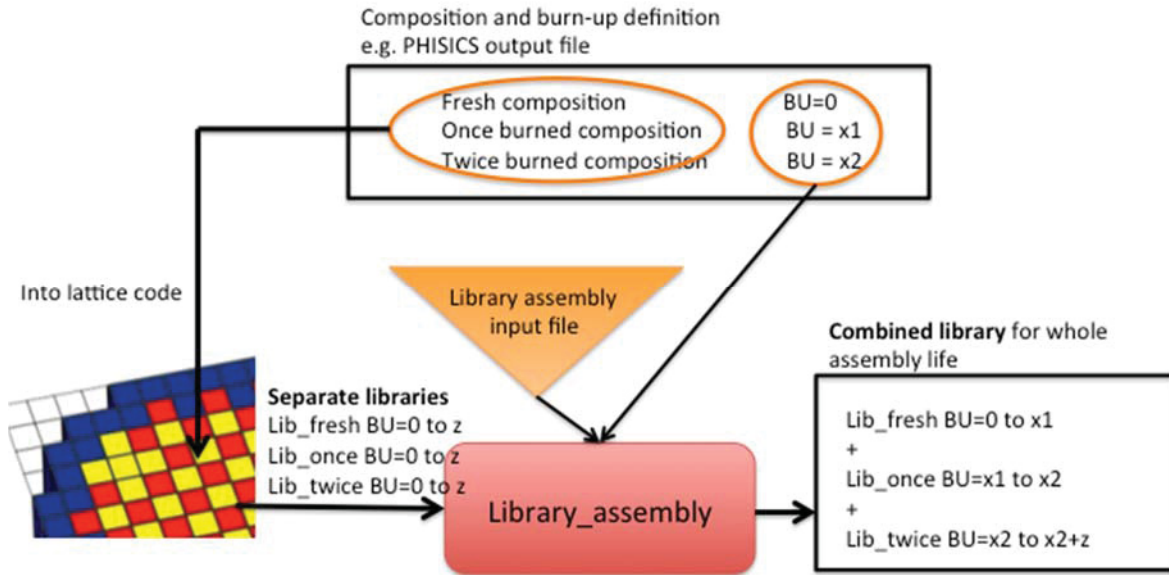


Figure 28. Library Assembly Tool Scheme.

- SPH tool*: After a new set of cross section libraries has been calculated, consistency between the lattice code and PHISICS calculation should be established. Since the PHISICS code does not support discontinuity factors yet, the super-homogenization method (SPH) has been implemented. The SPH method compares reaction rates from the lattice calculation and the PHISICS calculation for different core states and adjusts the cross section libraries, so that the PHISICS calculation matches the lattice calculation. The iteration scheme is shown in Figure 29. Once cross sections have been generated with the lattice code, a PHISICS input has to be developed that represents the same 2D geometry used in the lattice code, but the materials are homogenized. Reaction rates from the PHISICS and the lattice calculation are then compared and correction factors computed. These correction factors are then applied to the cross section library. The 2D PHISICS calculation is then repeated with the corrected cross section library and the resulting reaction rates are again compared to the reaction rates computed by the lattice code. This procedure is repeated until convergence is reached, i.e. the computed correction factors do not change anymore between iterations. The so corrected cross section library can then be used in the subsequent 3D core calculations. At the moment, isotropic rates are compared and isotropic (s0) correction factors are produced. To further improve this method, it is foreseen to include the first order anisotropic (p1) correction factors as well in the future.

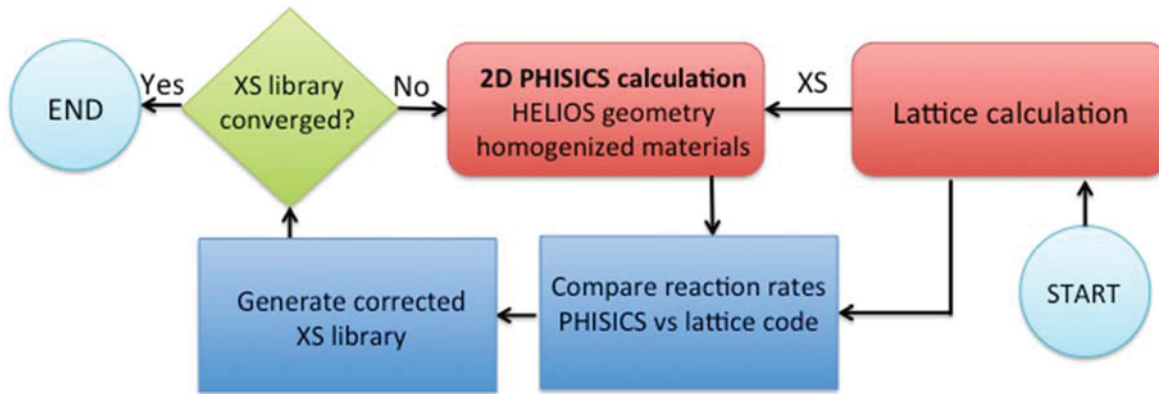


Figure 29. SPH Iteration Scheme.

- *Pin power reconstruction tool:* This tool collects pin power distributions from the lattice calculation. These can then be used to reconstruct pin powers in the 3D PHISICS core calculation results. The tool simply multiplies the assembly-averaged power from the PHISICS calculation with the pin power distribution from the lattice code. The pin power distributions from the lattice code are burnup dependent. The tool can interpolate these distributions to the burnup level of each assembly at any time during the cycle, for example at BOC or EOC.

The interface for the PHISICS/RELAP5-3D side is fixed and part of the PHISICS package. The lattice code side of the interface (subroutines to read/write material compositions, etc.) has to be implemented for each lattice code individually, since the input file structure is different for each code. As already mentioned, HELIOS-2 has been used for the LOTUS demonstration. Consequently, a PHISICS/RELAP5-3D interface for HELIOS-2 has been developed.

4.5.2 Equilibrium Cycle Strategy

In order to demonstrate the LOTUS tool methodology, two generic PWR design options based on the BEAVRS geometry have been realized. The equilibrium cycles for these generic PWRs have been analyzed. The calculations to provide initial data for the LOCA analysis are done with the above-described PHISICS/RELAP5/HELIOS-2 code, including cross section generation. Figure 30 shows the A11 core design strategy. HELIOS-2 and PHISICS inputs for the two design options have been created. Cross sections for the both initial guess configurations have been computed. At least 8 cycles have then been computed until the equilibrium cycle is reached. The equilibrium cycles have then been analyzed for both options in terms of desired cycle length, maximum assembly burnup as well as radial and axial power distributions. The designs have then been adjusted to meet the design goals and the equilibrium cycle has been recomputed for both core design options. Once the design goals have been reached, cross sections have been recomputed with HELIOS-2 for the new designs. The equilibrium cycles have then been recomputed with the new cross sections and have been reanalyzed. Since the equilibrium cycle characteristics may have changed due to the updated cross sections,

further optimization and changes in the core design may have become necessary. These “inner” (change core design and recomputed equilibrium cycle) and “outer” (recomputed cross sections) loops as shown in Figure 30 have been repeated until convergence has been reached for both core design options.

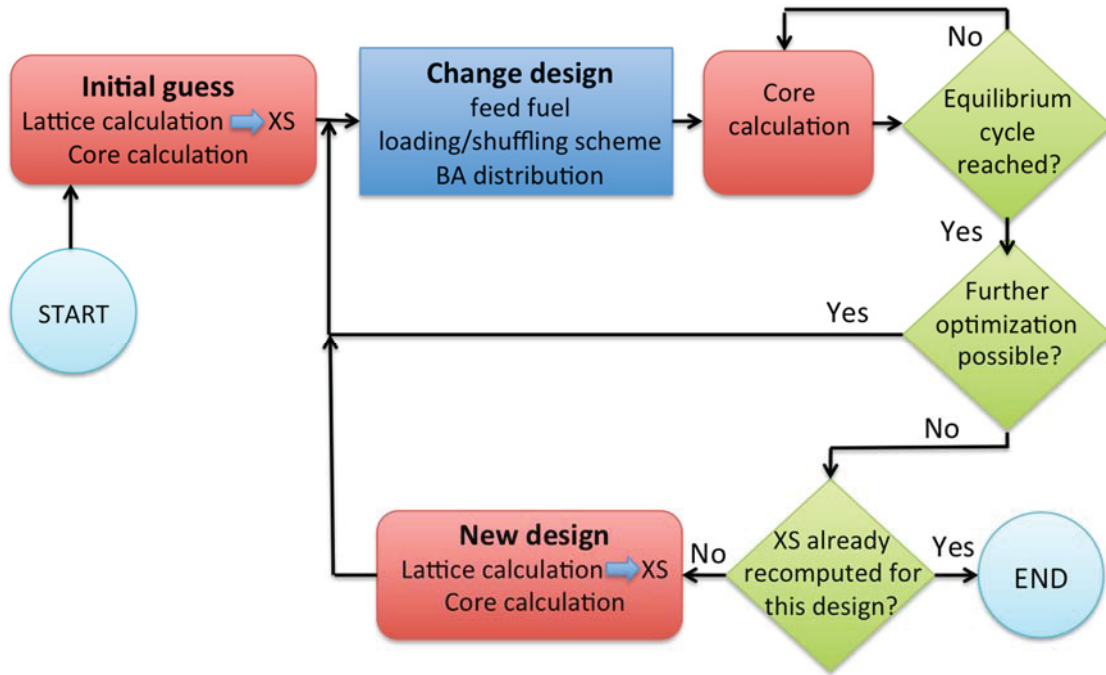


Figure 30. IA1 Demonstration of a PWR Design Strategy.

4.5.3 Cross Section Library Calculations

As mentioned, for the calculation of the homogenized cross sections, the lattice code HELIOS-2 has been used. In order to identify the number of cross sections sets needed to employ in this calculation, the “proximity” approach has been employed: even if the number of compositions are limited, an assembly is considered different with respect to another when the neighboring ones are different (e.g. different composition, structural material, instrumentation tube locations, etc.). This approach led to the identification of 29 different cross sections sets for the fuel region and one for the radial reflector, composed by the baffle, water between the baffle and the barrel, the barrel and the thermal shield. A detailed 2D representation of 1/8 of the core has been modeled with HELIOS-2 for both core options. Figure 31 shows the full HELIOS-2 model (including a zoom on one assembly) and Figure 32 left) shows the locations of the different cross section libraries produced.

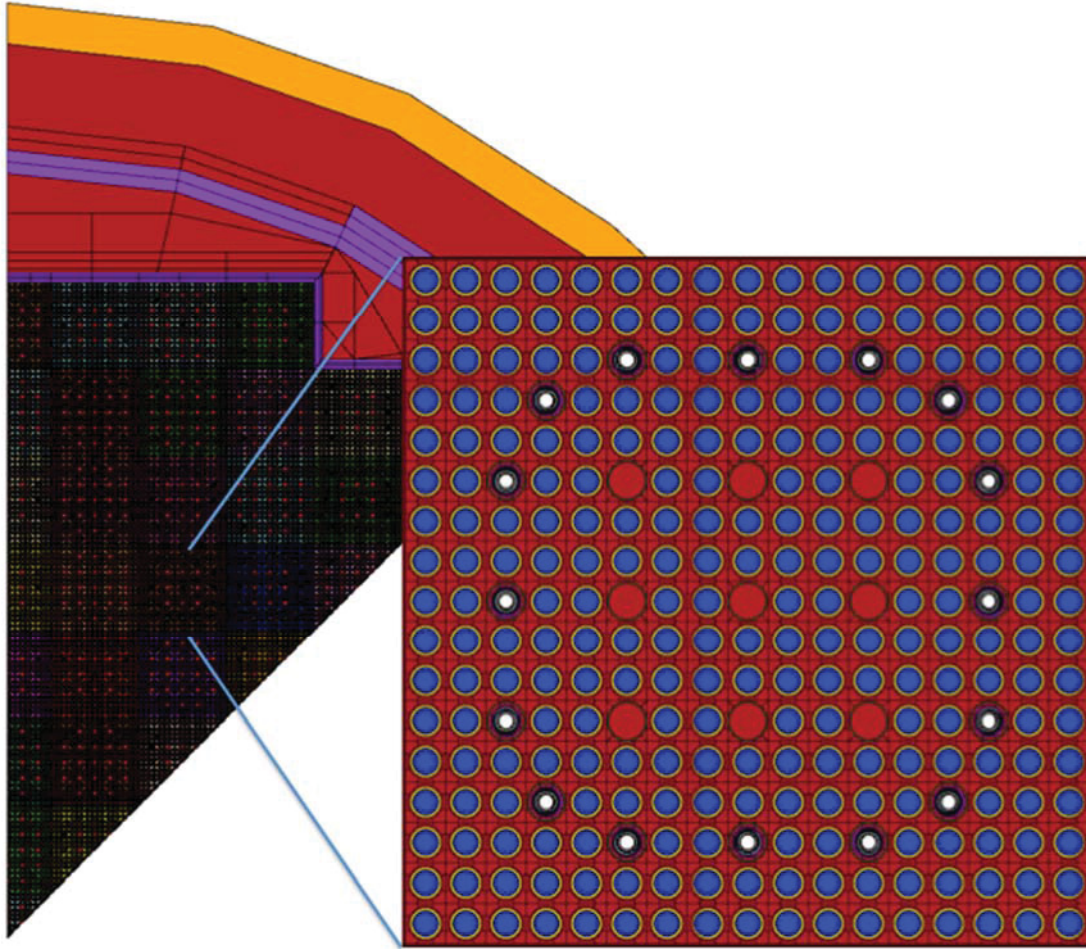


Figure 31. HELIOS-2 Model for an IA1 PWR Demonstration (An Assembly for Option 1 with WABA Pins Is Shown).

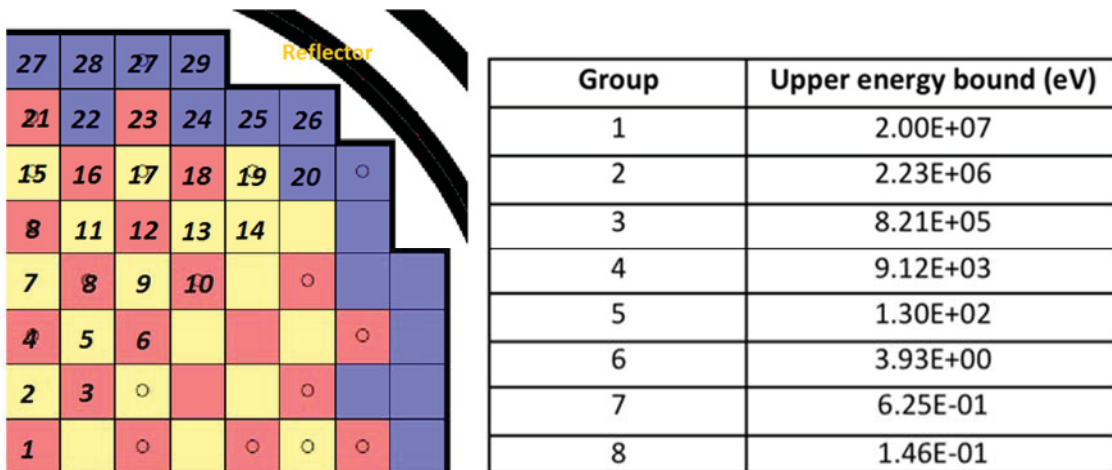


Figure 32. Left) Cross Section Library Locations Generated with HELIOS-2, Right) 8 Group Energy Structure Generated with HELIOS-2.

The lattice calculations are generally started from pre-collapsed multi-group neutron energy structures. For the computation of the different cross sections sets, lattice calculations have been performed starting from a 44-energy group structure, then collapsed into an 8-group structure in the homogenization procedure. In Figure 32 right) the collapsed energy structure is reported.

The reactor calculation involves the simulation of the reactor during several operational cycles and during transient/maneuver events. In order to exchange feedback between the core design tools (PHISICS) and the thermal-hydraulic code (RELAP5-3D), the microscopic cross sections sets for all isotopes except the moderator are tabulated with respect to several field parameters for each library. The cross section for the moderator regions have been tabulated as macroscopic cross sections. This allows us to treat the boron that is in solution in the moderator (this is a tabulation dimension) and the boron in the burnable absorbers (tabulated microscopic cross sections) separately. The following parameters and tabulation points have been computed for both core design options:

• Boron concentration in H2O (ppm):	0.0	1000	1900	
• Moderator density (kg/m ³):	640.8	833.0	945.2	1000
• Fuel temperature (K):	573.2	1073.2	1273.2	
• Burnup (GWd/tHM):	0.0	0.152	15	25

The tabulation dimensions lead to the construction of a complete N-Dimensional (4-Dimensional in this case) grid that is characterized by 108 tabulation points in total. It should be mentioned here, that the burnup points are for each cycle since cross section libraries are computed for fresh, once burned and twice burned assemblies. These libraries are then assembled as explained for the *Library assembly tool* above. The actual maximum burnup in the combined libraries for one assembly is then the burnup at for a twice-burned assembly at the beginning of cycle plus 25 GWd/tHM.

The SPH method is then applied for all 64 generated cross section libraries as explained in the SPH tool section above. Finally, as mentioned, the *library assembly tool* according to the shuffling scheme then assembles the libraries. The result is one library for each fresh fuel assembly that contains the burnup points for all the three cycles this assembly will go through.

4.5.4 Coupled PHISICS/RELAP5-3D Calculation

In order to assess the compliance of the existing power plants to the proposed rule, the LOCA accident scenario needs to be initiated from equilibrium cycle conditions. Hence, the reactor evolution needs to be followed for several operational cycles, until reaching the reference equilibrium cycle (see Figure 30). From a loading point of view, the equilibrium cycle can be considered as the cycle from which the fuel-reloading pattern is almost constant (i.e. same composition and spatial loading of the fuel batches). The equilibrium cycle might be “reached” after several reloads. In this study, we assume that the equilibrium cycle is reached after the 8th reload.

The PHISICS code is coupled with the thermal-hydraulic code RELAP5-3D. For the search of the equilibrium cycle, the thermal-hydraulic model of the reactor has been set-up considering the reactor core only (without a primary or a secondary system). The approach to consider only the core region without the primary system can be taken for base irradiation calculations (like the search for the equilibrium cycle for a given core configuration), since the system does not influence the core during normal operation. For this reason, the primary system is modeled only considering the upper and lower plenum of the core. In order to be as accurate as possible for the determination of the initial conditions for the subsequent LOCA analysis, the core is modeled using one core channel per fuel assembly (193 in total). The radial reflector is modeled as a bypass channel (6% of the mass flow). Figure 33 shows the RELAP5-3D nodalization used in the core design automation studies. It should be noted that this RELAP5-3D model is different than the one used in the subsequent LOCA analysis.

The PHISICS calculation of this coupled calculation is set-up as the full core, i.e. all the 193 assemblies are modeled explicitly. The materials are assembly homogenized. One ring of assemblies containing a water/steel mixture has been placed around the active core to represent the reflector. The 3D PHISICS calculation uses 18 axial layers. The cross section libraries are associated to the assemblies as shown in Figure 32 left).

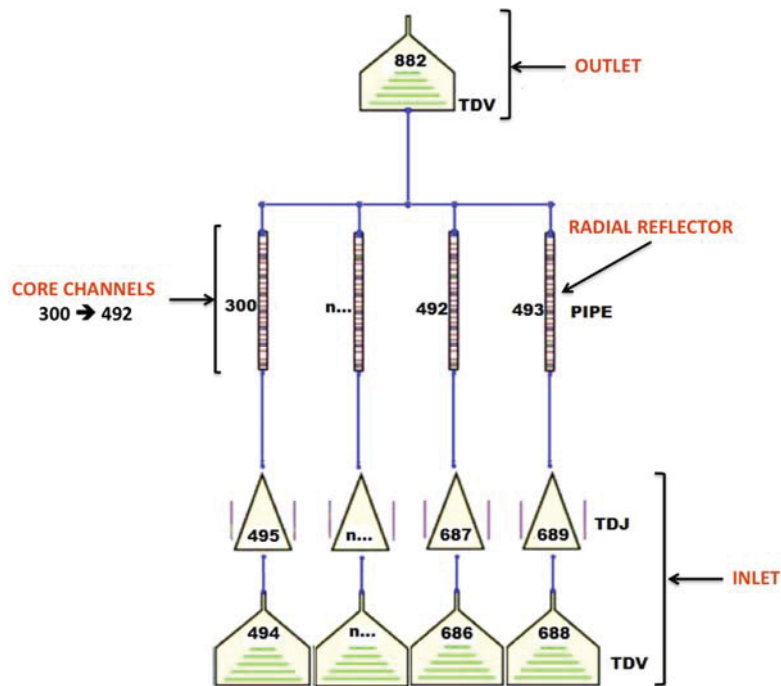


Figure 33. RELAP5-3D Core Nodalisation Used for the Core Simulation.

4.5.5 Transient Power Maneuvers

As it is well known, the core status at BOC, MOC and EOC does not impose challenging conditions for the LOCA analysis. Therefore, the LOCA scenarios for the assessment of the safety margins are generally performed considering the reactor right after

a maneuver, for example a xenon transient. The goal is to skew the axial power shapes in order to get bottom peaked, cosine and top peaked power shapes. It might be needed to run different maneuvers to obtain all three different power shapes. For the scope of this work, one load-following maneuver has been considered. The power history is shown in Figure 34. At the end of the maneuver, the LOCA analysis is initiated, having as boundary conditions the current status of the plant (burnup, power shape, etc.).

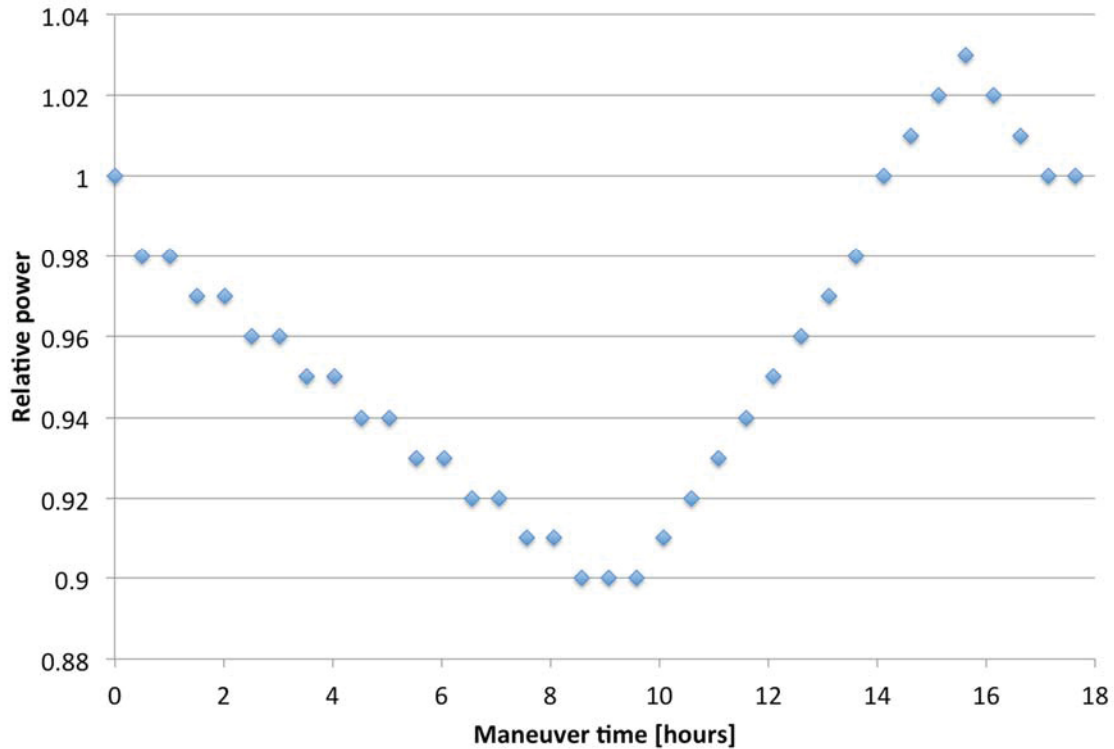


Figure 34. Load Following Maneuver Power History.

For this type of maneuver the power history is an input of the simulation, hence the reactivity insertion due to the cooling down of the reactor when the power decreases (due to the Doppler effect), is automatically compensated by PHISICS, determining through its Criticality Search module the critical insertion of the control rods. Figure 35 shows the control rod banks. Four banks being considered. The different banks get inserted in the sequence shown in Figure 35. For example, the first bank is inserted until half of its length, then bank one and two are inserted simultaneously until bank one is fully inserted and bank two is half inserted. At this point, bank 3 starts getting inserted, and so on. This control rod pattern is used for both core design options.

Since the maneuver can happen at any time during the equilibrium cycle and the LOCA accident can happen any time during the maneuver, these two variables can be treated stochastically. The RAVEN code has been used to sample different maneuver start times during the equilibrium cycle as well as different LOCA start times during the maneuver (see Figure 36). RAVEN runs then RELAP5 in “multi-deck” mode, i.e. it runs

the equilibrium cycle base irradiation to the desired time and then starts the maneuver transient in one run.

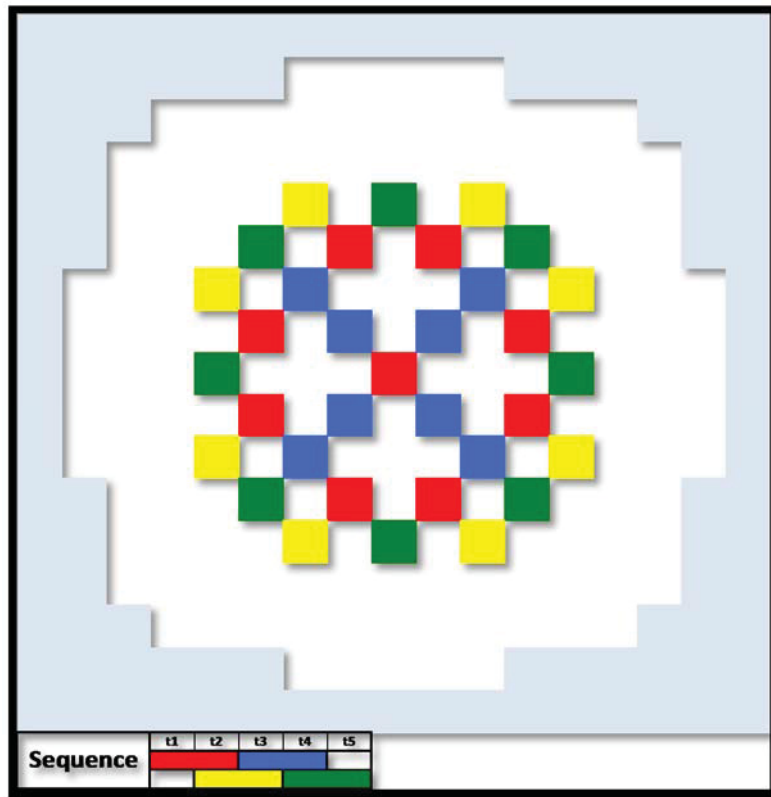


Figure 35. Control Rod Positions and Insertion Sequence.

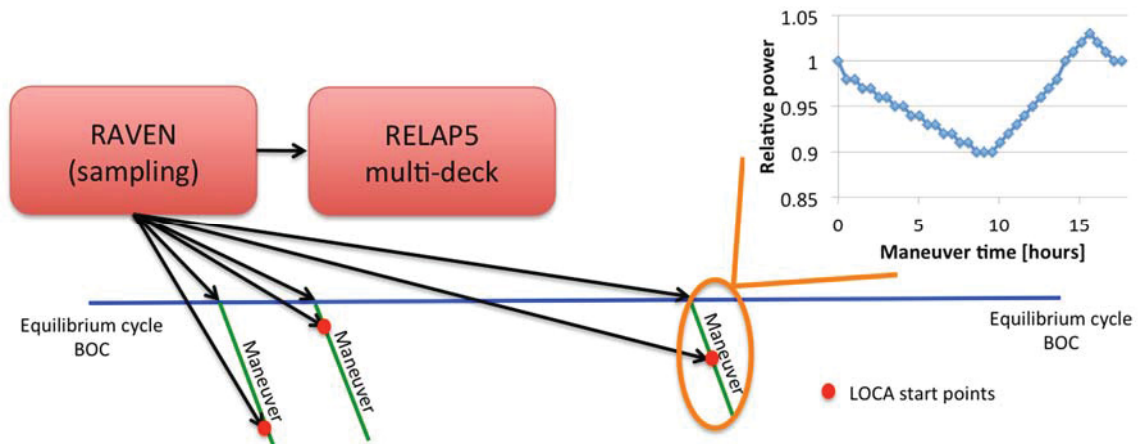


Figure 36. RAVEN Samples the LOCA Start Times and Runs RELAP5 in Multi-Deck Mode.

4.6 Fuels Performance

Fuel rod design information is necessary for reactor core design, fuel performance, and reactor system analysis codes as input parameters. To ensure data consistency, a common set of fuel rod design input data should be shared among all the codes. Table 2 shows several common fuel rod design input data needed for different codes. Note that these fuel rod data may vary with time and have to be updated under different conditions.

For baseline calculation purpose, we choose FRAPCON code for our fuel performance steady state calculations. Power history and axial power profile from the output of core design codes such as PHISICS are required as FRAPCON inputs. The linear heat generation rate (kW/m) at each time step of FRAPCON simulation should also be provided.

Table 2. Common Data from Fuel Rod Design for Different Physics in LOCA Analysis.

Fuel Rod Data	Fuel Performance	Core Design	System Code
Rod geometry information such as cladding outer diameter, cladding thickness, fabricated gap, active fuel length, and plenum length	☑	☑	☑
Spring dimensions such as outer diameter of plenum spring, diameter of the plenum spring wire, and number of turns in the plenum spring	☑	☑	☐
Pellet shape such as height (length) of each pellet, height (depth) of pellet dish, pellet end-dish shoulder width, Chamfer height and width	☑	☐	☐
Pellet isotopics such as fuel pellet U-235 enrichment, oxygen-to-metal atomic ratio, weight fraction of gadolinia in urania-gadolinia fuel pellets, Boron-10 enrichment in ZrB ₂ , parts per million by weight of moisture in the as-fabricated pellets, and parts per million by weight of nitrogen in the as-fabricated pellets	☑	☑	☐
Pellet fabrication such as as-fabricated apparent fuel density, open porosity fraction for pellets, the fuel pellet surface arithmetic mean roughness, etc.	☑	☑	☑
Cladding fabrication such as cladding type, the cladding surface arithmetic mean roughness, as-fabricated hydrogen in cladding, etc.	☑	☑	☑
Rod fill conditions such as initial fill gas pressure, Initial fill gas type and their mole fractions	☑	☑	☑
Fuel assembly geometry such as pitch	☑	☑	☑

System code RELAP5-3D already has some simple fuel performance models such as the rupture model and ballooning model, but it could not provide detailed analysis of fuel rods' behaviors such as the fission gas released, rod internal pressure, and fuel-cladding mechanical interaction, etc., which requires the simulation from fuel performance codes.

The most important issue when coupling the system code and fuel performance code is to make sure that the stored energy in the fuel pin for the RELAP5 steady state result equals to the stored energy calculated by the fuel performance code. The stored energy in the fuel rod is calculated by summing the energy of each pellet ring calculated at the ring temperature. The expression for stored energy is

$$E_s = \frac{\sum_{i=1}^I m_i \int_{298K}^{T_i} c_p(T) dT}{m} \quad (1)$$

where m_i is mass of ring segment i , T_i is temperature of ring segment i , $C_p(T)$ is specific heat evaluated at temperature T , m is total mass of the axial node, I is the number of annular rings. The stored energy is calculated for each axial node.

The fuel performance codes were developed only for single fuel rod calculations so that they are not capable of capturing the detailed TH conditions due to the impact from neighboring fuel rods and assemblies. System codes have best-estimate two phase flow and heat transfer models which can provide local steady state TH data at different depletion cycle points as input for FRAPCON simulations. By using axial dependent cladding surface temperature and coolant pressure for each fuel rod of interest, more accurate results can be obtained from fuel performance codes. In the meantime, part of the outputs from FRAPCON simulations are used to prepare for the steady state run of a system LOCA model, ensuring correct stored energy and initial conditions for the transient fuel performance models.

4.7 Systems Analysis

System analysis normally starts with building a plant model with a reactor system analysis code. As an example, a typical four-loop pressurized water reactor (PWR) with 3411 MW rated thermal power has been selected for analysis with RELAP5-3D. The accident scenario selected is a LB-LOCA with a double-ended guillotine break in a cold leg. The nodalization diagram of the RELAP5-3D model for the typical PWR is shown in Figure 12. The safety criteria are the generic acceptance criteria for the peak clad temperature and the maximum oxidation rate (as shown in Figure 1) proposed in the rulemaking. Since both PCT and ECR limits are burnup-dependent, this added complexity requires defining new safety metrics that would synthesize PCT and ECR with fuel rod dependent cladding pre-transient hydrogen content. The safety metrics are defined as the ratios of the calculated PCT over PCT limits for each fuel rod, as well as the ratios of the calculated ECR over ECR limits for each fuel rod and are expressed in the following:

$$PCTR = \frac{PCT^{Calculated}}{PCT^{Limit}} \quad (2)$$

$$ECRR = \frac{ECR^{Calculated}}{ECR^{Limit}} \quad (3)$$

If we define PCTRmax and ECRRmax as the maximum value of PCTR and the maximum value of ECRR, respectively, the acceptance criteria for the safety metrics are the following:

$$1) PCTR_{max} < 1.0$$

or

$$2) ECRR_{max} < 1.0$$

Using the above criteria, the limiting fuel rods can be identified as the fuel rods with PCTRmax or the ECRRmax.

The reactor core modeling in RELAP5-3D used different homogenization approaches for thermal fluid dynamics calculations than for the heat conduction and clad oxidation calculations in the fuel rods. A multiple channel approach was used for the thermal fluid dynamics calculation, as illustrated in Figure 37. Specifically, the assemblies in the core were grouped into various regions based on their burnup history. The assemblies with fresh fuel, once burned fuel and twice burned fuel were grouped together respectively. Two flow channels – one average channel and one hot channel – were built to represent each group of assemblies. Hence there are a total of six flow channels in this study. The flow channels are connected in the lateral direction to allow crossflow to be calculated. Crossflow is modeled at each axial elevation in the core between the three average core channels. It is also modeled at each axial elevation between the hot channels and the adjacent average channels. This allows flow to be redistributed around a blockage caused by cladding ballooning or rupture. The crossflow area is based on the minimum gap between the fuel rods along one side of a fuel assembly and the number of fuel assembly sides at the interface between the three average core channels; for example, for the hot assembly in each region, there are four sides at the interface. Loss coefficients are approximated based on flow across in-line and staggered rows of tubes, with the average distance of travel estimated to be about half an assembly width.

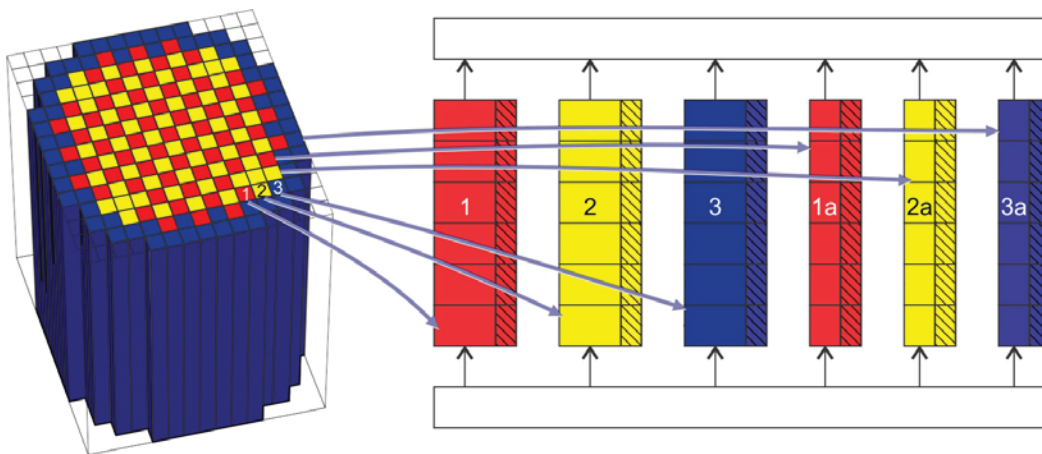


Figure 37. Schematic Illustration of the Mapping between the Core Design Analysis and the RELAP5-3D Analysis Core Model for a typical Four-Loop PWR.

For heat conduction and clad oxidation calculations, it is computationally prohibitive to consider all the fuel rods in the reactor core. Instead a homogenization technique is used to reduce the number of fuel rods to be simulated. Two sets of heat structures were used for each assembly – one set represents the highest power rod or the hot rod in the assembly and the other set represents the average of the remaining fuel rods in the assembly. This is

a reasonable approximation given that the fuel rod burnup normally does not vary too much within a PWR assembly and the hot rod in an assembly would be the limiting rod for that assembly.

As a result, heat structures for the highest power assembly (hot assembly) and its hot rod in each group of assemblies were built and attached to the hot channel, as shown schematically in Figure 38 such that the PCT and ECR in the average rods and hot rod can be calculated. Analogously, the heat structures for the other assemblies and their respective hot rods were built and connected to the average channel, as shown in Figure 39, such that the PCT and ECR can be calculated for the average rods and hot rod in each assembly. Therefore, there are a total of 386 sets of heat structures for the fuel in this study (193 for assemblies plus 193 for hot rods). It is noted that the hot rod power has been subtracted from each assembly to yield the correct power for the average fuel rods in each assembly such that the reactor total power is conserved.

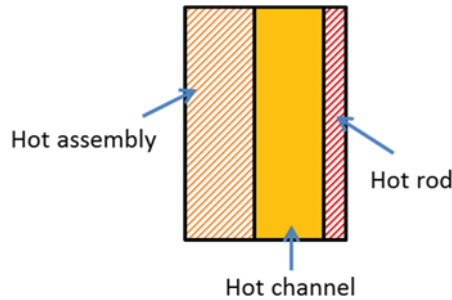


Figure 38. Schematic Illustration of the Heat Structure Mapping for the Hot Assembly and Its Hot Rod with the Hot Channel (One for Each Group of Assemblies).

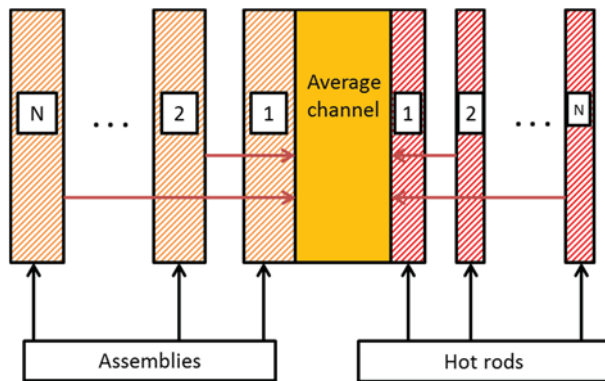


Figure 39. Schematic Illustration of the Heat Structure Mapping for Average Assemblies and their Respective Hot Rods with the Average Flow Channel.

In order to perform BEPU analysis, the important phenomena affecting the progression of the LB-LOCA accident are first determined by the phenomena identification and ranking table (PIRT) process. A large number of studies have been done previously to identify the important phenomena. A PIRT analysis has been conducted in this work with

input from FPoliSolutions LLC. For demonstration purposes, a reduced set of parameters with high importance to LB-LOCA has been selected and is shown in Table 3.

Table 3. Distribution of Parameter Uncertainties.

Parameter	PDF type	Min	Max	Comments
Reactor thermal power	Normal	0.98	1.02	Multiplier
Reactor decay heat power multiplier	Normal	0.94	1.06	Multiplier
Accumulator pressure	Normal	-0.9	1.1	Multiplier
Accumulator liquid volume (m ³)	Uniform	-0.23	0.23	Additive
Accumulator temperature (K)	Uniform	-11.1	16.7	Additive
Subcooled multiplier for critical flow	Uniform	0.8	1.2	Multiplier
Two-phase multiplier for critical flow	Uniform	0.8	1.2	Multiplier
Superheated vapor multiplier for critical flow	Uniform	0.8	1.2	Multiplier
Fuel thermal conductivity	Normal	0.93	1.07	Multiplier
Average core coolant temperature (K)	Normal	-3.3	3.3	Additive
Film boiling heat transfer coefficient	Uniform	0.7	1.3	Multiplier

The uncertainty quantification of the LB-LOCA analysis is carried using the Monte Carlo approach to determine the 95/95 upper tolerance limits.

Since a LOCA event is equal-probable in time, the time in a cycle is an additional random variable whose uncertainty is propagated through the analysis in a typical LB-LOCA analysis conducted in the current practice. Including the time in a cycle as a random variable would require LOCA calculations to be carried out on a very large number of exposure points, which is not practical. As a result, in our demonstration calculations we selected a few specific exposure points in a cycle and then propagated all the uncertainties for each exposure point.

The exposure points selected for the LB-LOCA calculations cover the entire range of the cycle length. The selected exposure points are at the beginning of cycle (BOC), 100 days, 200 days, 300 days, 400 days, 500 days and end of cycle (EOC). This way, the dynamic response of the plant with regards to LB-LOCA transients would be fully characterized at different core conditions during the entire cycle.

A set of 1000 RELAP5-3D input files has been prepared respectively at each of the seven selected exposure points by randomly perturbing the input parameters using their associated probability density functions defined in Table 3. All the RELAP5-3D cases were run to steady state first. Large break LOCA cases were then initiated by assuming a double-ended guillotine break. Following the initiation of the LB-LOCA, a fast depressurization of the primary system ensues. The ECCS is activated to provide emergency cooling water to the core. The entire process lasts about 10 minutes. To be conservative, in our RELAP5-3D plant model simulations, the shutdown of the reactor following the initiation of LB-LOCA is achieved through the negative reactivity feedback, rather than through the scram of the reactor. In our LB-LOCA runs, it is assumed that only two out of the three ECCS systems in the intact loops are functioning and able to inject water into the reactor core.

However, as passive components, it is assumed that all three accumulators in the intact loops are functioning and able to inject water into the reactor core.

The LOTUS toolkit automatically samples each uncertain parameter shown in Table 3 from its distribution. For a uniform distribution, the minimum and maximum values are the boundaries of the sampling. For a normal distribution, the sampling boundaries were truncated at the minimum and maximum values, which is effectively a truncated normal distribution. No dependencies between parameters were considered in the sampling. The LOTUS toolkit then modifies the RELAP5-3D input files according to the perturbed values. It automatically drives the desired number of RELAP5-3D runs on Idaho National Laboratory's high performance computers (HPC). The toolkit also performs the postprocessing of the RELAP5-3D output files and presents the PCTRmax and ECRRmax values according to the Monte Carlo approach.

4.8 Risk Assessment

In this section the uncertainty propagation and risk assessment techniques employed by LOTUS to compare statistical plant operation with regulatory limits are considered. The uncertainty propagation and risk assessment are performed using RAVEN. The algorithms for uncertainty propagation and limit surface search algorithms are addressed first, leading to the beneficial introduction of reduced-order models and surrogate models. Additionally, input space reduction through sensitivity screening is introduced.

4.8.1 Uncertainty Propagation

Traditional approaches to NPP operation analysis and safety margin involve strong conservatism and sometimes unphysical assumptions. BEPU seeks to refine that analysis to return margin to the operator and better characterize plant operation. Key to the BEPU approach in margin characterization is propagation of input uncertainties to statistics of the figures of merit. Traditional approaches to quantifying uncertainty for NPP include the Wilks method and the more costly but arguably more reliable Monte Carlo method. Recent studies have suggested that while Wilks requires relatively few samples to produce statistics, the fluctuation of those statistics is significant; Monte Carlo, on the other hand, requires many samples to produce reliable statistics, but does so in a consistent and reliable manner [16]. Other methods for efficient uncertainty quantification have risen in popularity recently, such as stochastic collocation for generalized polynomial chaos [17]. Collocation methods can provide savings over Monte Carlo in systems that are regular or have an effective input space with low dimensionality.

Ultimately, uncertainty propagation produces the likely values and dispersion of response figures of merit. Likely value is given by the expectation value (or mean) of a sample set, and dispersion is demonstrated by statistics such as the standard deviation (or sigma), variance, and 5th or 95th percentiles. In NPP margin characterization, the 95th percentile is used to compare to operational limits such as PCT and ECR.

4.8.2 Limit Surface Search

For providing more access to safety margin to plant operators, it is desirable to determine what portions of the input uncertainty space can result in undesirable plant operation, such as approaching operation limits. Because there are many input parameters with associated uncertainty as part of simulating NPP operation, especially during accident scenarios, it is difficult to manually explore the input space and determine what combination of parameters is resulting in undesirable behavior. A powerful tool in the RAVEN framework is the Limit Surface Search algorithm, which will explore the input space near changes in desired output and create a hypersurface that separates desirable response values from undesirable. Once this surface is obtained, it is simple to acquire statistics such as failure probability.

One drawback to the Limit Surface Search algorithm is the requirement that many exploratory samplings of the input space are required, which in turn requires many independent runs of the plant simulation. Because of the complexity of plant physics, plant simulations are expensive, which makes searching for the limit surface prohibitively expensive. Three tools can be used to mitigate this expense: reduced-order models, surrogate models, and input space reduction through sensitivity screening.

4.8.3 Reduced-Order Models and Surrogate Models

Both reduced-order models (ROMs) and surrogate models attempt to reduce the cost of evaluating expensive simulations by representing a limited scope of the simulation in an algorithm that is efficient to evaluate. ROMs reduce the cost by simplifying the physics involved in the simulation, by making assumptions or limiting the range of input values. Methods such as Catton's lumped parameter models [18] are employed for producing representative ROMs in this work.

Surrogate models, on the other hand, use evaluations of the original models to produce mathematical representations that are very cheap to evaluate. Once a ROM or surrogate model is constructed for a simulation model, it can be used in place of the original (based on the assumptions made when constructing the ROM or surrogate). With each costly code represented by an inexpensive model, expensive tools such as Monte Carlo uncertainty propagation and Limit Surface Search can be employed much more efficiently.

To demonstrate the LOTUS framework, we employ a set of ROMs that individually use lumped-parameters based on Catton models [18]. There is a ROM each for core design, fuels performance, and systems analysis. The core design ROM determines the burnup states of characteristic fuel assemblies (region) in the core as well as peak assembly and peak rod ratios for each region. The fuels performance ROM takes the burnup and peaking ratios from the core design ROM and approximates conductivities for the clad, gap, and fuel of each region's characteristic rods. Finally, the systems analysis ROM simulates first steady-state temperature profiles then the temperature of the cladding as a large-break loss of coolant accident is simulated.

One of the benefits of this system of ROMs is cheap calculations. This allows experimentation with uncertainty quantification techniques that require a great number of samples to be effective, such as Monte Carlo benchmarking and limit surface search algorithms.

4.8.4 Sensitivity Screening

Another obstacle to some uncertainty propagation techniques as well as Limit Surface Search algorithms is the dimensionality of the uncertain input space. As the number of uncertain inputs grows, the number of samples required to represent that space accurately grows exponentially. To help alleviate this problem, global sensitivity analysis can be employed. In global sensitivity analysis, the effect of perturbing an input on the moments of a response is quantified. Often, a response is much more sensitive to some inputs than others. In some cases, no responses are sensitive to perturbations of a particular input. If this is discovered, the uncertainty in that parameter can be ignored without negatively impacting the BEPU analysis. Each such reduction in uncertain space dimensionality greatly improves the performance efficiency of Limit Surface Search and dimension-dependent uncertainty propagation techniques.

5. LOTUS DEMONSTRATION RESULTS

5.1 Core Design Automation

The above described core design methodology and the new lattice code interface have been applied to two cases: A first “simple” option based on the BEAVRS [25] benchmark, evolved to a “high energy-low-leakage” (HE-LL) loading geometry; and a second, more complex, option based on publicly available PWR data from recent years (see Appendix 1), called HE-LL-Optimized (HE-LL-O). The PHISICS/RELAP5-3D core simulator has been used to compute assembly-homogenized quantities (burnup maps, assembly power peaking maps, power history, etc.) together with pin power reconstruction (from HELIOS-2) in these two applications. This is an acceptable current state-of-the-art methodology to provide input data for safety analysis, like LOCAs. It should be noted that PHISICS/RELAP5-3D and the developed lattice code interface can also do pin averaged calculations, as it will be helpful in best-estimate-plus-uncertainty (BEPU) safety analysis.

5.1.1 Common Core Geometry for HE-LL and HE-LL-O Core Designs

Both core design options considered for the Industry Application #1 LOTUS demonstration are based on the BEAVRS benchmark geometry. In particular, the water reflector and the pressure vessel geometry are kept the same for both options. The main differences between the two options are the fuel assembly design and the loading patterns, as it will be shown later. Figure 40 (Left) shows the radial layout of the BEAVRS reactor including the reflector and the pressure vessel. The figure shows the key plant parameters on the right. Figure 40 shows as an example the fuel assembly enrichments and layout for the BEAVRS design. The HE-LL and HE-LL-O core designs are derived from a multi-cycle reload analysis in which BEAVRS is the starting cycle in a multi-cycle sequence.

5.1.2 Option 1: HE-LL Core

In order to demonstrate the LOTUS tool methodology, it is helpful to be able to analyze higher burnup fuel, which will challenge the proposed rulemaking “10 CFR 50.46c” acceptance criteria. The goal of the first Industrial Application reference core design is to reach these higher burnups using a most simple core design. This includes the use of only one fresh fuel assembly enrichment for the whole core, no axial lower enriched fuel zones on the assemblies and the use of Wet Annular Burnable Absorbers rods (WABA). Furthermore, to have a modern low-leakage loading scheme that allows reaching higher burnups, but still keeping it as simple as possible, all twice burned fuel has been placed at the periphery. It is worth mentioning that for this simple design, the main goal is to reach higher burnups, therefore, it is deemed acceptable that some of the other design goals, like power peaking may not fully be reached.

For the first core design option, HE-LL, the starting point is the BEAVRS design. For the fuel design, the axial fuel enrichment is constant and a variable number of WABA rods are used to flatten the radial power distribution in the core. The assembly design is shown in Figure 41. This is a 17 x 17 assembly with 264 fuel rods and 25 non-fuel locations. The non-fuel locations contain the guide tubes, the WABA rods and the instrumental tubes.

The starting point, i.e. the initial guess for the core design and material compositions are the ones specified in the BEAVRS benchmark. Using the cross-sections computed for the BEAVRS design, the BEAVRS feed fuel and loading pattern have been changed. The BEAVRS reloading pattern is a “low-energy/high-leakage” one. For this work, our goal is to perform analysis on a realistic loading pattern. Hence, a transition from the BEAVRS “low-energy/high-leakage” to the desired “high-energy/low-leakage” (HE-LL) reloading pattern is performed. During this multi-cycle equilibrium analysis, the fuel enrichment is optimized for an 18-month cycle. A “manual optimization” of the core is performed where the shuffling scheme, the loading pattern and the burnable absorber distribution (WABAs) in the core are optimized in order to minimize the needed enrichment to reach the 18 month cycle as well as to minimize certain thermal-hydraulic characteristics, such as $F\Delta h$ and Fq . For each step in the optimization, at least 8 cycle sequences are computed, in order to reach the equilibrium cycle for this configuration. At the end of the manual optimization, new cross section libraries for the adjusted core design are recomputed and the SPH correction is applied to them. The “manual optimization” is then repeated. For this demonstration PWR design, three of these iterations are performed, i.e. cross sections are recalculated three times.

HELIOS-2 calculations, i.e. cross-section libraries at two different axial heights have been generated: one in the region where there is only fuel and one in the region where there is a spacer. In addition, a library for the bottom reflector and a library for the top reflector have been generated. This leads to a total of 62 libraries (2*29 fuel assemblies + 2 radial reflectors, one for the fuel and one for the spacer region + 2 top and bottom reflectors). Axially, the libraries prepared for the spacer region are associated to the axial layers containing a spacer and the “normal” fuel libraries are associated to the other axial layers. The libraries prepared to the top, bottom and radial reflectors are associated with the corresponding reflector assemblies.

The boundary conditions for the thermal-hydraulics have been taken from the BEAVRS benchmark specifications. Therefore, the inlet temperature has been set to 560K and the upper plenum pressure has been set to 157bars in the RELAP5-3D model. The mass flow has been set to 88.5kg/s for each assembly and 1375kg/s for the reflector region.

Using the described core design strategy (see Figure 30), a “high-energy/low-leakage” (HE-LL) core has been designed. As mentioned, the starting point was the BEAVRS geometry. From there, the feed fuel composition and enrichment, as well as the loading pattern, shuffling scheme and burnable poison distribution have been changed “arbitrarily” by hand to find a reasonable PWR core design without having to use proprietary plant information. It has to be noted that the resulting design intends in no way to be an optimized core design that is or should be used in an operating power plant. The goal is to create a generic PWR 18-month equilibrium cycle design that is reasonable in terms of fuel enrichment and certain thermal-hydraulic characteristics, such as $F\Delta h$ and Fq for the demonstration of the LOTUS tool.

The enrichment found in order to reach, at the equilibrium, a cycle length of 18 months is 4.8%. Figure 42 shows the core configuration including loading map and number of burnable absorbers (WABA) in the fresh fuel assemblies.

1.61	1.45	1.47	1.22	1.62	1.17	1.11	0.27
1.65	1.50	1.51	1.26	1.67	1.21	1.15	0.28
1.93	1.72	1.73	1.42	1.94	1.38	1.33	0.33
0.00	25.45	20.85	29.51	0.00	29.47	0.00	52.57
1.45	1.69	1.55	1.66	1.35	1.53	0.67	0.24
1.50	1.74	1.60	1.71	1.39	1.58	0.69	0.25
1.72	2.06	1.86	1.99	1.59	1.83	0.79	0.30
25.45	0.00	19.63	0.00	27.64	0.00	47.04	52.54
1.47	1.57	1.70	1.45	1.56	1.10	1.02	0.24
1.51	1.61	1.76	1.50	1.60	1.13	1.06	0.25
1.73	1.88	2.08	1.73	1.86	1.29	1.23	0.29
20.85	19.19	0.00	24.48	0.00	31.89	0.00	52.50
1.22	1.67	1.46	1.60	1.18	1.33	0.47	0.15
1.26	1.72	1.50	1.64	1.22	1.37	0.49	0.15
1.42	2.00	1.74	1.91	1.39	1.59	0.57	0.19
29.51	0.00	24.15	0.00	31.49	0.00	51.84	52.52
1.62	1.35	1.55	1.17	1.35	0.68	0.24	
1.67	1.39	1.60	1.21	1.39	0.70	0.25	
1.94	1.59	1.85	1.39	1.62	0.81	0.30	
0.00	27.56	0.00	31.53	0.00	30.49	51.01	
1.17	1.52	1.08	1.31	0.67	0.28	0.11	
1.21	1.57	1.11	1.35	0.69	0.29	0.11	
1.38	1.82	1.26	1.56	0.80	0.34	0.14	
29.47	0.00	32.28	0.00	30.32	51.15	44.23	
1.11	0.67	1.00	0.44	0.22	0.11		
1.15	0.69	1.03	0.46	0.23	0.11		
1.33	0.79	1.20	0.53	0.28	0.14		
0.00	47.27	0.00	51.84	53.59	43.91		
0.27	0.23	0.23	0.14				
0.28	0.24	0.23	0.14				
0.33	0.29	0.28	0.18				
52.57	53.58	52.50	52.65				

	max	Fresh
Pbar	1.70	Once burned
FDH	1.76	Twice burned
Fq	2.08	
Burnup	53.59	

1.49	1.25	1.22	1.21	1.43	1.15	1.26	0.36
1.54	1.29	1.25	1.25	1.47	1.19	1.30	0.37
1.87	1.70	1.56	1.48	1.65	1.35	1.43	0.45
31.30	51.91	47.08	52.57	30.50	50.99	20.83	58.22
1.25	1.49	1.29	1.52	1.25	1.46	0.73	0.34
1.29	1.54	1.33	1.57	1.29	1.51	0.75	0.35
1.70	1.89	1.65	1.79	1.47	1.67	0.85	0.42
51.91	31.95	47.56	31.52	52.61	27.62	59.86	57.73
1.22	1.29	1.53	1.31	1.44	1.15	1.21	0.34
1.25	1.33	1.57	1.35	1.49	1.18	1.25	0.35
1.56	1.65	1.80	1.56	1.65	1.36	1.37	0.44
47.08	47.32	32.32	51.41	29.52	52.40	19.58	56.50
1.21	1.53	1.31	1.45	1.18	1.40	0.56	0.23
1.25	1.57	1.35	1.50	1.21	1.44	0.58	0.24
1.48	1.79	1.56	1.67	1.38	1.57	0.67	0.30
52.57	31.57	51.20	30.33	53.55	24.42	56.90	55.91
1.43	1.25	1.44	1.18	1.57	0.87	0.34	
1.47	1.29	1.49	1.21	1.62	0.89	0.35	
1.65	1.47	1.64	1.38	1.78	1.03	0.42	
30.50	52.54	29.47	53.53	25.49	44.19	56.23	
1.15	1.46	1.14	1.39	0.86	0.40	0.20	
1.19	1.51	1.18	1.43	0.89	0.41	0.21	
1.35	1.67	1.35	1.56	1.02	0.54	0.26	
50.99	27.54	52.56	24.13	43.88	57.31	46.92	
1.26	0.73	1.20	0.54	0.33	0.20		
1.30	0.75	1.23	0.55	0.34	0.20		
1.43	0.85	1.36	0.64	0.41	0.25		
20.83	60.00	19.21	60.76	58.53	46.56		
0.36	0.34	0.33	0.22				
0.37	0.35	0.34	0.23				
0.45	0.41	0.41	0.28				
58.22	58.66	57.44	55.80				

	max	Fresh
Pbar	1.57	Once burned
FDH	1.62	Twice burned
Fq	1.89	
Burnup	60.76	

Figure 43. Option 1 (HE-LL): Pbar, Fdh, Fq and Burnup for Each Assembly at BOC (Top) and EOC (Bottom).

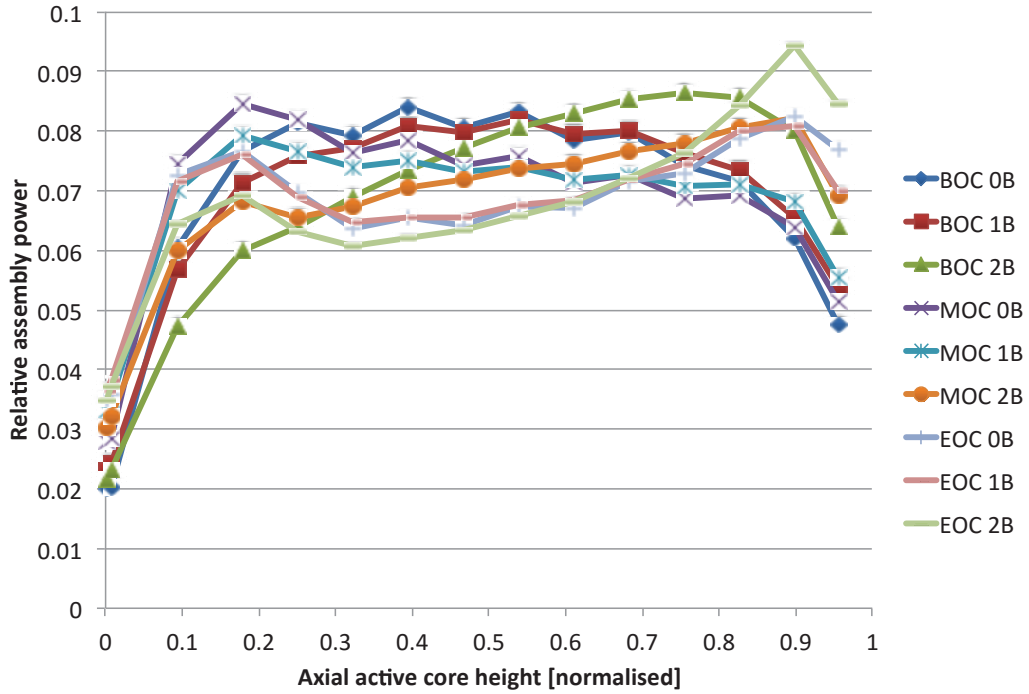


Figure 44. Option 1 (HE-LL): Core Averaged Axial Power Distribution for Fresh (0B), Once Burned (1B) and Twice Burned (2B) Fuel Assemblies at BOC, MOC and EOC.

1.06 1.02	1.04 1.03	1.05 1.03	1.06 1.04	1.07 1.04	1.06 1.05	1.07 1.06	1.06 1.07
1.04 1.03	1.06 1.02	1.05 1.03	1.06 1.02	1.04 1.03	1.07 1.04	1.05 1.06	1.07 1.07
1.05 1.03	1.05 1.03	1.06 1.02	1.04 1.03	1.07 1.04	1.06 1.05	1.07 1.05	1.07 1.07
1.06 1.04	1.06 1.02	1.04 1.03	1.06 1.02	1.06 1.05	1.07 1.05	1.05 1.05	1.06 1.06
1.07 1.04	1.04 1.03	1.07 1.04	1.06 1.05	1.07 1.04	1.07 1.07	1.07 1.07	
1.06 1.05	1.07 1.04	1.06 1.05	1.07 1.05	1.07 1.07	1.06 1.06	1.06 1.06	
1.07 1.06	1.05 1.06	1.07 1.05	1.05 1.06	1.07 1.07	1.06 1.06		
1.06 1.07	1.07 1.07	1.07 1.07	1.06 1.06				

	max	Fresh
BOC	1.07	Once burned
EOC	1.07	Twice burned

Figure 45. Option 1 (HE-LL): Maximum Pin Peaking Factors for Each Assembly at BOC and EOC.

5.1.3 Option 2: HE-LL-Optimized Core (HE-LL-O)

The option 1 HE-LL core design provides the desired burnup for an 18 month cycle, but the needed fuel enrichment as well as the maximum radial and axial power peakings are somewhat high. In order to go to a more realistic core design than the simple HE-LL core presented in option 1, a second option has been designed. The goal of the second IA1 reference core is still to reach high burnup, but lower the radial power peaking and to flatten the axial power profiles towards more realistic current core conditions. Furthermore, the fresh fuel enrichment should be in a realistic range for an 18-month cycle.

The optimized design allows therefore for more complex features, such as two batches of fresh fuel assemblies with different enrichments, the addition of axial lower enriched fuel zones (blankets) on the top and bottom of the assemblies and the use of Integral Fuel Burnable Absorber rods (IFBA), instead of the traditional WABA rods. The constraint, that for a low leakage core, all twice-burned fuel has to be placed at the periphery is also lifted. Instead, a modified, publicly available real, recent PWR plant-loading pattern has been used (see Appendix A). The starting point for the option 2 HE-LL-O core design is the publicly available data in Appendix A. The assembly design is shown in Figure 46. It's a 17 x 17 assembly with 264 fuel rods and 25 non-fuel locations. All non-fuel locations are guide or instrument tubes. The IFBA rods are normal fuel rods that have a boron absorber coating sprayed on the cladding, as opposed to the WABA rods, that are annual boron rods. The assembly shown in Figure 46 on the left has 128 IFBA pins, but other assembly designs with 64 and 104 IFBA pins exist. The fuel rods contain a low enriched zone at the top and bottom. These blankets are about 20cm long and contain 2.6% enriched fuel as shown in Figure 46 on the right. The IFBA coating does not extend to the blanket regions, i.e. the burnable absorber is only sprayed on the high-enriched center part of the fuel rods.

As a starting point, the cross sections from option 1 have been used. The degrees of freedom for the optimization are the shuffling scheme, since this is not known from the open literature, the fuel enrichments for the two fresh fuel batches (since they are given as ranges only in the open literature) and the IFBA rod distribution. Starting from an initial guess, the feed fuel enrichment and shuffling pattern have been changed by leaving the loading pattern untouched. The fuel enrichments has been searched to obtain an 18-month cycle. A “hand-optimization” of the core has been performed where the shuffling scheme, and the burnable absorber distribution (IFBAs) in the core has been changed in order to minimize the needed enrichment to reach the 18 month cycle as well as to minimize certain thermal-hydraulic characteristics, such as $F\Delta h$ and Fq . For each step in the optimization, at least 8 cycles have been computed, in order to reach the equilibrium cycle for this configuration. When this optimization has been finished, new cross section libraries for the adjusted core design have been computed and the SPH correction has been applied to them. The “hand-optimization” has then been repeated. For this demonstration PWR design, two of these iterations have been performed, i.e. cross sections have been recalculated two times.

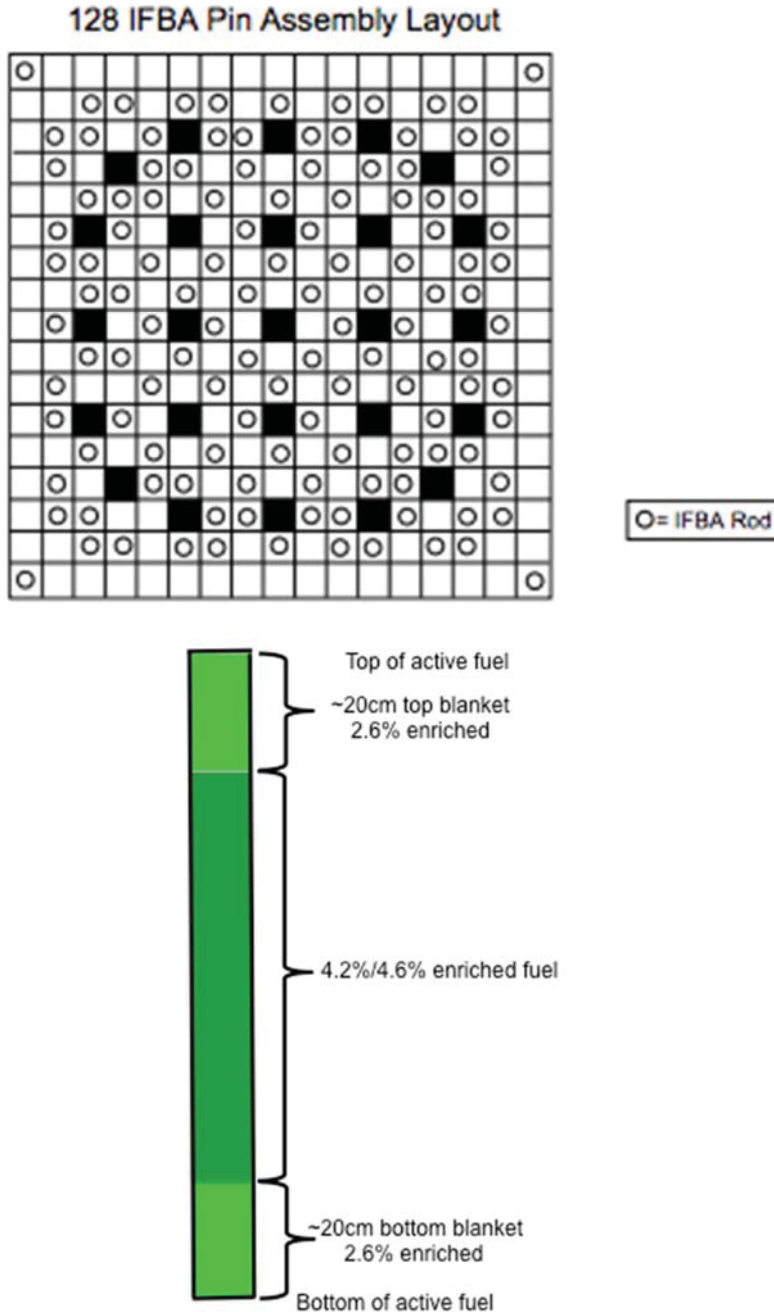


Figure 46. Option 2 (HE-LL-O): Left) Current 17x17 Pin Assembly. In this Example Shown with 128 IFBA Rods (Circles) and 25 Guide Tubes (Black); Right) Axial Fuel Pin Design: High Enriched Center Part with Top and Bottom Blankets 2.6% Enriched.

HELIOS-2 calculations, i.e. cross-section libraries at two different axial heights have been generated: one in the fuel region and one in the blanket region. In addition, a library for the bottom reflector and a library for the top reflector have been generated. This leads to a total of 34 libraries (29 fuel assemblies + 1 blanket + 2 radial reflectors, one for the fuel and one for the blanket region + 2 top and bottom reflectors). Axially, the libraries

prepared for the fuel regions are associated to the axial layers containing the corresponding fuel and the one blanket library is associated to all blanket regions in the core. The libraries prepared to the top, bottom and radial reflectors are associated with the corresponding reflector assemblies.

The boundary conditions for the thermal-hydraulics have been taken from the open literature as well (see again Appendix A). Therefore, the inlet temperature has been set to 560K and the upper plenum pressure has been set to 157bars in the RELAP5 model as for the option 1. The mass flow has been set to 90.6kg/s for each assembly and 1375kg/s for the reflector region for core design option 2, which means there somewhat more core flow in the HE-LL-O core design compared to the HE-LL one.

As mentioned, the feed fuel composition and enrichment, as well as the shuffling scheme and burnable poison distribution have been changed “arbitrarily” by hand to find a reasonable PWR core design without having to use proprietary plant information. It has to be noted that the resulting design intends in no way to be an optimized core design that is or should be used in an operating power plant. The goal is to create a generic PWR 18-month equilibrium cycle design that is reasonable in terms of fuel enrichment and certain thermal-hydraulic characteristics, such as $F\Delta h$ and Fq for the demonstration of the LOTUS tool, but at the same time allows for more complexity than the simple option 1 HE-LL core design.

The two enrichments found in order to reach, at the equilibrium, a cycle length of 18 months are 4.2% and 4.6%. Figure 47 shows the core configuration including loading map and number of burnable absorbers (IFBA) in the fresh fuel assemblies.

The k_{eff} at BOC has been found to be 1.10462 and the cycle ends when the k_{eff} falls below 1.0. Assuming a realistic boron worth of $\sim 10\text{pcm/ppm}$, the maximum boron concentration in the core at BOC is expected to be $\sim 1000\text{ppm}$ which is in the range of boron concentrations reported in the open literature. Figure 48 shows the radial assembly power peaking factors (P_{bar}), the thermal-hydraulic quantities $F\Delta h$ and Fq and the average burnup for each assembly at BOC end EOC. Furthermore, the figure shows the core wide maximums for these quantities. For the readers convenience, the assemblies are colored the same way as in Figure 47, i.e. fresh fuel in yellow (green is not used), once burned in orange and twice burned in blue.

The core average axial power distributions for the fresh, once and twice burned fuel assemblies at BOC, MOC and EOC are shown in Figure 49. Figure 50 shows the maximum pin peaking for each assembly. These values are computed with HELIOS-2 and are shown for BOC and EOC.

0.96	1.35	1.23	1.18	1.28	1.11	0.92	0.53
1.01	1.44	1.31	1.24	1.35	1.18	0.98	0.57
1.08	1.59	1.41	1.34	1.46	1.32	1.10	0.64
35.90	0.00	20.17	21.17	17.24	26.05	25.78	25.77
1.35	1.01	1.34	1.01	1.39	1.24	1.18	0.58
1.44	1.06	1.41	1.06	1.46	1.31	1.26	0.62
1.59	1.14	1.55	1.14	1.59	1.45	1.37	0.68
0.00	37.40	0.00	37.31	0.00	23.68	0.00	26.10
1.23	1.33	0.96	1.35	1.27	1.25	1.22	0.55
1.31	1.40	1.01	1.42	1.36	1.32	1.29	0.59
1.41	1.53	1.09	1.56	1.46	1.45	1.42	0.64
20.17	0.00	37.40	0.00	20.00	24.32	0.00	26.29
1.18	0.96	1.33	0.99	1.34	1.13	1.07	0.31
1.24	1.01	1.40	1.05	1.42	1.19	1.13	0.33
1.34	1.09	1.54	1.13	1.57	1.29	1.26	0.36
21.17	35.90	0.00	37.16	0.00	26.00	0.00	42.29
1.28	1.36	1.24	1.33	0.82	1.07	0.45	
1.35	1.44	1.32	1.40	0.86	1.15	0.48	
1.46	1.57	1.42	1.55	0.93	1.28	0.52	
17.24	0.00	21.06	0.00	42.44	0.00	41.80	
1.11	1.23	1.24	1.12	1.06	0.87	0.26	
1.18	1.30	1.31	1.18	1.14	0.92	0.28	
1.32	1.44	1.43	1.28	1.27	1.03	0.30	
26.05	23.64	24.24	25.83	0.00	0.00	41.26	
0.92	1.18	1.21	1.05	0.43	0.27		
0.98	1.25	1.28	1.12	0.46	0.28		
1.10	1.36	1.42	1.25	0.49	0.31		
25.78	0.00	0.00	0.00	45.05	39.18		
0.53	0.58	0.55	0.31				
0.57	0.62	0.59	0.33				
0.64	0.68	0.64	0.36				
25.77	25.98	26.29	42.84				

				max	Fresh			
				Pbar	1.39	Once burned		
				FDH	1.46	Twice burned		
				Fq	1.59			
				Burnup	45.05			
0.93	1.30	1.08	0.98	1.04	0.94	0.91	0.60	
0.97	1.34	1.13	1.01	1.08	0.97	0.95	0.65	
1.04	1.45	1.22	1.10	1.18	1.09	1.05	0.73	
53.43	25.29	41.43	40.92	38.80	44.74	42.17	35.63	
1.30	0.98	1.35	0.94	1.27	1.06	1.32	0.68	
1.34	1.02	1.40	0.98	1.31	1.10	1.39	0.72	
1.45	1.10	1.53	1.07	1.41	1.22	1.52	0.79	
25.29	55.83	25.61	55.35	25.56	44.72	23.24	37.17	
1.08	1.35	0.99	1.38	1.10	1.08	1.35	0.66	
1.13	1.39	1.03	1.42	1.15	1.12	1.43	0.70	
1.22	1.53	1.10	1.56	1.25	1.23	1.58	0.76	
41.43	25.49	55.42	26.07	41.93	45.52	23.90	37.20	
0.98	0.91	1.38	1.01	1.37	1.05	1.11	0.37	
1.01	0.96	1.42	1.05	1.42	1.09	1.19	0.39	
1.10	1.04	1.56	1.13	1.54	1.19	1.30	0.43	
40.92	53.21	25.82	55.57	25.54	45.62	19.83	48.27	
1.04	1.27	1.09	1.37	0.90	1.22	0.52		
1.08	1.31	1.14	1.42	0.94	1.30	0.55		
1.18	1.41	1.23	1.55	1.01	1.43	0.59		
38.80	25.30	42.50	25.38	57.81	20.83	50.28		
0.94	1.06	1.08	1.05	1.22	1.05	0.33		
0.97	1.10	1.12	1.09	1.30	1.12	0.35		
1.09	1.22	1.23	1.19	1.42	1.24	0.38		
44.74	44.59	45.30	45.34	20.70	16.97	46.26		
0.91	1.32	1.35	1.11	0.50	0.34			
0.95	1.39	1.43	1.19	0.54	0.36			
1.05	1.52	1.58	1.30	0.58	0.40			
42.17	23.20	23.81	19.65	53.15	44.29			
0.60	0.69	0.66	0.37					
0.65	0.72	0.70	0.39					
0.73	0.80	0.76	0.43					
35.63	37.06	36.94	48.72					

Figure 48. Option 2 (HE-LL-O): Pbar, Fdh, Fq and Burnup for each Assembly at BOC (Top) and EOC (Bottom).

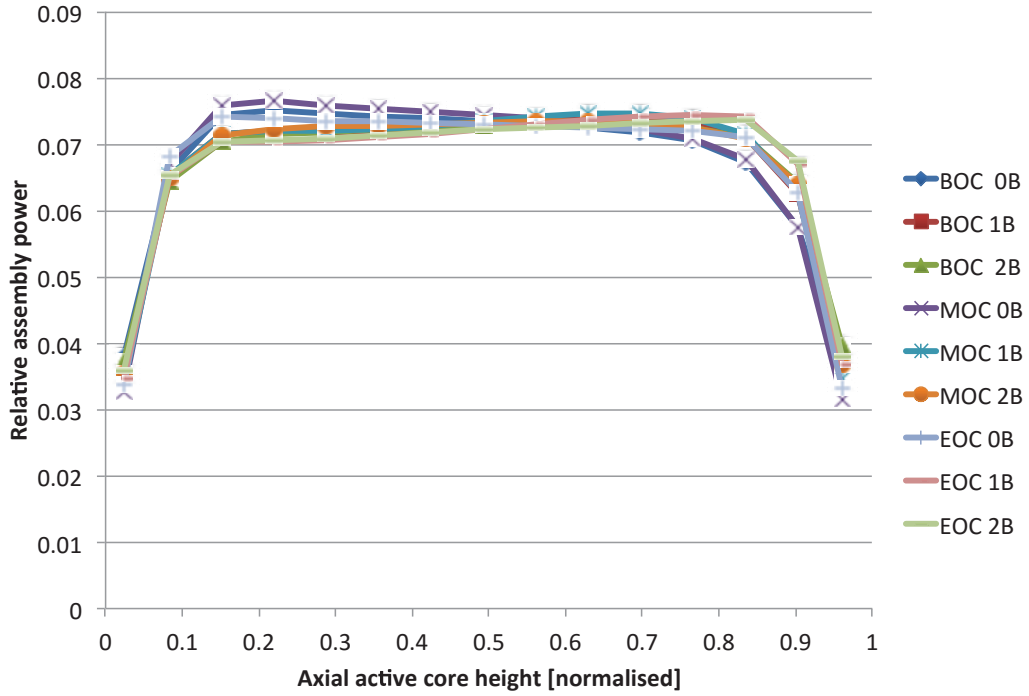


Figure 49. Option 2 (HE-LL-O): Core Average Axial Power Distribution for Fresh (0B), Once Burned (1B) and Twice Burned (2B) Fuel Assemblies at BOC, MOC and EOC.

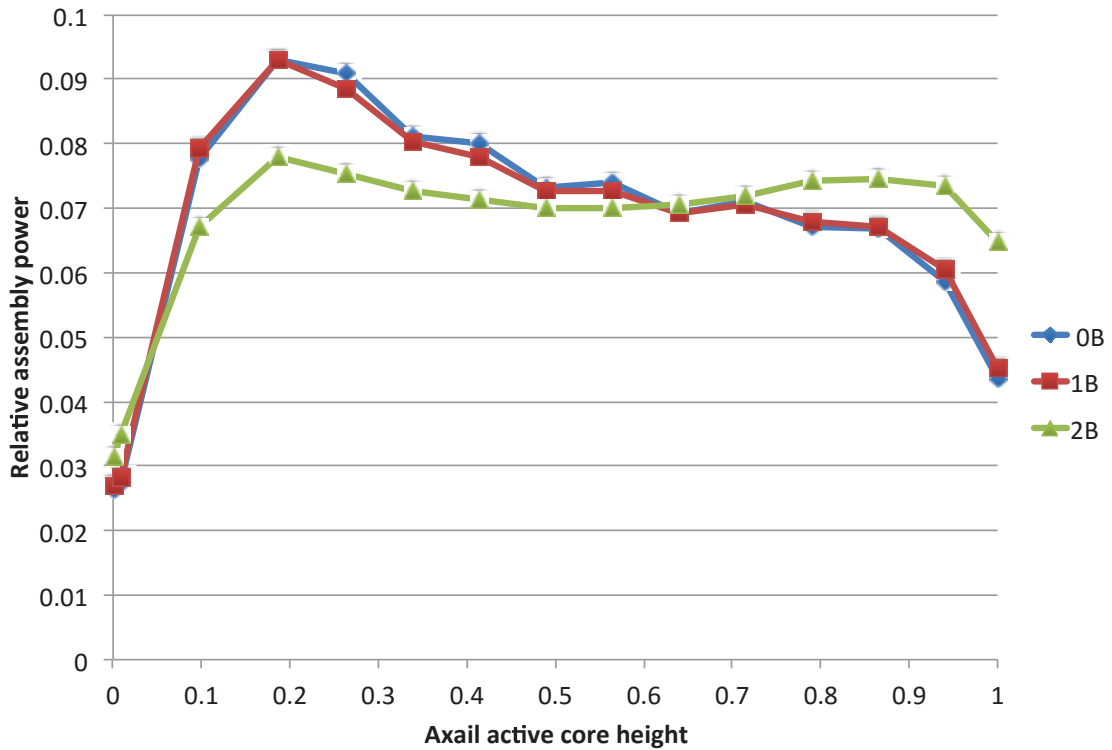
1.05 1.04	1.06 1.03	1.06 1.05	1.06 1.04	1.06 1.04	1.06 1.04	1.06 1.05	1.08 1.08
1.06 1.03	1.06 1.04	1.05 1.03	1.06 1.05	1.06 1.04	1.06 1.04	1.06 1.05	1.06 1.05
1.06 1.05	1.05 1.03	1.06 1.04	1.05 1.03	1.06 1.05	1.06 1.04	1.06 1.06	1.06 1.05
1.06 1.04	1.06 1.05	1.05 1.03	1.06 1.04	1.06 1.03	1.05 1.04	1.06 1.07	1.06 1.05
1.06 1.04	1.06 1.04	1.06 1.05	1.06 1.03	1.06 1.05	1.07 1.06	1.06 1.07	
1.06 1.04	1.06 1.04	1.06 1.04	1.05 1.04	1.07 1.06	1.06 1.07	1.07 1.07	
1.06 1.05	1.06 1.05	1.06 1.06	1.06 1.07	1.06 1.07	1.07 1.07		
1.08 1.08	1.06 1.05	1.06 1.05	1.06 1.05				

	max	Fresh
BOC	1.08	Once burned
EOC	1.08	Twice burned

Figure 50. Option 2 (HE-LL-O): Maximum Pin Peaking Factors for each Assembly at BOC and EOC.

5.1.4 Transient Power Maneuvers for HE-LL and HE-LL-O Core Designs

For the demonstration of LOTUS, RAVEN was instructed to sample the LOCA start times on a grid, instead of continuously in time. Therefore the power shapes passed to the subsequent LOCA analysis are at the end of the maneuver for BOC, 50 days, 100 days, 200 days, 300 days, 400 days, 500 days and EOC. As an example, Figure 51 shows the skewed axial power shapes at the end of the load following maneuver for BOC, 300 days and EOC for core design option 1 (HE-LL), while Figure 52 shows the same skewed power shapes for the core design option 2 (HE-LL-O).



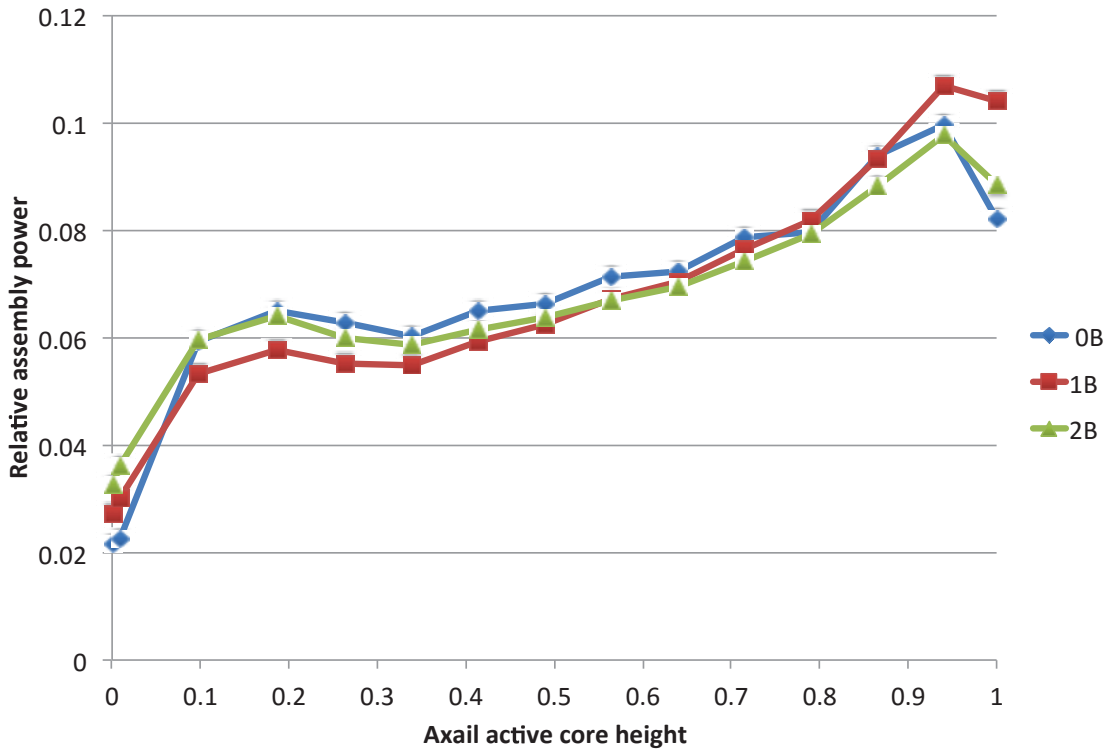
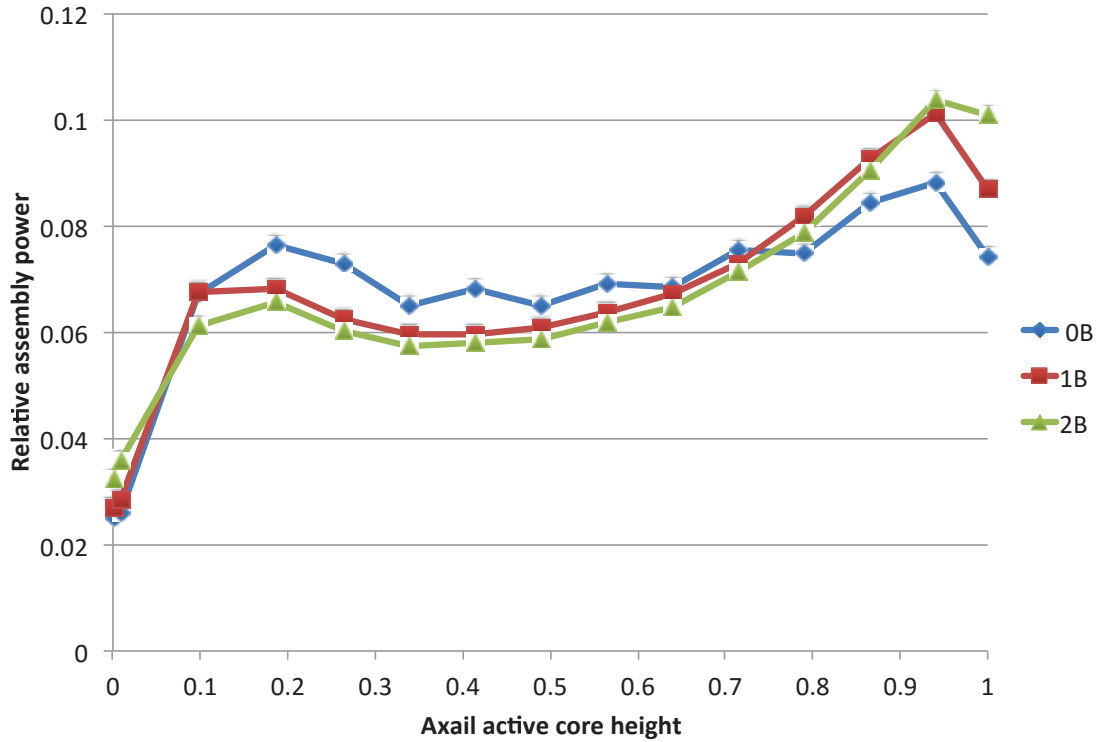
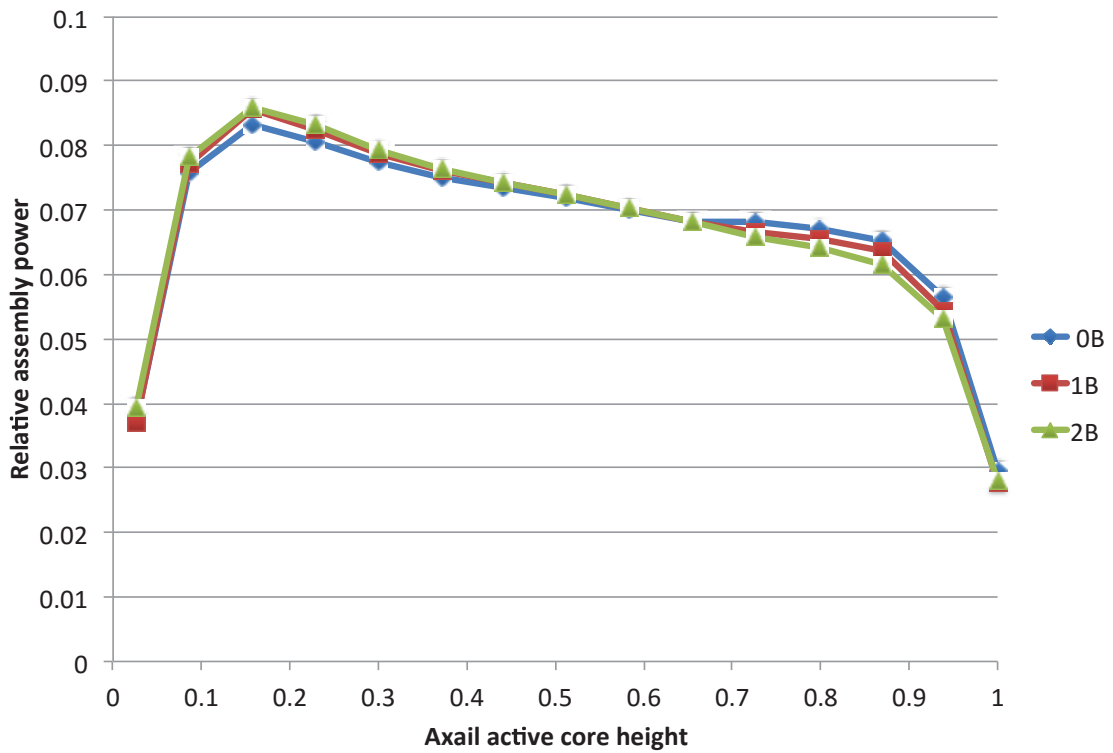
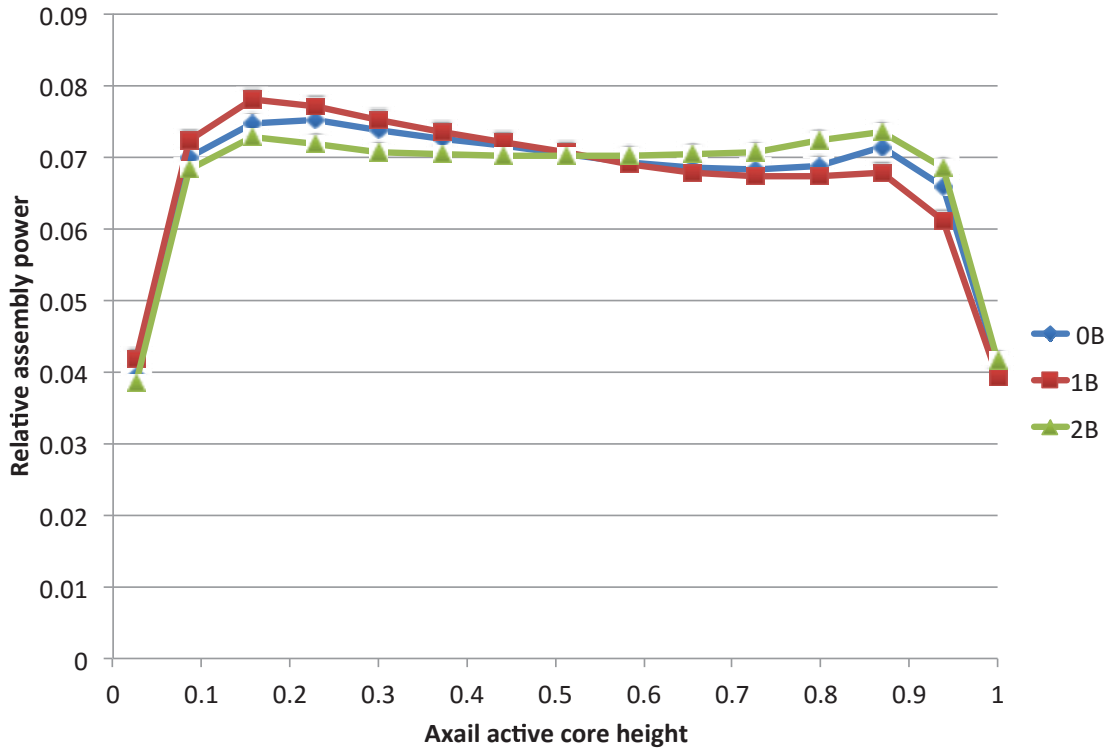


Figure 51. Option 1 (HE-LL): Skewed Power Shapes at the End of the Maneuver at BOC (Top), at 300 Days (Middle) and at EOC (Bottom). Shown Are Core Average Axial Power Distributions for Fresh (0B), Once Burned (1B) and Twice Burned (2B) Fuel Assemblies.



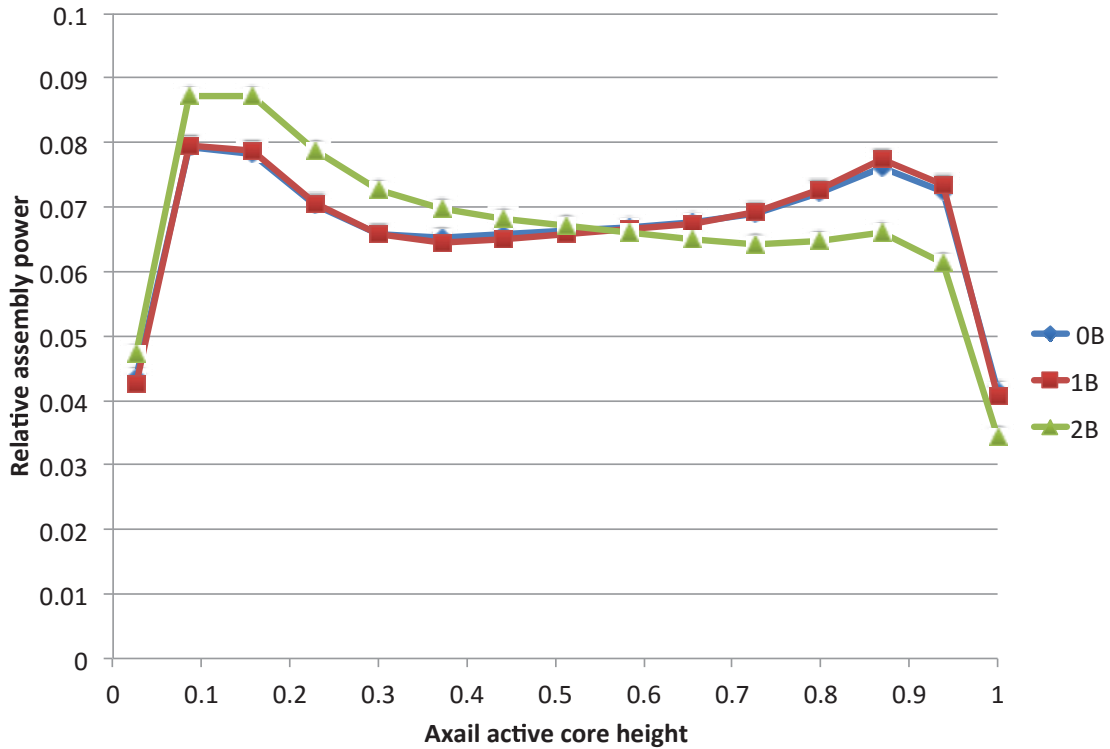


Figure 52. Option 2 (HE-LL-O): Skewed Power Shapes at the End of the Maneuver at BOC (Top), at 300 Days (Middle) and at EOC (Bottom). Shown Are Core Average Axial Power Distributions for Fresh (0B), Once Burned (1B) and Twice Burned (2B) Fuel Assemblies.

5.2 Fuels Performance

The proposed 10 CFR 50.46c rulemaking implies that all the fuel rods (more than fifty thousands) have to be analyzed in order to find the rods with the limiting PCTR and ECRR values. However, analyzing every fuel rod in a core is not practical to perform LB-LOCA analyses, we built two fuel rod models for each assembly, one for the hot rod and the other one for the average rods. In this way, the total number of simulated fuel rods in LB-LOCA simulations is reduced to a manageable number of 386. The hot rod is defined as the highest power rod in each assembly. The remaining fuel rods in an assembly is lumped together and represented by one FRAPCON model to simulate the behavior of the average rods. The cladding material is ZIRLO™. The NRC’s fuel performance code FRAPCON is the code of choice to perform fuel performance calculations in this work. The FRAPCON input file preparation and code execution were carried out automatically by LOTUS. The power histories required in the FRAPCON calculations were automatically retrieved from the core design results. The FRAPCON calculations were done at the selected cycle exposures of BOC, 100 days, 200 days, 300 days, 400 days, 500 days and EOC. The parameters required to provide the correct steady-state initialization of the RELAP5-3D simulations are subsequently obtained from the FRAPCON output files

by LOTUS and mapped into the RELAP5-3D input models. These parameters include the fuel rod internal pressure, gap gas mole fraction, etc.

5.2.1 HE-LL Core Design

In this subsection, selected results from the FRAPCON runs are presented to demonstrate the automation capability of LOTUS with respect to fuel performance calculations for the HE-LL core design. Figure 53 shows the power history used for the hot rod in a twice burned fuel assembly. The power history data is automatically retrieved by LOTUS from the core design results and included in the FRAPCON input file prepared by LOTUS. Figure 54 shows the maximum hydrogen contents calculated by FRAPCON versus fuel rod averaged burnup for the HE-LL core design.

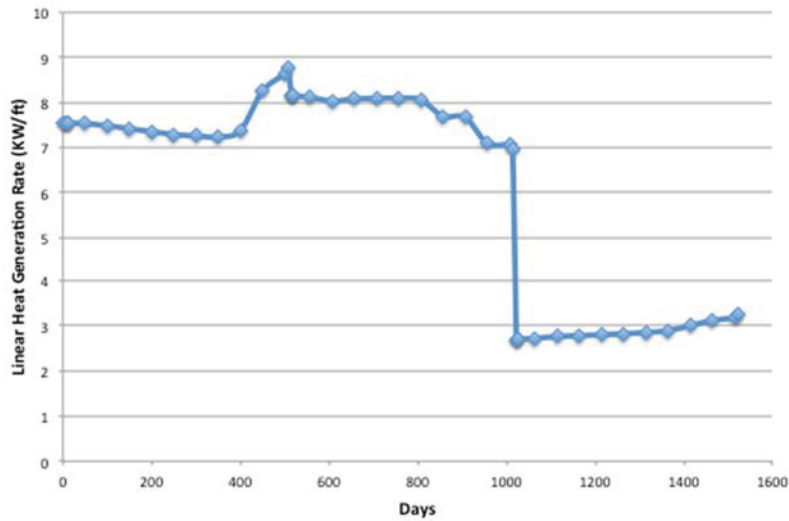


Figure 53. Power History for the Hot Rod in a Twice Burned Fuel Assembly.

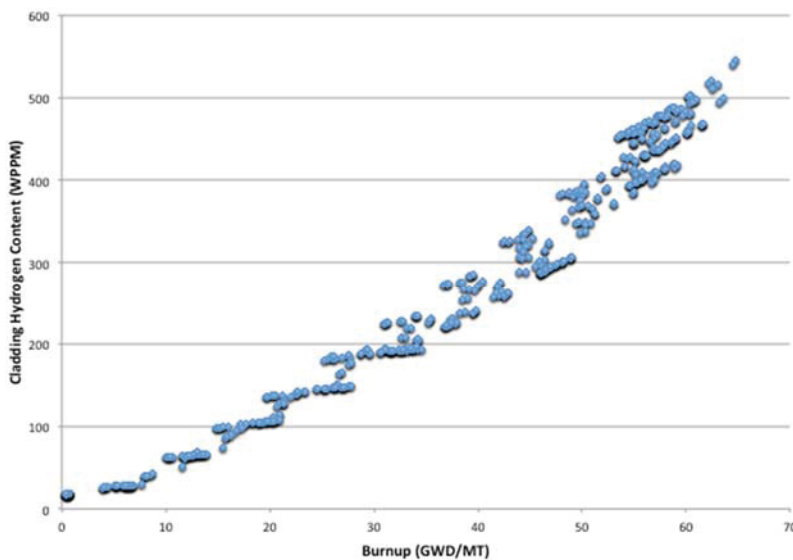


Figure 54. Cladding Hydrogen Content versus Rod Average Burnup.

5.2.2 HE-LL-Optimized Core Design

In this subsection, the results from the FRAPCON runs are presented to demonstrate the automation capability of LOTUS with respect to fuel performance calculations for the HE-LL-Optimized core design. Figure 56 shows the power history used in the FRAPCON calculations for the hot rod in a twice burned assembly. Figure 56 shows the maximum cladding Hydrogen contents versus fuel rod averaged burnup for the HE-LL-Optimized core design.

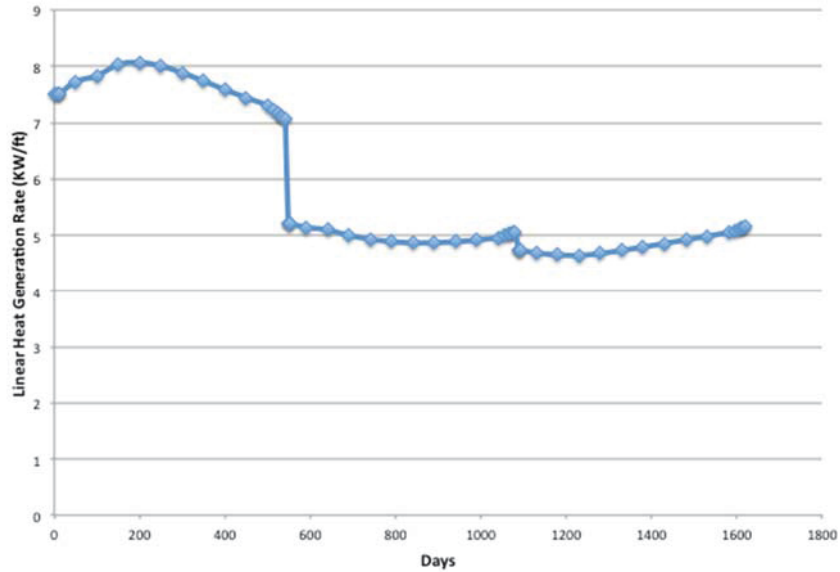


Figure 55. Power History for the Hot Rod in a Twice Burned Fuel Assembly.

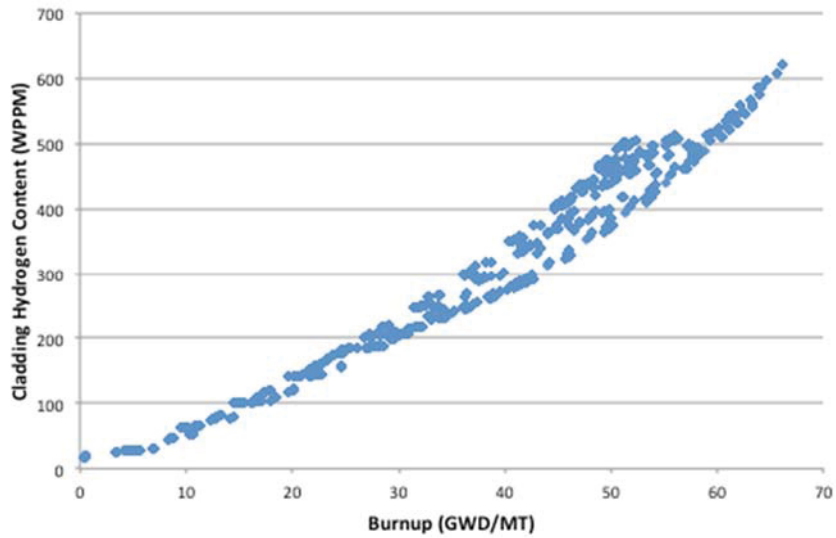


Figure 56. Cladding Hydrogen Content versus Fuel Rod Average Burnup.

5.3 Systems Analysis

RELAP5-3D is the code of choice to perform LB-LOCA analyses. The LOTUS-Baseline automation process starts with an existing RELAP5-3D plant system model and automatically mapped in certain required parameters from fuel performance and core design calculations. To be consistent with fuel performance calculations, two sets of heat structures were built for each fuel assembly – one for the hot rod and the other for the average rods. From the fuel performance calculations, the required parameters such as rod internal pressure, gap gas mole fraction, etc. are automatically obtained from the FRAPCON output files and mapped into the respective fuel rod models in the RELAP5-3D input files. From the core design calculations, the power shapes from the power maneuvering calculations are automatically obtained from the PHYSICS calculations and mapped into the RELAP5-3D input files. The best-estimate plus uncertainty (BEPU) analyses for LB-LOCA were subsequently carried out with the Monte Carlo method. A set of thirteen uncertain input parameters, such as reactor power, decay heat, accumulator conditions, fuel thermal conductivity, heat transfer coefficients, etc., as shown in Table 3, were randomly sampled in the BEPU analyses. The cladding pre-transient hydrogen uptake contents were also obtained from the FRAPCON output files. These are used in the determination of PCTR and ECRR calculations post RELAP5 LB-LOCA calculations. The direct Monte Carlo simulations were carried out. One thousand LB-LOCA cases with RELAP5-3D have been run on Idaho National Laboratory’s high performance computers (HPC), respectively, at seven selected cycle exposure points at BOC, 100 days, 200 days, 300 days, 400 days, 500 days and EOC. The $PCTR_{max}$ and $ECRR_{max}$ values from each RELAP5-3D output file were obtained and sorted by LOTUS among the 1000 runs, respectively, at the selected cycle exposure points. The probability distribution function (PDF) and the cumulative distribution function (CDF) of the figures of merit (PCTR and ECRR) were subsequently obtained. From the CDF and PCTR and ECRR, the 95 percentile values of PCTR and ECRR, as well as their corresponding PCT and ECR values, are obtained and their associated 95% confidence intervals are subsequently calculated to construct the estimators of the 95/95 upper tolerance limits for PCT and ECR. The 95/95 estimators are then compared to the proposed 10 CFR 50.46c rule to demonstrate compliance. The 95% limit values with 95% confidence interval can be expressed as:

$$Y_{95/95} = \mu_{95\%} \pm 2.11 * SE_M \quad (4)$$

where $\mu_{95\%}$ is the 95 percentile values of PCT and ECR and SE_M is the standard error of the sample mean value.

5.3.1 HE-LL Core Design

The results for the RELAP5-3D LB-LOCA simulations for the HE-LL core design are summarized in this subsection. Since the equilibrium cycle length for the HE-LL design is 507 days, the calculations at 500 days are omitted. For illustrative purpose, the PDF and CDF for PCTR at EOC is shown in Figure 57 and the PDF and CDF for ECRR at EOC is shown in Figure 58. The 95% percentile value with 95% confidence interval are calculated following the 1000 RELAP5-3D LB-LOCA simulations at the selected cycle exposure point and the results are summarized in Table 4. The limiting cases are identified from the

LB-LOCA simulations and the PCT and ECR values for the hot rod in each assembly in the limiting cases are obtained by LOTUS and shown in Figure 59 for PCT and Figure 60 for ECR. Figure 61 shows the correlation between ECR and PCT for the limiting cases identified in the LB-LOCA simulations.

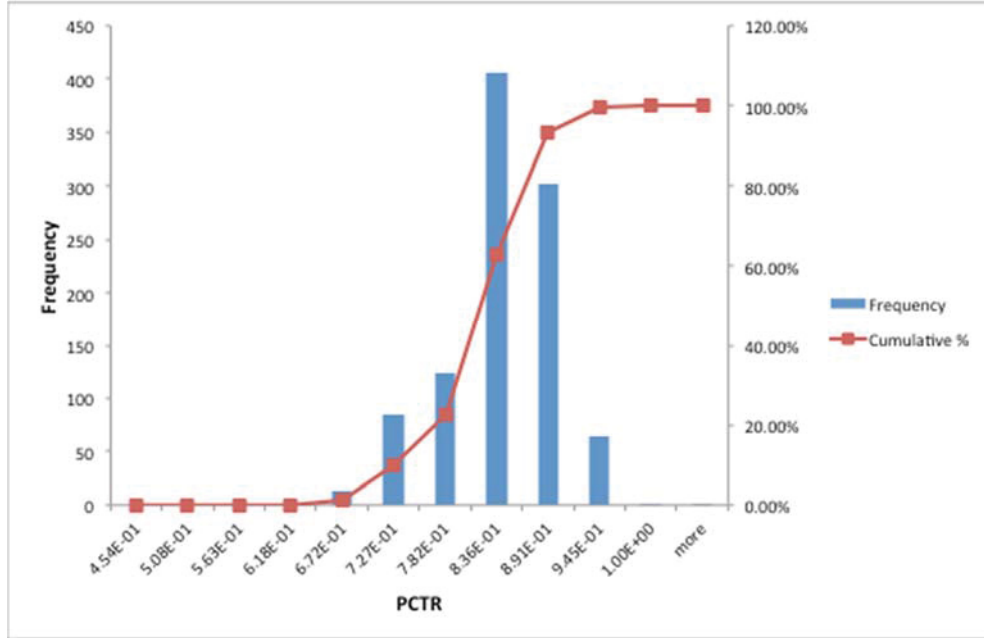


Figure 57. PDF and CDF for PCTR at EOC.

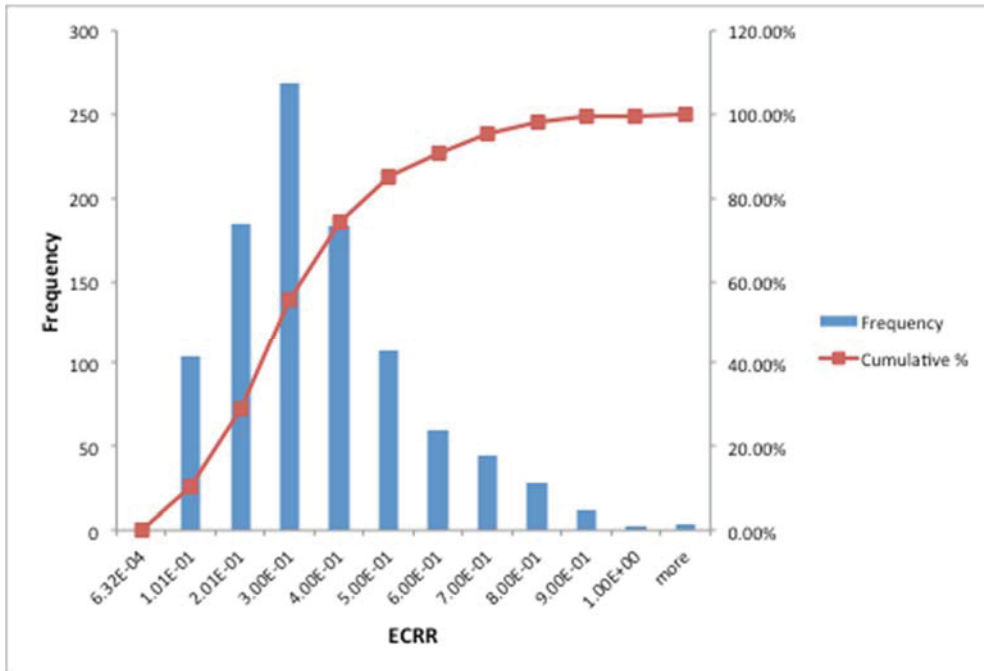


Figure 58. PDF and CDF for ECRR at EOC.

Table 4. Summary of the 95/95 Estimators for PCT and ECR for the HE-LL Core Design.

	PCT (K)		ECR (%)	
	$\mu_{95\%}$	$2.11 * SE_M$	$\mu_{95\%}$	$2.11 * SE_M$
BOC	1404.82	8.54	6.27	0.17
100 Days	1279.86	6.40	2.78	0.08
200 Days	1269.28	4.39	4.43	0.08
300 Days	1412.45	6.38	8.17	0.16
400 Days	1320.00	4.64	6.77	0.10
EOC	1250.39	5.74	3.75	0.09

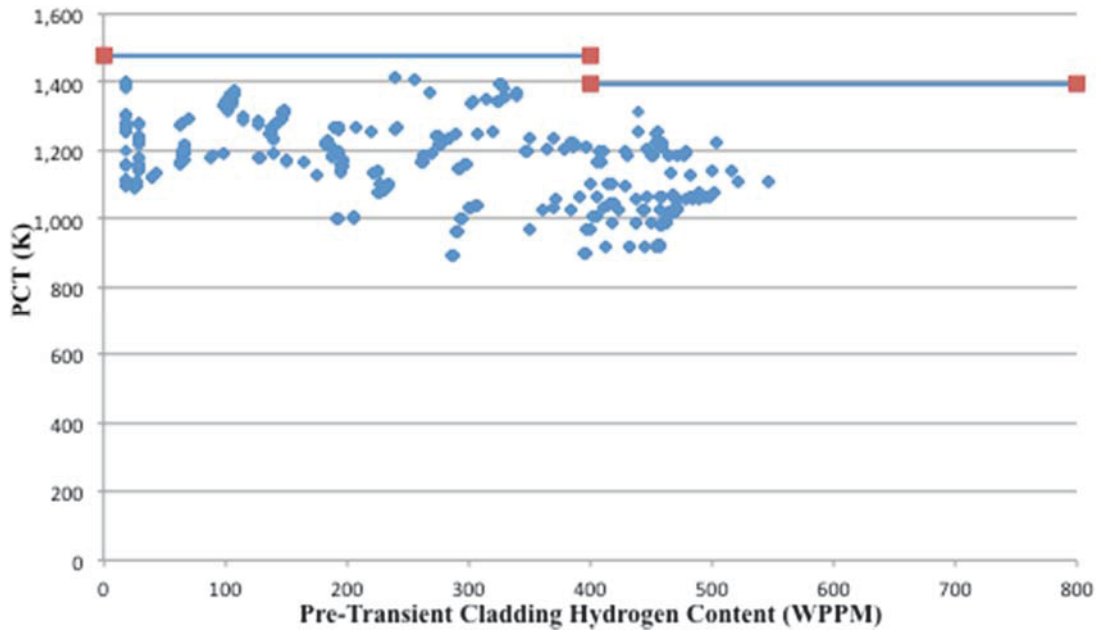


Figure 59. PCT versus Pre-Transient Cladding Hydrogen Content.

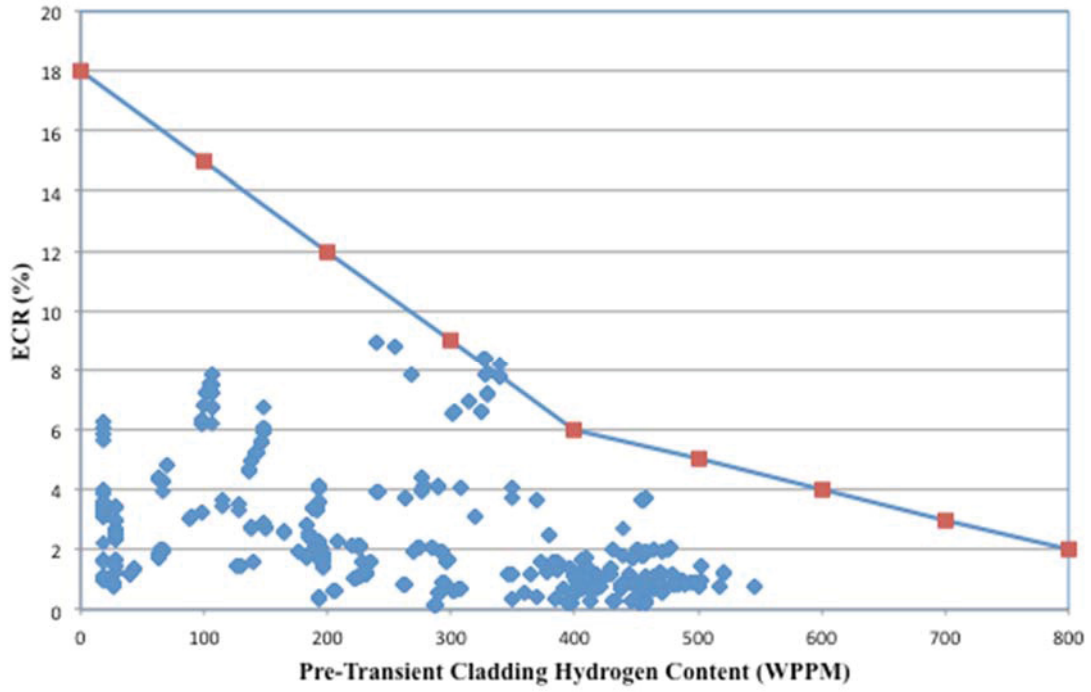


Figure 60. ECR versus Pre-Transient Cladding Hydrogen Content.

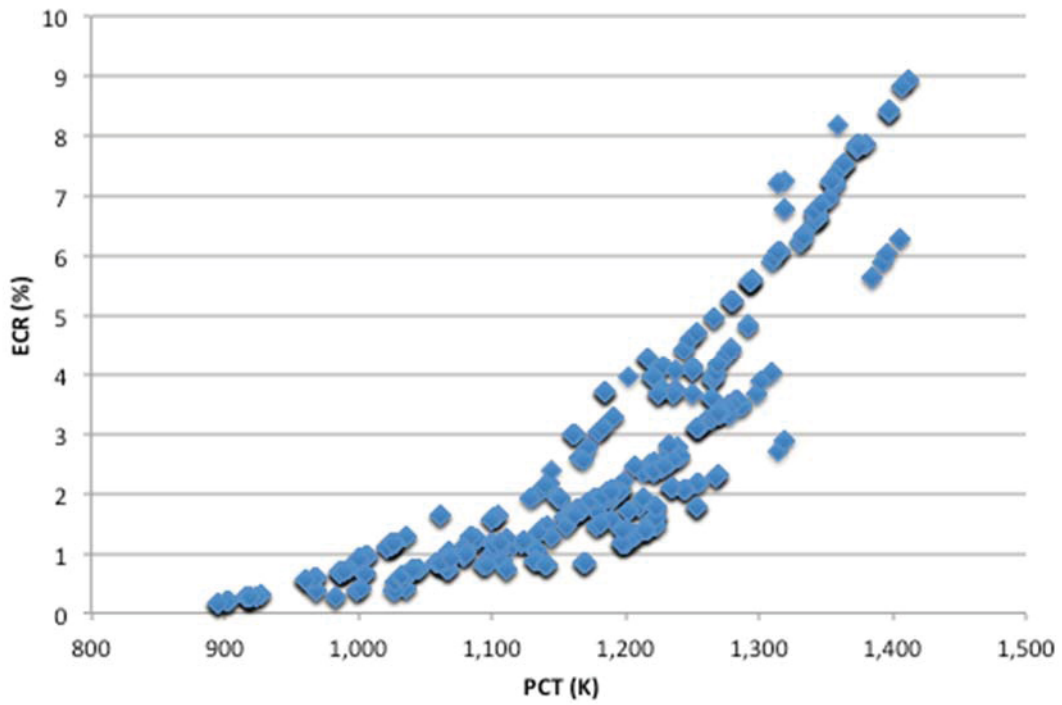


Figure 61. ECR versus PCT for the Limiting Cases.

5.3.2 HE-LL-Optimized (HE-LL-O) Core Design

The results for the RELAP5-3D LB-LOCA simulations for the HE-LL-Optimized core design are summarized in this subsection. The 95% percentile value with 95% confidence interval are calculated following the 1000 RELAP5-3D LB-LOCA simulations at the selected cycle exposure point and the results are summarized in Table 5. The limiting cases are identified from the LB-LOCA simulations and the PCT and ECR values for the hot rod in each assembly in the limiting cases are obtained by LOTUS and shown in Figure 62 for PCT and Figure 63 for ECR. Compared to the results obtained for the HE-LL core design, the HE-LL-Optimized core design has less power peaking and hence the PCT and ECR responses are much less than the acceptance criteria.

Table 5. Summary of the 95/95 Estimators for PCT and ECR for the HE-LL-Optimized Core Design.

	PCT (K)		ECR (%)	
	$\mu_{95\%}$	$2.11 * SE_M$	$\mu_{95\%}$	$2.11 * SE_M$
BOC	1148.45	3.59	1.84	0.03
100 Days	1167.81	3.60	1.32	0.03
200 Days	1154.00	3.62	1.82	0.03
300 Days	1170.57	3.77	1.83	0.03
400 Days	1180.30	3.89	2.14	0.03
500 Days	1189.65	3.76	2.24	0.04
EOC	1243.35	4.07	2.82	0.05

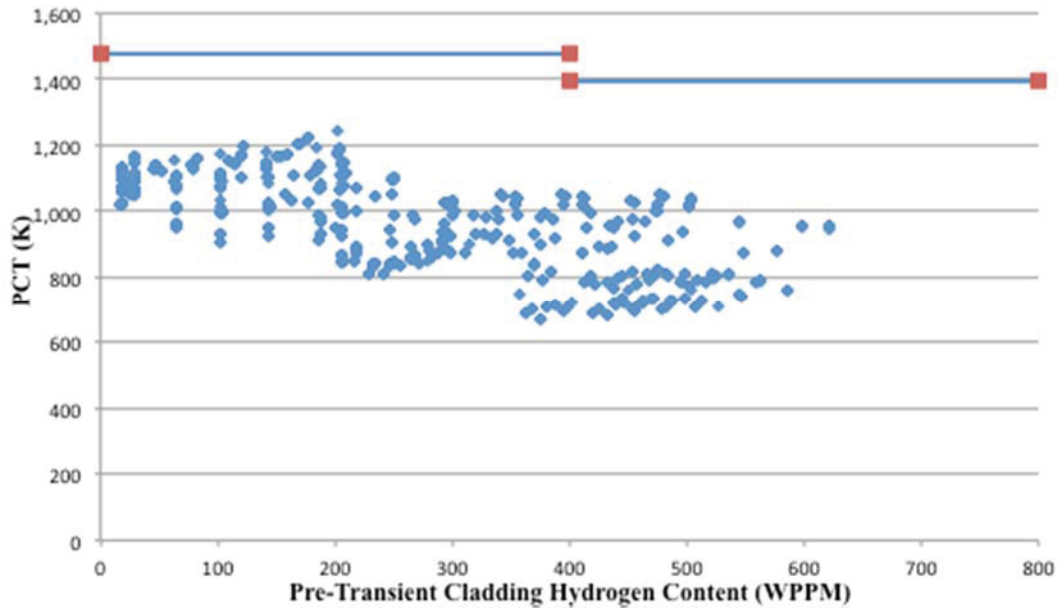


Figure 62. PCT versus Pre-Transient Cladding Hydrogen Content for the Limiting Cases.

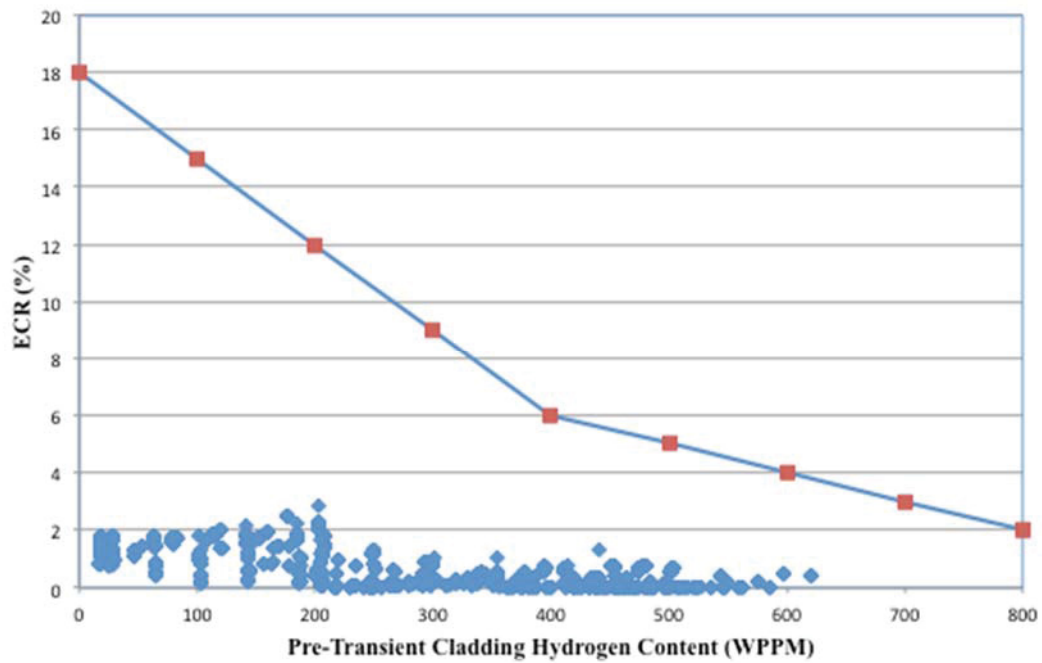


Figure 63. ECR versus Pre-Transient Cladding Hydrogen Content for the Limiting Cases.

5.4 Risk Assessment

In [2] a series of lumped-parameter reduced-order models are presented, in which large-break LOCA analysis can be approximated using simple physics-based equations without the time-consuming rigor of more robust codes. These ROMs divide the core into six characteristic fuel assembly regions: one for each of three fuel burnups (fresh, once burned, and twice burned), as well as a “hot assembly” for each region (fresh, once burned, and twice burned fuels). Simulations for core design, fuel performance, power shaping, steady-state thermal hydraulics, and LOCA analysis are all found in the ROMs. While this work was originally constructed using MATLAB, the ROMs have been replicated in a modular fashion in Python in order to be compatible with MOOSE-based codes and RAVEN in particular.

The process of simulating a LOCA event using these ROMs is as follows. First, the core design ROM is used to determine the burnup of both hot and average assemblies in each region, as well as the relative pin power peaking factors in the same. Second, six distinct fuels performance calculations are performed, one for each average and hot fuel rod in each region. These fuel performance simulations each calculate fuel conductivity properties at each requested axial elevation. Third, the core design and fuels performance data acts as inputs to the steady-state thermal hydraulics ROM, which determines the initial temperature condition before the accident scenario begins. Fourth and finally, the LOCA ROM uses all the previous ROM data to simulate the time, region, and axially-dependent clad temperature as the LOCA progresses.

In order to perform uncertainty quantification, RAVEN was used to perturb inputs unique to each ROM and run the collection. RAVEN was provided the template input file to perturb, and distributions for each uncertain input. RAVEN runs each collection of ROMs in parallel, with a full collection taking a few seconds to evaluate. RAVEN was instructed to take ten thousand Monte Carlo samples, collect the resulting PCTs and ECRs, and perform statistical analysis on them including the expected value of each ROM as a function of burnup and region, as well as the 5th and 95th percentile of the samples. The results of the RAVEN calculation are shown in Figure 64.

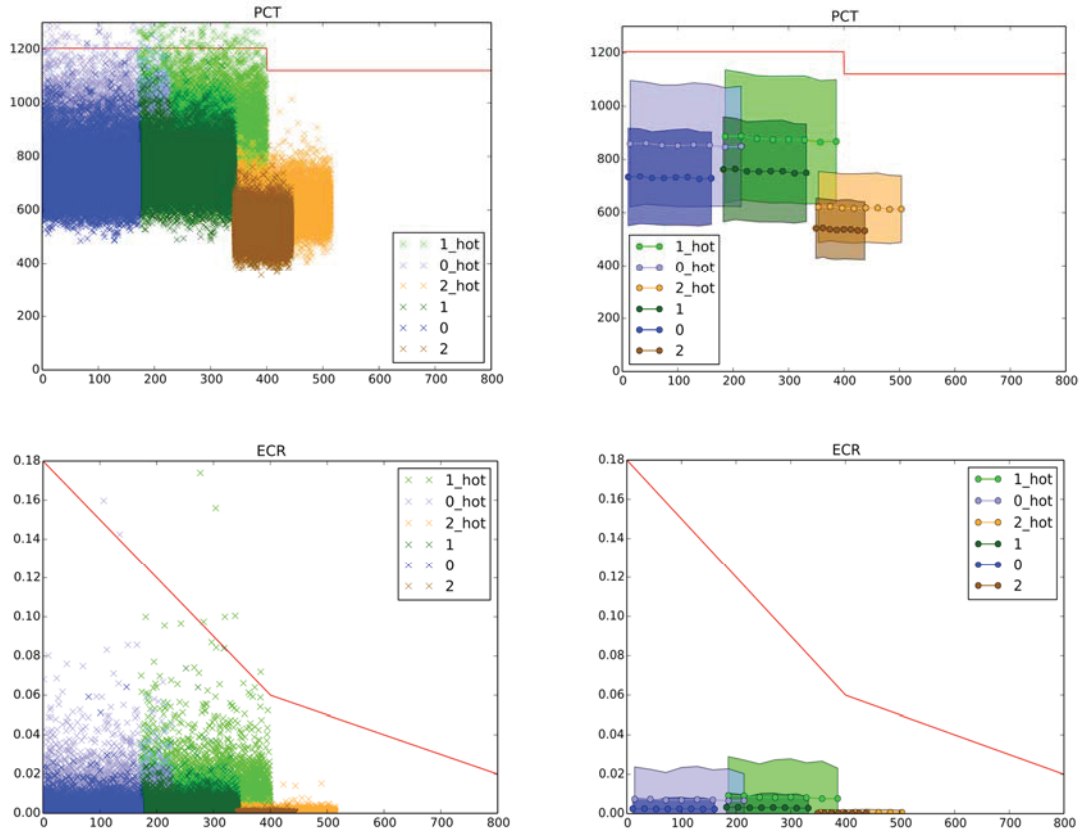


Figure 64. PCT (Top) and ECR (Bottom) ROM Uncertainty Quantification by Region: (Left) Monte Carlo Samples; (Right) Mean with 5-95 Percentiles; (Red) Proposed Limit.

The PCT and ECR samples are shown in Figure 64. On the left are the individual ten thousand Monte Carlo samples, and on the right are the binned mean samples per burnup, along with two standard deviations above and below the mean in solid color (5-95 percentiles). The red line is the NRC proposed regulatory limit. In comparing to the original work presented in [2], the PCT values are nearly identical. The mean values for the ECR are indistinguishable from the original work as well; however, the 95th percentile values are approximately 15% smaller for these models in comparison with the original. It should be noted that the results presented here are obtained using exclusively Gaussian normal distributions for all inputs, while this information was not included in [2]. While there are a few incidents of ECR values exceeding the proposed limit, the probability of these occurring is statistically insignificant, as can be seen by the spread of the 5-95 bands.

6. CONCLUSIONS, FUTURE WORK AND THE PATH FORWARD

6.1 Results Conclusions

The results from the previous sections indicate that the PCT and ECR responses are well characterized by performance based modeling under large break LOCA conditions with two different core design strategies (i.e. the HE-LL and HE-LL-O core designs). It is apparent from Figure 60 that the proposed ECR acceptance criteria may have been violated for the HE-LL core design strategy explored in this study, which would present a challenge in safety margin management had this happened for an operating plant. However, further refinement and additional analyses to the initial models used in this study need to be considered before reaching such conclusion.

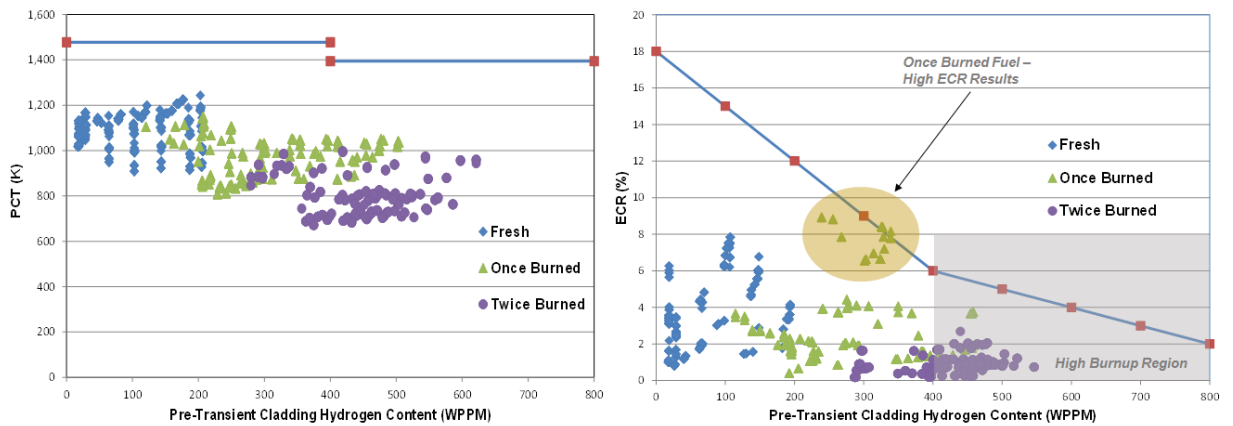


Figure 65. PCT (Left) and ECR (Right) Results by Fuel Type (Burnup) for a HE-LL Core Reload and Design Strategy.

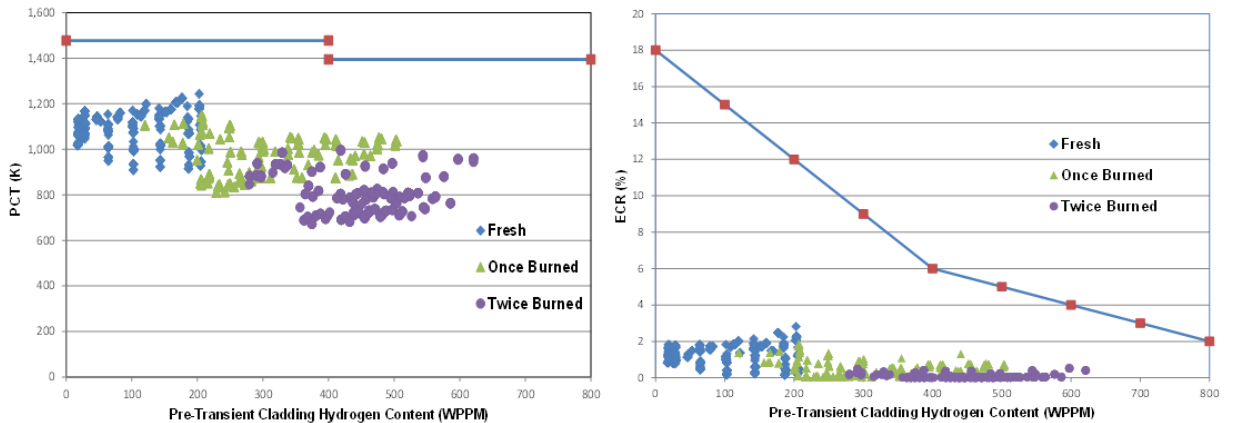


Figure 66. PCT (Left) and ECR (Right) Results by Fuel Type (Burnup) for a HE-LL-Optimized Core Reload and Design Strategy.

In Figure 65 two regions of interest are identified for ECR results (Right): (a) a region with once burned fuel with ECR results approaching a proposed 50.46c limit (yellow-shaded area); and (b) a high burnup region with pre-transient cladding hydrogen contents above 400 wppm (gray-shaded area). A closer look at the fuel performance history and behavior in region (a) is warranted. This could indicate that core designs should be optimized to reduce the peaking for once burned fuel. On the other hand, for the HE-LL-Optimized core design, with results shown in Figure 66, the compliance to the proposed acceptance criteria is demonstrated with significant safety margin available. Fuel behavior in region (b) is also important, and deserves further analysis. Modeling behavior of high burnup fuel is a challenge with today's tools, as post-LOCA fuel/clad behavior is poorly understood.

As shown in Figure 65 and Figure 66, these demonstration calculations illustrate the importance of exploring core design optimization capabilities within the LOTUS framework in order to provide a complete toolkit to perform Risk-Informed Safety Margin Management for the existing LWR fleet. Core design optimization is essential for fuel cycle economics, safety margin management and planning for future cycles. Since nuclear fuel typically stays in a reactor for three (and possibly more) consecutive cycles, planning of loading and operating strategies needs to be well thought of. Therefore, a robust optimization capability would play an essential role to keep the current LWR fleet operating economically.

6.2 IA1 Future Work

In this section we discuss areas of interest of future work needed to further improve our modeling capabilities and understanding of complex phenomena such as time dependent core and fuel performance under various realistic conditions. We identify five areas of interest. They are described below in no particular order of importance.

The **first area of future work** going forward in the LOTUS framework development would be on developing the core design optimization capability.

Figure 60 shows that the ECR values are close to the acceptance criteria for the twice burned fuel which has high burnup. High burnup fuel behavior under transient conditions is not yet well characterized and understood. Thus far in our demonstration calculations, fuel performance calculations were used to provide the correct steady-state initialization of the fuel rods in the core prior to LOCA calculations. We rely on the simplified fuel performance model in RELAP5 to capture the fuel behavior under LOCA conditions. Since the metal-water reaction model developed by Cathcart is implemented in RELAP5-3D, the ECR values calculated using RELAP5-3D are adequate to demonstrate the compliance to the 10 CFR 50.46c rules. However, in order to provide more mechanistic modeling of fuel behavior under LOCA conditions such as fuel rod balloon and burst, fuel fragmentation, relocation and dispersal, fuels performance codes have to be coupled with system analysis codes. Additionally, the effects of oxygen diffusion from the cladding inside surfaces have to be considered for high burnup fuel under LOCA conditions. Oxygen sources may be present on the inner surface of irradiated cladding due to gas-phase UO₃ transport prior to gap closure, fuel-cladding-bond formation, and the fuel bonded to this layer. Under LOCA

conditions, this available oxygen may diffuse into the base metal of the cladding. Currently no models exist to account for the oxidation of the clad inner surfaces. One approach is to take the ECR values calculated from the clad outer surface oxidation and multiply them by 2 to account for the “double-sided oxidation” effect. Given the fact that the available ECR acceptance criteria are much reduced for the high burnup fuel with the new rules, this approach may be too conservative and mechanistic modeling would be required. Therefore, the **second area of future work** for the LOTUS framework development is to couple FRAPTRAN and BISON with system analysis codes such as RELAP5 and RELAP-7 to provide a comprehensive evaluation of clad inner surface oxidation, balloon and burst potential, fuel fragmentation, relocation and dispersal taking into consideration burnup under LOCA conditions. It is noted that clad inner surface oxidation, fuel fragmentation, radial relocation and dispersal models are to be developed in FRAPTRAN and BISON. This effort will help the development of FRAPTRAN (NRC) and BISON (CASL) on their development activities to address these very challenging issues under LOCA conditions.

The **third area of the future work** is to extend the LOTUS analysis capability to support the development and licensing of the accident tolerant fuel (ATF). Accident tolerant fuel aims at developing advanced cladding materials and fuel designs to achieve superior performance under accident conditions such as LB-LOCA. It has the potential to enable fuel to have high enrichment and to achieve much higher burnup beyond the current licensing limit of 62 GWd/tHM such that the fuel cycle economics and reactor safety can be greatly improved. However in order to achieve this objective, experiments are needed to support the characterization and the licensing of ATF. The TREAT facility at INL will be used to conduct the experiments for ATF. The LOTUS framework can be used to perform risk-informed simulations to inform the design and the execution of the experiments to be conducted at TREAT and to analyze experiments after they are done.

The **fourth area of future work** is to work with current plant operators in using the RISMC toolkit to achieve as effective, efficient core performance as possible. The South Texas Project (STP) plant, with the assistance of the Texas A&M University TAMU) have expressed interest in building a generic PWR plant model to represent the STP PWR plant. In this generic PWR plant model, all important core and fuel design, and thermal hydraulics components will be incorporated into a LOTUS modeling environment to study and optimize plant performance.

The **fifth area of future work** is to further develop the LOTUS framework such that detailed information for limiting fuel rod performance can be readily obtained such as the location, fuel type, burnup condition, peaking condition, etc., so that fuel behavior can be better understood.

6.3 Path Forward

The idea behind the first Industry Application is the development of an Integrated Evaluation Model that is motivation to revisit how risks and uncertainties are quantified across the physical disciplines for the safety analysis in the proposed NRC rule 10 CFR 50.46c. The use of an integrated approach in managing the data stream across the various engineering calculations in this Industry Application is one of the most challenging aspects

of the INL research and development. The Integrated Evaluation Model developed in by INL for Industry Application #1 (IA1) (LOTUS) is proposing a solution to this problem.

From the nuclear power perspective, we are engaging staff from both South Texas Project (STP) and the Texas A&M University (TAMU) in the research for constructing LOTUS tailored to an existing nuclear power plant. The TAMU researchers offer collaborative expertise for design, modeling, and simulation of the pressurized water reactor. Toward that end, TAMU is assisting INL on the development and application of LOTUS for STP by constructing the associated thermal-hydraulics model that was used for the large break LOCA demonstration in this study. While the thermal-hydraulics model is built using existing plant information, to the extent possible, plant and fuel proprietary information is being replaced by generic and/or publicly available information in order to facilitate the sharing of information to all interested stakeholders.

Further, with the assistance of STP, TAMU has started the construction of a database of information that will assist in the core design automation, the fuel/clad modeling, and the thermal-hydraulics systems analysis. These items are deemed essential to conduct future modeling and simulation and safety analyses activities using the LOTUS framework.

The importance of the LOTUS framework also extends to current and future nuclear fuels applications. The technical basis for burnup extension (to higher limits) will require additional data to better model fuel behavior at the expected new burnup limit. During FY2016, we collaborated with the EPRI Fuels Reliability Program on IA1. Out of this interaction, we have key specific data and modeling needs that are considered of high priority to the industry. For example, a majority of high burnup fuel is expected to operate at low power in the last cycle of operation and should not pose a challenge from fuel fragmentation perspective. However, during a postulated LOCA, the question of whether a rod bursts or not depends on the emergency core cooling system (ECCS) performance and thus complicates the fuel fragmentation impact evaluation. A comprehensive evaluation of balloon and burst potential, taking into consideration burnup, is needed to gauge both the magnitude and disposition of the issue. The RISMC IA1 framework has tools suitable for this evaluation. These RISMC tools could be used to perform a sensitivity/probabilistic evaluation, taking into consideration a targeted plant's systems, to obtain fuel rod balloon and burst potential/pin count. Such higher fuel burnup applications and the potential for evaluation models that offer solutions to these issues is appealing to organization such as Southern Co., Exelon, and the Tennessee Valley Authority.

The progress shown on the Industry Application #1 will also provide secondary benefits for other technical challenges such as the evaluation and characterization of accident tolerant fuels (ATF) being researched by DOE. Having an integrated multi-physics toolkit that is fuel/clad-, fuel cycle-, and scenario-centric provides a ready platform for the analysis of novel fuel and cladding systems. The importance of ATF applications in the current operating nuclear fleet has been emphasized by NEI, Exelon, and others at the 2016 ANS Utility Working Conference in August 2016, at which the INL RISMC researchers were invited to present our ATF work. At the opening plenary session of this venue, entitled "Delivering the Nuclear Promise / Light Water Reactor Sustainability," Scot Greenlee, Senior Vice President of Engineering and Technical Services for Exelon

Nuclear, spoke of the importance and relevance of ATF in achieving the efficiency goals of the Delivering the Nuclear Promise Initiative. Dr. Kathy McCarthy, Director of the Light Water Reactor Sustainability Program Technical Integration Office, followed by explaining how the DOE LWRS Program is engaged in assisting the nuclear industry to achieve such goals. Mr. Greenlee went further in describing “game changing” attributes of the Delivering the Nuclear Promise Initiative that have the potential to transform the nuclear industry; these elements are: (a) Risk-Informed Regulation and Thinking; (b) Accident Tolerant Fuel; and (c) the Digital Plant. Items (a) and (b) are the focus of several of the RISMC industry applications.

Lastly, an important facet of the engagement related to RISMC Tool development is continued interaction with the U.S. Nuclear Regulatory Commission. Engagement with the NRC includes technical briefings by the RISMC research team, updates on the RISMC Tools development and applications, and overview of the IA1 approach being used by RISMC, highlighting the advanced tools and integration approach we are using to solve this complex issue. The value of interacting with the NRC on the RISMC research and development, especially for Industry Application #1 is echoed by the industry and academic communities.

7. REFERENCES

1. U.S. NRC, Draft Regulatory Guide DG-1263, ADAMS Accession Number ML111100391, U.S. NRC, Washington, DC, <http://pbadupws.nrc.gov/docs/ML1111/ML111100391.pdf>.
2. R. Szilard, et. al., "Industry Application Emergency Core Cooling System Cladding Acceptance Criteria Early Demonstration," Idaho National Laboratory, INL/EXT-15-36541, September 2015.
3. R. Szilard, et. al., "R&D Plan for RISMC Industry Application #1: ECCS/LOCA Cladding Acceptance Criteria," Idaho National Laboratory, INL/EXT-16-38231, April 2016.
4. R. H. Szilard, et. al., "Industry Application Emergency Core Cooling System Cladding Acceptance Criteria Problem Statement," INL-EXT-15-35073, April 2015.
5. S. S. Wilks, "Determination of Sample Sizes for Setting Tolerance Limits," *The Annals of Mathematical Statistics*, Vol. 12, no. 1, pp. 91-96, 1941.
6. C. Rabiti, et. al., "New Simulation Schemes and Capabilities for the PHISICS/RELAP5-3D Coupled Suite," *Nuclear Science and Engineering*, **Vol. 182**, 104-118, January 2016.
7. Y. Wang, et. al., "Krylov Solvers Preconditioned with the Low-Order Red-Black Algorithm for the PN Hybrid FEM for the INSTANT Code," *Proc. Conf. M&C 2011*, Rio de Janeiro, Brazil, 2011.
8. A. Alfonsi, et. al., "PHISICS Toolkit: Multi-Reactor Transmutation Analysis Utility-MRTAU," *Proc. Conf. Advances in Reactor Physics (PHYSOR 2012)*, Knoxville, Tennessee, April 15-20, 2012.
9. A. Epiney, et. al., "PHISICS Multi-Group Transport Neutronic Capabilities for RELAP5," *Proc. Int. Congress Advances in Nuclear Power Plants (ICAPP 2012)*, Chicago, Illinois, June 24 –28, 2012, American Nuclear Society (2012).
10. N. P. Luciano, et. al., "THE NESTLE 3D NODAL CORE SIMULATOR: MODERN REACTOR MODELS," *ANS MC2015 Joint International Conference on Mathematics and Computation (M&C), Supercomputing in Nuclear Applications (SNA) and the Monte Carlo (MC) Method*, Nashville, TN, April 19-23, 2015, on CD-ROM, American Nuclear Society, LaGrange Park, IL (2015).
11. F. N. Gleicher, J. Ortensi, et. al. "The Coupling of the Neutron Transport Application RATTLESNAKE to the Fuels Performance Application BISON," International Conference on Reactor Physics (PHYSOR 2014), Kyoto, Japan, (May 2014).
12. CASL-U-2014-0014-002, "VERA Common Input User Manual, Version 2.0.0," Revision 2, February 2015.
13. CASL-U-2015-0077-000, "MPACT User's Manual Version 2.0.0," February 2015.

14. C.A. Wemple, H-N.M. Gheorghiu, R.J.J. Stamm'ler, E.A. Villarino, "The HELIOS-2 Lattice Physics Code," 18th AER Symposium on VVER Reactor Physics and Reactor Safety, 19-23 September 2011, Eger, Hungary.
15. CASL-U-2015-0055-000, "CTF – A Thermal-Hydraulic Subchannel Code for LWRs Transient Analysis," February 2015.
16. S. W. Lee, et. al., "Analysis of Uncertainty Quantification Method by comparing Monte-Carlo Method and Wilks' Formula," *Nuclear Engineering and Technology*, **Vol. 46**, 481-488, August 2014.
17. D. Ayres, et. al., "Uncertainty Quantification in Nuclear Criticality Modelling Using a High-Dimensional Model Representation," *Annals of Nuclear Energy*, **Vol. 80**, 379-402, May 2015.
18. I. Catton, et. al., "Application of Fractional Scaling Analysis to Loss of Coolant Accidents: Component Level Scaling for Peak Clad Temperature," *Journals of Fluids Engineering*, **Vol. 131**, no. 121401, 2009.
19. K. J. Geelhood, et. al., "FRAPCON-4.0: A Computer Code for the Calculation of Steady-State, Thermal-Mechanical Behavior of Oxide Fuel Rods for High Burnup," PNNL-19418, Vol. 1 Rev. 2, September 2015.
20. K. J. Geelhood, et. al., "FRAPTRAN-1.5: A Computer Code for the Transient Analysis of Oxide Fuel Rods," NUREG/CR-7023, Vol. 1 Rev. 1, PNNL-19400, Vol. 1 Rev. 1, May 2014.
21. J. D. Hales, et. al., "BISON Theory Manual, The Equations behind Nuclear Fuel Analysis," Idaho National Laboratory, Jan., 2015.
22. INL, *RELAP5-3D Code Manual Volume I: Code Structure, System Models and Solution Methods*, INEEL-EXT-98-00834, Rev. 4, June, 2012.
23. RELAP-7 Theory Manual, INL/EXT-14-31366, Idaho National Laboratory, February 2014.
24. D. Mandelli, et. al., "BWR Station Blackout: A RISMC Analysis Using RAVEN and RELAP5-3D," *Nuclear Technology*, vol. 193, 161-174, January 2016.
25. N. Horelik, B. Herman, B. Forget, K. Smith, "Benchmark for Evaluation and Validation of Reactor Simulations (BEAVRS), v1.0.1," Proc. M&C 2013, Sun Valley, Idaho, May 5-9, 2013.



APPENDIX

HE-LL and HE-LL-O Core Design Characteristics

A.1. INTRODUCTION

This appendix section provides referenced data for the development of a PWR Westinghouse 4-Loop High-Enrichment Low-Leakage (HE-LL) core. The information reported hereafter has been collected from publicly available documentation. The HE-LL and HE-LL-O cores are the reference cores for the development of the Industrial Application #1 (LOCA analyses) of the DOE LWRS/RISMC program, in FY 2016 [A.1]. High fuel enrichment (up to 5 w/o %) and high burnup (up to 62 GWd/tHM) are currently used by the nuclear industry. The information provided in this report (fuel design, core loading scheme, etc.) may allow the development of a state-of-the-art lattice physics model and of a coupled three-dimensional neutronic/thermal-hydraulic model.

This appendix is divided into four sections. In Section A.2, information about the Westinghouse high-burnup fuel, the core design, the fuel loading scheme and the core physics parameters is provided. In Section A.3, expected results for the validation of the computational models are reported. Section A.4 lists the references.

A.2. FUEL CYCLE SPECIFICATIONS

A.2.1. Nuclear Power Plant Characteristics

The reference nuclear power plant (NPP) is a Westinghouse 4-Loops plant having a reactor power of 3411 MW_{th}. Several units with similar characteristics are in operation in the U.S., e.g. Seabrook NPP, McGuire and Catawba NPPs [A.2]. Some of these units have recently performed a power uprate. The information about the HE-LL fuel cycle design reported in this document is for a Rated Thermal Power (RTP) of 3648 MW_{th}, which is the power achieved from the reference plant after a Measurement Uncertainty Recapture (MUR) power uprate. The rightmost column of Table A.1 is reporting the bounding values for the corresponding design.

Table A.1. NPP General Parameter.

<u>Reactor Parameter</u>	Reference Design	Power Uprate
Reactor core heat output (MW _{th})	3411	3659
Heat generated in fuel (%)	97.4	97.4
System pressure, nominal (psia)	2250	2250
Total thermal flow rate (10 ⁶ lb _m /hr)	145.73	142.759
Effective flow rate for heat transfer (10 ⁶ lb _m /hr)	138.73	133.09
<u>Coolant Temperature</u>		
Nominal inlet (F)	559.53	557.54
Average rise in core (F)	60.63	67.24
<u>Heat Transfer</u>		
Active heat transfer surface area	59,700	59,700
Average heat flux (Btu/hr-ft ²)	189,800	203,500
Maximum heat flux for normal operation (Btu/hr-ft ²)	474,5005	508,8005
Average linear power (KW/ft)	5.445	5.845
Peak linear power for normal operation (KW/ft)	13.65	14.65
<u>Pressure Drops</u>		
Across core (psi)	28.5±2.857	28.6
Across vessel, including nozzle (psi)	48.7±7.37	48.7

A.2.2. Core Characteristics

The core is cooled and moderated by light water at a pressure of 2250 pounds per square inch absolute (psia) in the Reactor Coolant System (RCS). 193 Westinghouse

Robust-Fuel Assemblies (RFA, see further) are arranged in a squared lattice. The main dimensions and characteristics of the core are reported in Table A.2.

Table A.2. Core Characteristics.

<u>Active Core</u>	
Equivalent diameter (in.)	132.7
Active fuel height, first core (in.)	144.0
Height-to-diameter ratio	1.08
Total cross section area (ft ²)	96.06
H ₂ O/U molecular ratio, lattice (Cold)	2.41
<u>Reflector Thickness and Composition</u>	
Top, water plus steel (in.)	~10
Bottom, water plus steel (in.)	~10
Side, water plus steel (in.)	~15

A.2.3. Fuel Design

A.2.3.1 Westinghouse Robust-Fuel-Assembly

The fuel mechanical design used in the fuel cycles reported in this document is the Westinghouse RFA (Robust FA) design. The RFA main characteristics are given in Table A.3 to Table A.5 and from Figure A.1 to Figure A.4.

All fuel utilizes (Optimized) ZIRLO™ for fuel clad, Control Rod Guide Tubes (CRGT) and instrument thimbles. The top and bottom grids are Inconel-718. The six Low-Pressure Drop (LPD) mid-zone and three Intermediate Flow Mixer grids (IFM) are ZIRLO™ with ZIRLO™ sleeves. In addition, all fuel contains a “Performance+” debris mitigation grid located at the bottom end plug of the fuel rod. The composition of this grid is Inconel-718.

Table A.3. Westinghouse RFA Characteristics.

<u>RFA Parameter</u>	
Number	193
Rod array	17x17
Rods per assembly	264
Rod pitch (in.)	0.496
Overall transverse dimensions (in.)	8.426x8.426
Fuel weight (as UO ₂) (lb. per assembly) [Approx.]	~1138
ZIRLO™ weight (lb. per assembly)	274
Number of grids per assembly	8 – Structural 3 – Intermediate Flow Mixing 1 – Protective Bottom Grid
Composition of grids	ZIRLO™ & Inconel-718
Weight of ZIRLO™ grids in active core region (lb. per assembly)	14.65
Weight of Inconel-718 grids in active core region (lb. per assembly)	2.22
Number of guide thimbles per assembly	24
Composition of guide thimbles	ZIRLO™
Number of instrumentation thimbles per assembly	1
Composition of instrumentation thimbles	ZIRLO™
Diameter of guide thimbles, upper part, above dashpot (in.)	0.442 I.D. x 0.482 O.D. [0.020 in. wall]
Diameter of guide thimbles, lower part, below dashpot (in.)	0.397 I.D. x 0.439 O.D. [0.021 in. wall]
Diameter of instrument guide thimbles (in.)	0.442 I.D. x 0.482 O.D. [0.020 in. wall]

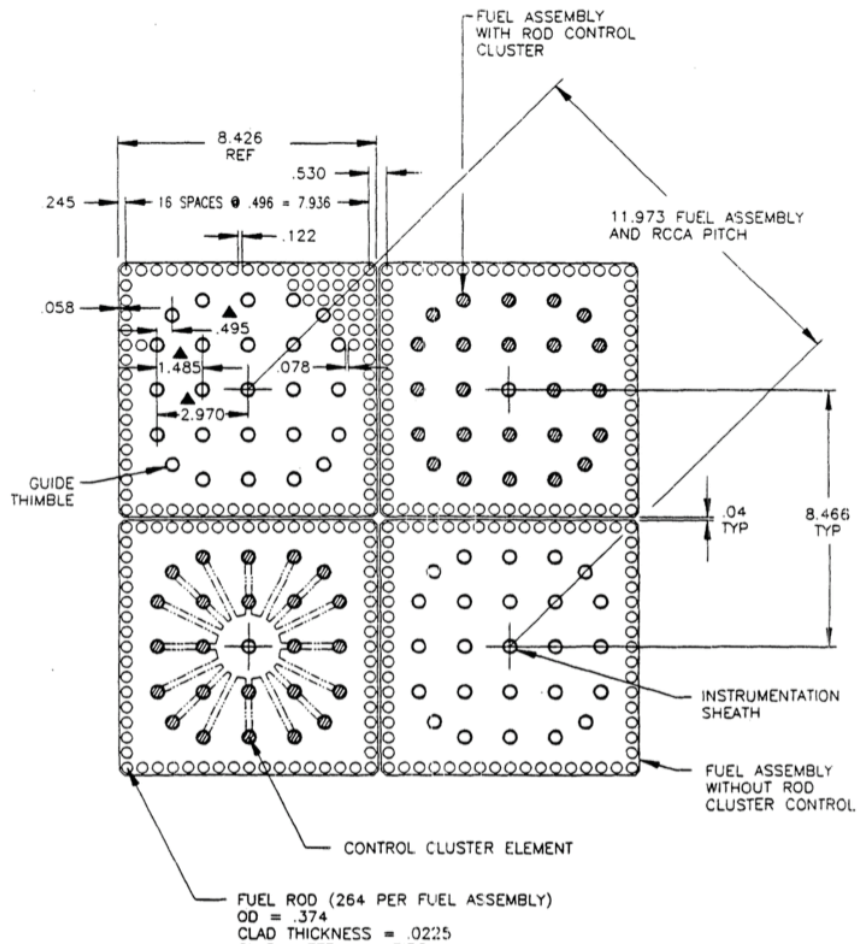


Figure A.1. RFA Core Arrangement.

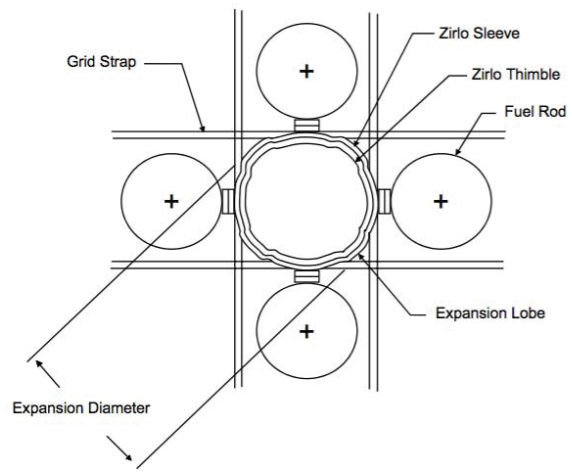


Figure A.2. Fuel Rod Dimensions.

Two hundred and sixty four fuel rods are mechanically joined in a square, 17x17 array to form a fuel assembly. The fuel rods are supported at intervals along their length by LPD grid assemblies and IFM grids, which maintain the lateral spacing between the rods throughout the design life of the assembly. The grid assembly consists of an "egg-crate" arrangement of interlocked straps. The straps contain springs and dimples for fuel rod support as well as coolant mixing vanes. The fuel rods consist of enriched uranium dioxide ceramic cylindrical pellets contained in hermetically sealed zirconium alloy tubing. All fuel rods are pressurized with helium during fabrication to reduce stresses and strains and to increase fatigue life.

Table A.4. RFA Fuel Rods Characteristics.

Fuel Rods	
Number	50,952
Outside diameter (in.)	0.374
Gap thickness (in.)	0.00325
Clad thickness (in.)	0.0225
Clad material	ZIRLO™ / Optimized ZIRLO™

Table A.5. Fuel Pellets Characteristics.

Fuel Pellets	
Material	UO ₂ Sintered
Density (percent of theoretical)	95
Fresh Fuel enrichments w/o	
Typical Low Enrichment	3.6-4.4
Typical High Enrichment	4.0-4.8
Diameter, typical (in.)	0.3225
Length, typical (in.)	0.387
Mass of UO ₂ per foot of fuel rod (lb./ft)	~0.363

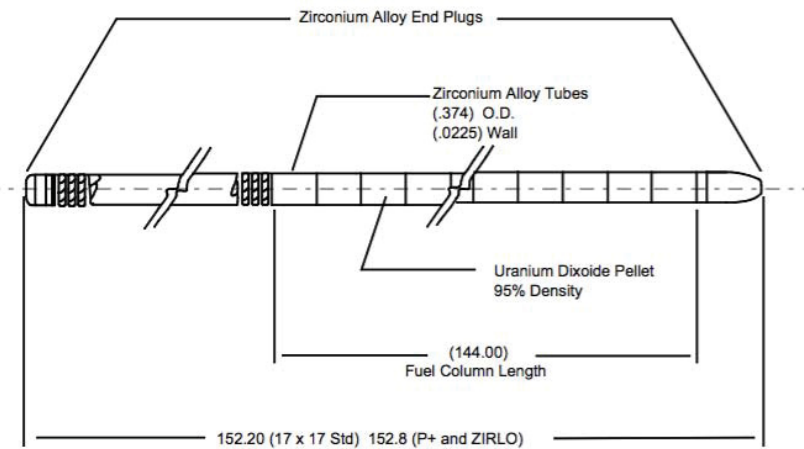
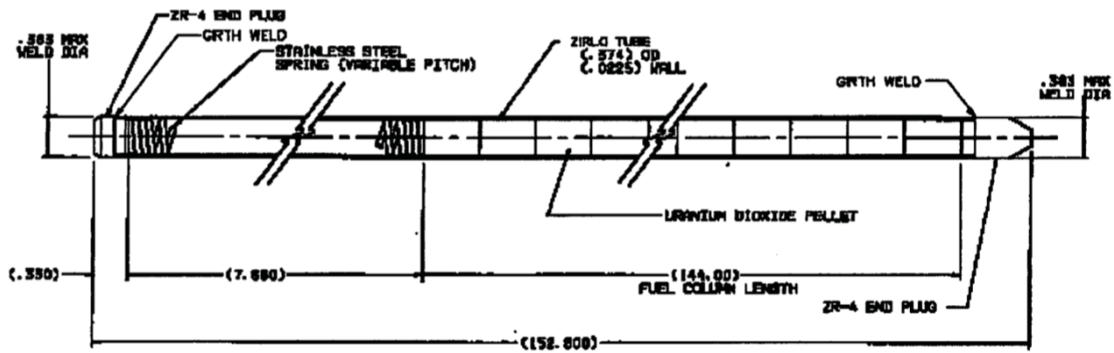


Figure A.3. Fuel Rod Dimensions.

The center position in the assembly is reserved for use by the in-core instrumentation, while the remaining 24 positions in the array are equipped with guide thimbles joined to the grids and the top and bottom nozzles. The guide thimbles may be used as core locations for Rod Cluster Control Assemblies (RCCAs), see further, neutron source assemblies, or burnable poison rods. Otherwise, the guide thimbles can be fitted with plugging devices to limit bypass flow.

The bottom nozzle is a bottom structural element of the fuel assembly, and admits the coolant flow to the assembly.

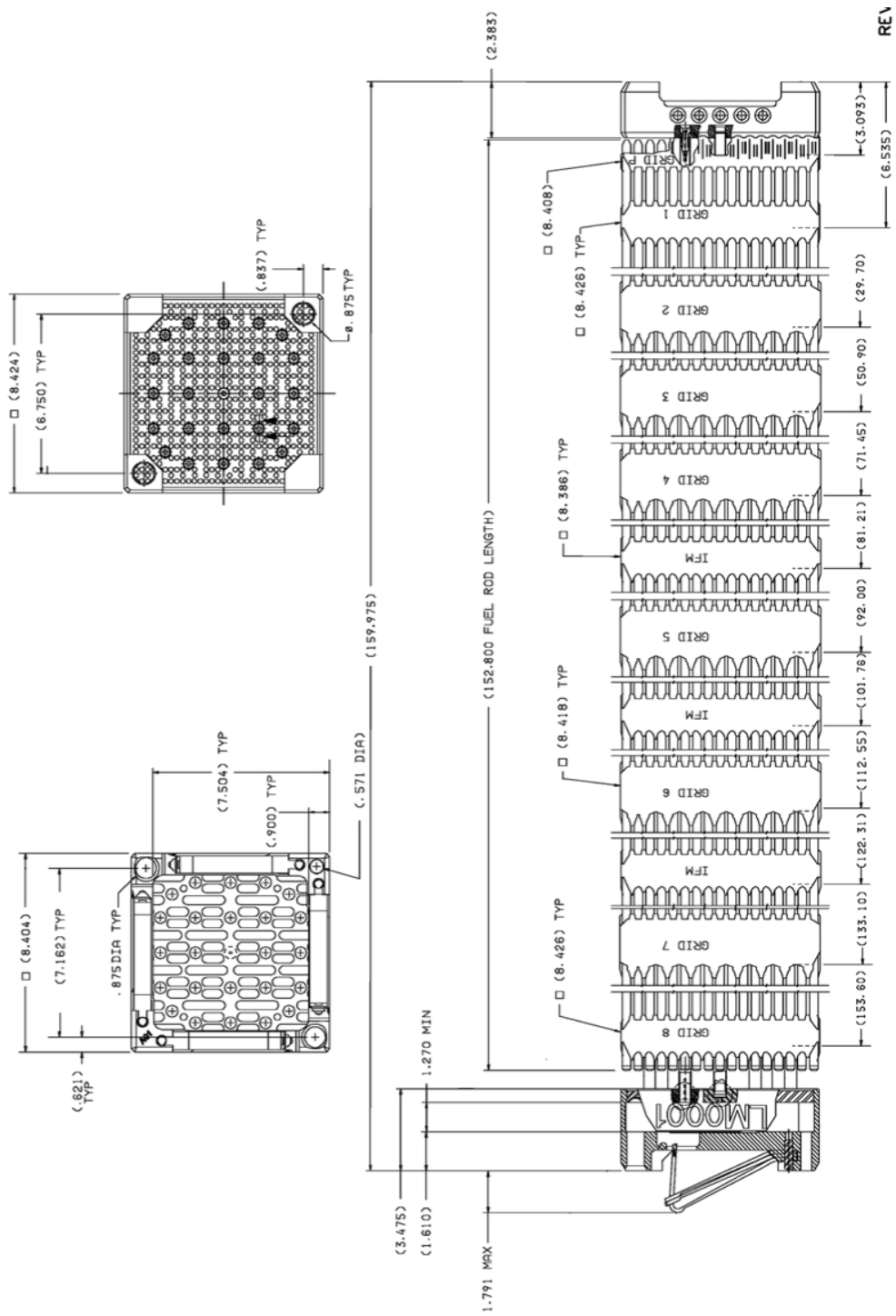


Figure A.4. Westinghouse RFA.

A.2.3.2 Integral Fuel Burnable Absorbers FA

Reactivity control is mainly performed by soluble boron dissolved in the moderator/coolant. Additional boron, in the form of burnable poison rods, were employed in the initial core (first cycle) to establish the desired initial reactivity. Integral Fuel Burnable Absorbers (IFBA) are instead employed in reload fuel for this purpose. IFBAs fuel rod design is identical to the Non-IFBA fuel rod design, with the following exceptions:

- Some of the fuel pellets are coated with a thin layer of zirconium diboride (ZrB_2) on the pellet cylindrical surface;
- The helium back fill pressure for the IFBA fuel rod is lower than the non-IFBA fuel rod.

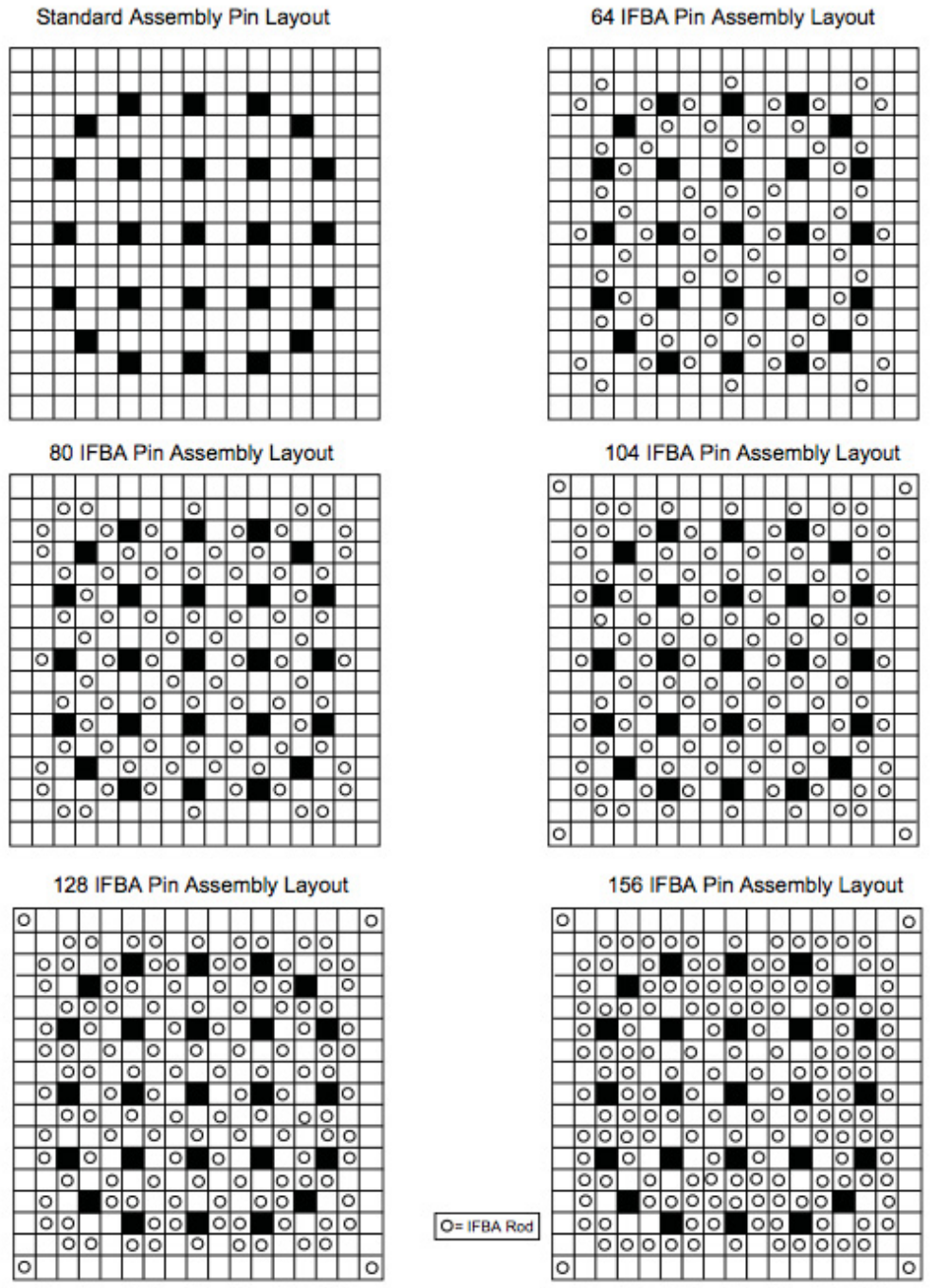
The ZrB_2 coating is referred to as IFBA design. The IFBA pellets are placed in the central portion of the fuel pellet stack (up to 134 inches). The lower back fill pressure for the IFBA rod offsets the increased rod pressure at end of life due to the production and release of helium from the ZrB_2 coating on the IFBA fuel pellets. The main characteristics of an IFBA FA are reported in Table A.6.

Table A.6. IFBA Characteristics.

Integral Fuel Burnable Absorbers (IFBA)	
Number	6,000 – 12,000 (typical)
Material	ZrB_2
Coating Thickness (in.)	0.0002 – 0.0004
B-10 loading (mg/in)	1.57 - 3.14
Initial reactivity worth (%)	Dependent on Number in Assembly

The boron in the rods is depleted with burnup but at a sufficiently slow rate so that the resulting critical concentration of soluble boron is such that the moderator temperature coefficient remains negative at all times for power operating conditions above 20% power.

The number and patter of IFBA rods loaded within an assembly may vary depending on the specific application. For the HE-LL core, Figure A.5 shows the typical IFBA fuel rods within a FA. Their loading pattern is shown in Figure A.6. It should be noted that their loading pattern corresponds to the fresh-fuel loading locations shown on Figure A.9.



G:\Word\images_PIUFSAR434.dwt

Figure A.5. IFBA Fuel Assemblies.

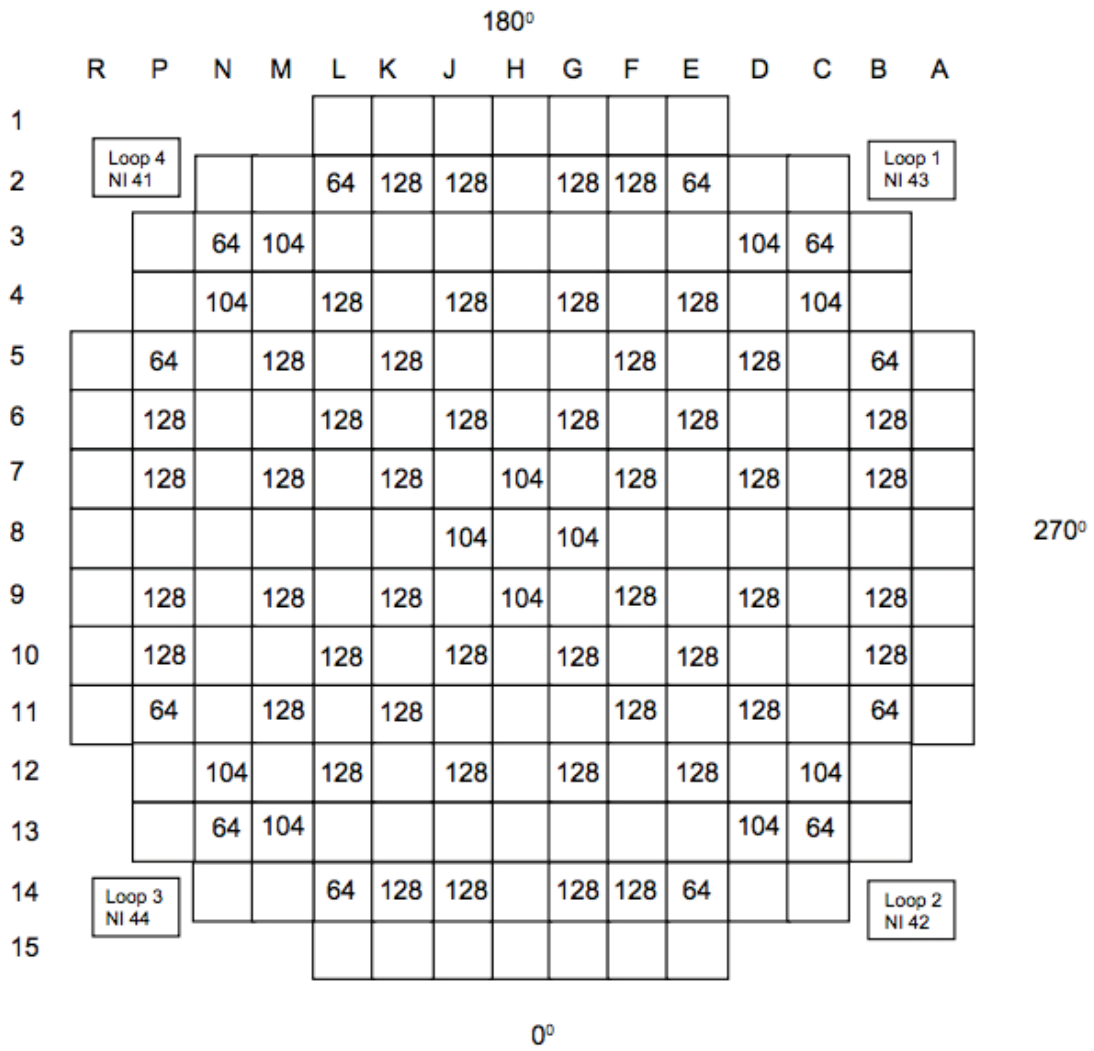


Figure A.6. IFBA Fuel Assemblies Loading Scheme.

A.2.3.3 Control Rod Assembly

The Rod Cluster Control Assemblies (RCCAs) each consist of a group of individual absorber rods fastened at the top end to a common hub called a spider assembly. These assemblies contain absorber material to control the reactivity of the core, and to control axial power distribution. The nuclear design analyses and evaluations establish physical locations for control rods. Moreover, the nuclear design, together with corrective actions of the reactor control and protective systems, provide adequate reactivity control even if the highest reactivity worth RCCA is stuck in the fully withdrawn position.

The RCCAs provide reactivity control for:

- Shutdown;
- Reactivity changes resulting from coolant temperature changes in the power range;
- Reactivity changes associated with the power coefficient of reactivity;
- Reactivity changes resulting from void formation.

Table A.7 reports the main characteristics of the RCCA.

Table A.7. Rod Cluster Control Assembly Characteristics.

Rod Cluster Control Assemblies	
Neutron absorber	Ag-In-Cd
Composition	80%-15%-5%
Diameter (in.)	0.341 Ag-In-Cd
Density (lb./in. ³)	0.367 Ag-In-Cd
Cladding material	Type 304, Cold Worked Stainless Steel
Clad thickness (in.)	0.0185
Number of clusters – full length	57
Number of absorber rods per cluster	24

The Ag-In-Cd Rod Cluster Control Assembly comprises 24-neutron absorber rods fastened at the top end to a common spider assembly. The absorber material used in the control rods is a silver-indium-cadmium alloy which is essentially "black" to thermal neutrons and has sufficient additional resonance absorption to significantly increase its worth. All components of the spider assembly are made from austenitic stainless steel or other corrosion-resistant material such as Inconel. Figure A.7 illustrates the RCCA and control rod drive mechanism assembly, in addition to the arrangement of these components in the reactor relative to the interfacing fuel assembly and guide tubes.

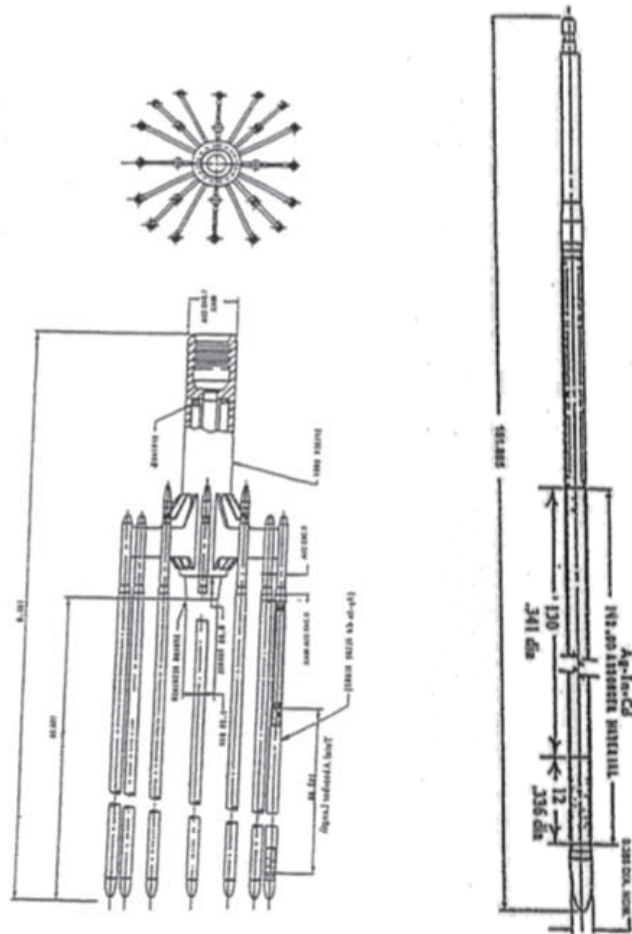


Figure A.7. RCCA & Absorber Rod Dimensions.

The overall length is such that when the assembly is withdrawn through its full travel, the tips of the absorber rods remain engaged in the guide thimbles so that alignment between rods and thimbles is always maintained.

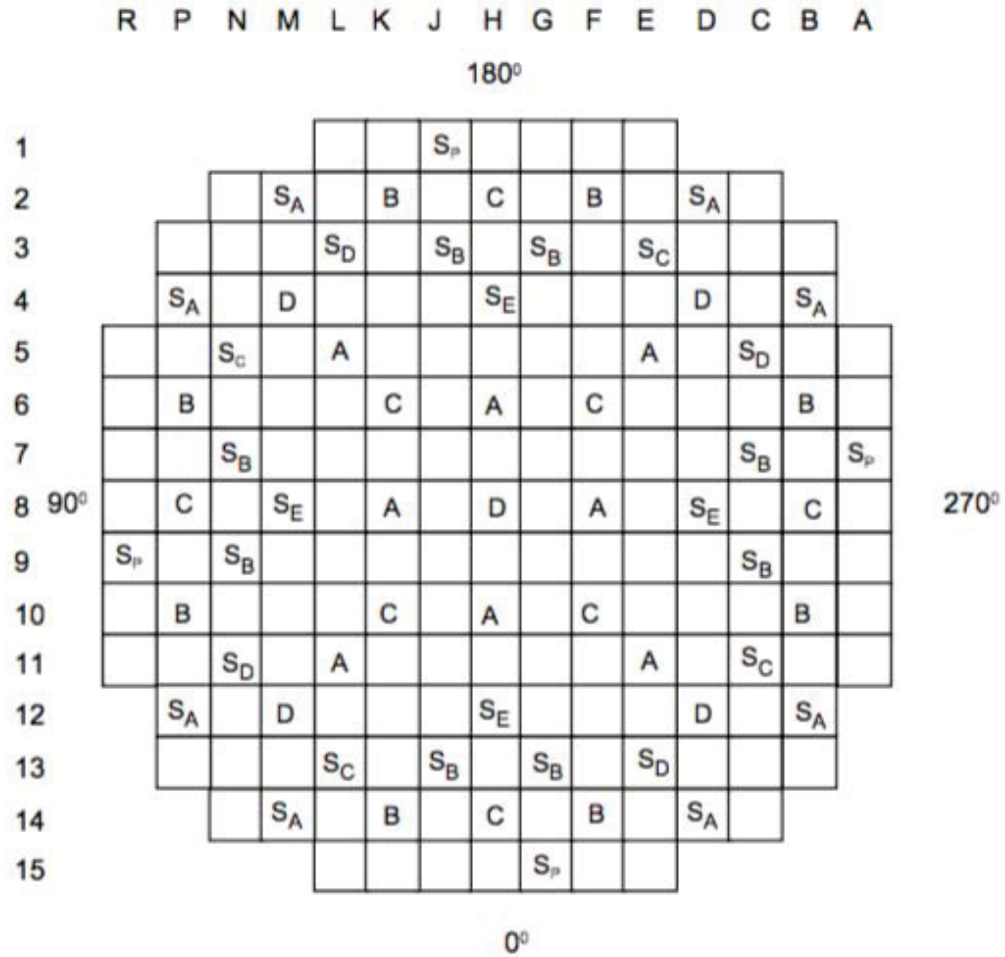
The RCCAs are divided into two categories: control and shutdown.

The control groups compensate for reactivity changes associated with variations in operating conditions of the reactor, i.e., power and temperature variations. These rods may be partially inserted at power operation (this implies that the total power peaking factor should be low enough to ensure that the power capability is met).

Additional shutdown banks are provided which, together with the control banks A, B, C and D, supply reactivity insertion to cover the power defect, plus:

1. transient cooldowns below the hot zero power critical state,
2. an NRC requirement for a minimum of 1 percent hot standby shutdown reactivity,
3. the worth of any full length control rod stuck out of the core,
4. a margin for uncertainty in rod worth and reactivity change calculations.

The control and shutdown groups together provide adequate shutdown margin. Figure A.8 provides a possible location of the RCCAs in a HE-LL type core.



<u>Control Bank</u>	<u>Number of Rods</u>		<u>Shutdown Bank</u>	<u>Number of Rods</u>
A	8		SA	8
B	8		SB	8
C	8	S _p - Spare Locations	SC	4
D	5		SD	4
<u>Total</u>	<u>29</u>		<u>SE</u>	<u>4</u>
			<u>Total</u>	<u>28</u>

Figure A.8. RCCAs Positions.

A.2.4. Nuclear Design Description

The fuel rods are designed for a peak rod burnup of approximately 60,000 megawatt-days per metric ton of uranium (MWd/tHM) in the fuel cycle equilibrium condition. Peak rod burnups as high as 62,000 MWd/tHM can be licensed.

The core will operate between eighteen and twenty-four months between refueling, accumulating between 16,000 MWd/tHM and 24,000 MWd/tHM per cycle.

The fuel rods within a given assembly have the same uranium enrichment in both the radial and axial planes. Fresh fuel assemblies of different enrichments are used in the reload core to establish a favorable radial power distribution. Figure A.9 shows a sample fuel-loading pattern to be used in the reload cores.

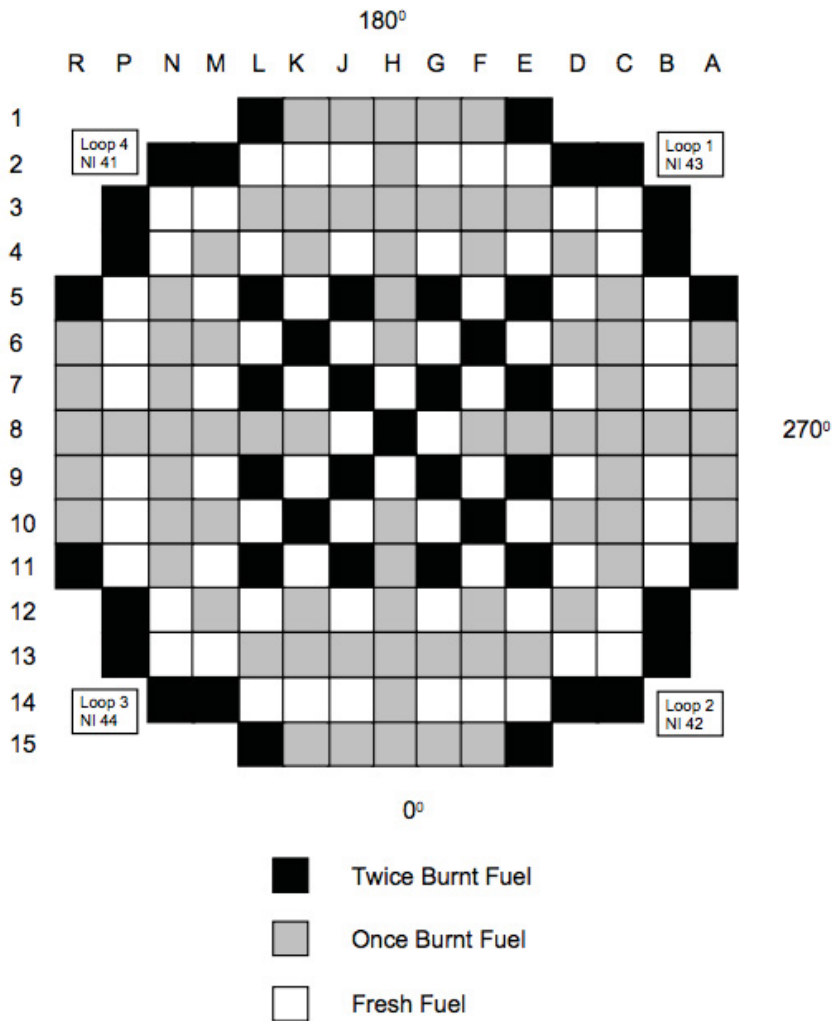


Figure A.9. Loading Arrangement for a Typical Low Leakage Scheme.

The premise for reload designs is for low radial leakage (HE-LL core), achieved by placing low reactivity assemblies around the perimeter of the core. Fresh assemblies are then distributed within the core interior to generate a favorable radial power distribution.

The enrichments for these cores vary with the expected cycle length; typical values are shown in Table A.8. Axial fuel blankets composed by mid-enriched annular fuel pellets are being used to reduce axial neutron leakage and improve fuel utilization.

Table A.8. Loading Sequence for High Burnup Fuel.

Cycle number	Number of fresh FA	FA Enrichments (w/o %)	Blanket Design	Design Burnup Operation
N	28 / 56 [84]	4.50 / 4.95	6 inches, Bottom & Top, Annular, 2.6% w/o enrich.	21,240 MWd/tHM & coastdown to 22,240 MWd/tHM
N+1	52 / 32 [84]	4.20 / 4.60	6 inches, Bottom & Top, Annular, 2.6% w/o enrich.	~21,000 MWd/tHM
N+2	24 / 60 [84]	4.40 / 4.80	6 inches, Bottom & Top, Annular, 2.6% w/o enrich.	~21,000 MWd/tHM
N+3	40 / 40 [80]	4.30 / 4.70	6 inches, Bottom & Top, Annular, 2.6% w/o enrich.	~21,000 MWd/tHM

A.2.5. Reactor Physics Parameters

A.2.5.1 Critical Boron Concentration

The moderator coolant contains boron as a neutron poison. The concentration of the soluble neutron absorber is varied to compensate for reactivity changes due to fuel burnup, fission product poisoning including xenon and samarium, burnable poison depletion, and the cold-to-operating moderator temperature change. Figure A.10 and Figure A.11 show the critical boron concentration for two HE-LL core configurations as function of burnup.

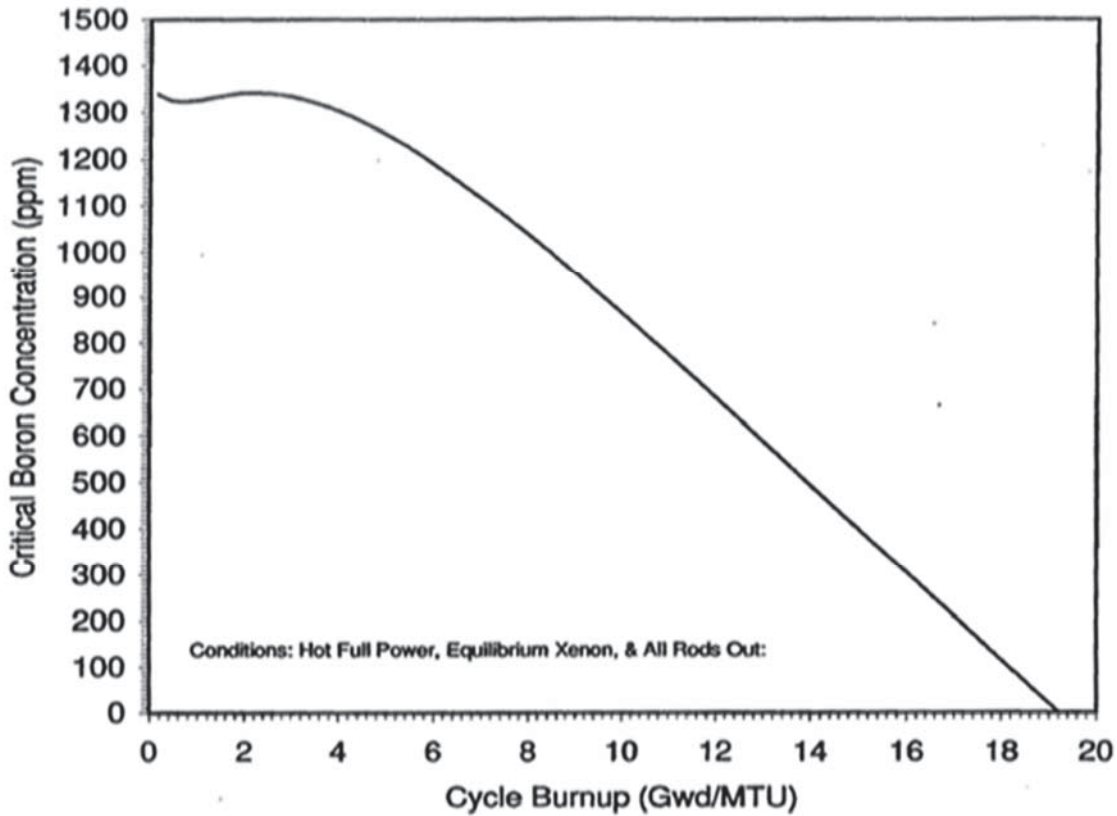


Figure A.10. Critical Boron Concentration for HE-LL Core.

As the boron concentration is increased, the moderator temperature coefficient becomes less negative. The use of a soluble poison alone would result in a positive moderator coefficient at beginning-of-life for the cycle. Therefore, burnable absorber fuel rods are used to reduce the soluble boron concentration sufficiently to ensure that the moderator temperature coefficient is negative for power operating conditions above 20% power.

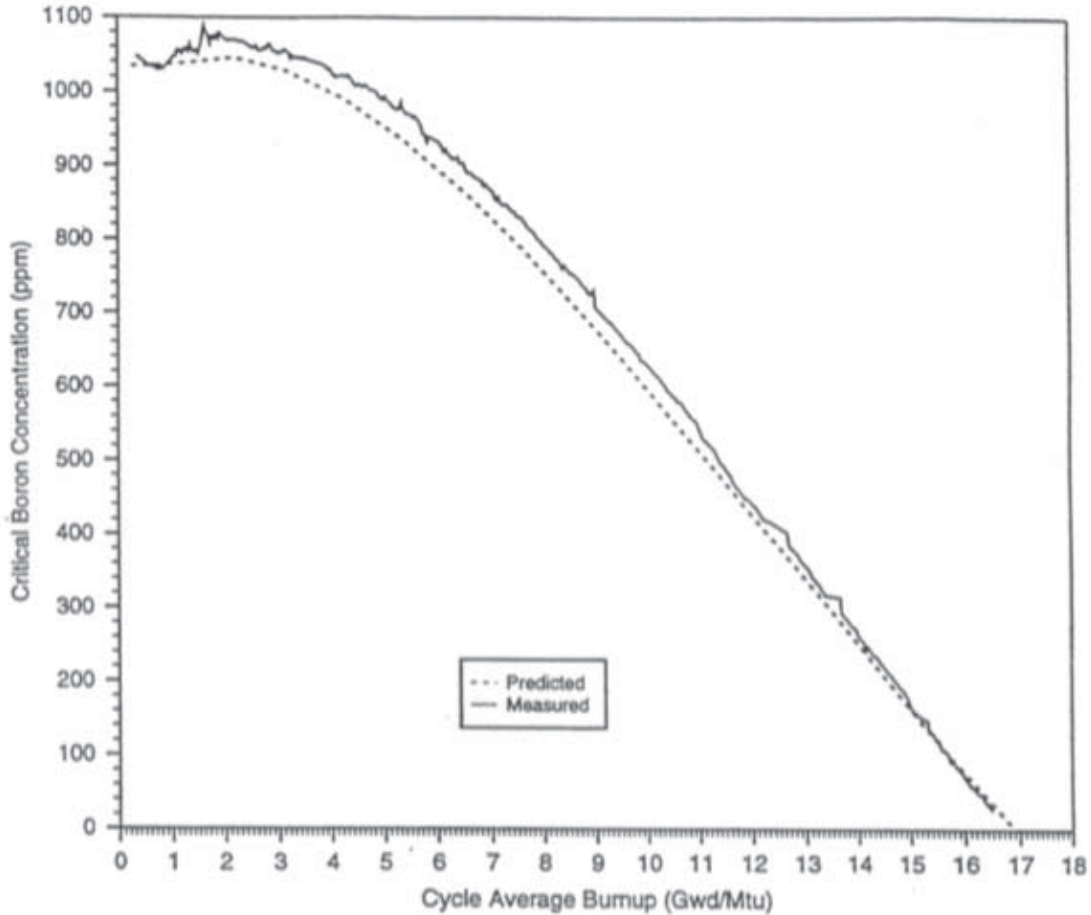


Figure A.11. Critical Boron Concentration for HE-LL Core.

A.2.5.2 Reactivity Coefficients

The fuel temperature coefficient will be negative and the moderator temperature coefficient of reactivity will be non-positive for power operating conditions, above 20% power, thereby providing negative reactivity feedback characteristics. Reactivity coefficients for a typical HE-LL core configuration are reported in Table A.9.

Table A.9. Reactivity Coefficients Range.

Reactivity Coefficients	Design Limits	Best Estimate
Doppler Temperature Coefficient, pcm/F	-3.2 to -0.9	-2.1 to -1.3
Moderator Temperature Coefficient, pcm/F	+5. to -55	+2. to -43.
Boron Coefficient, pcm/ppm	-16 to -5	-14.5 to - 6.5

Note: 1 pcm = (percent mille) $10^{-5} \Delta\rho$, where $\Delta\rho$ is calculated from two statepoint values of k_{eff} by $\ln(k_2/k_1)$

A.2.5.3 Delayed Neutron Fractions

Typical delayed neutron fractions for BOL and EOL for an HE-LL core are reported in Table A.10.

Table A.10. Delayed Neutron Fractions.

Delayed Neutron Fraction, β_{eff}	
BOL	EOL
0.0065	0.0048

A.2.5.4 Power Distributions

A.2.5.4.1 Definitions

Power distributions are quantified in terms of hot channel factors. These factors are a measure of the peak pellet power within the reactor core and the total energy produced in a coolant channel and is expressed in terms of quantities related to the nuclear or thermal design, namely:

- Power density, is the thermal power produced per unit volume of the core (KW/liter).
- Linear power density, is the thermal power produced per unit length of active fuel (KW/ft). Since fuel assembly geometry is standardized, this is the unit of power density most commonly used.
- Average linear power density, is the total thermal power produced in the fuel rods divided by the total active fuel length of all rods in the core.
- Local heat flux, is the heat flux at the surface of the cladding (Btu/ft²-hr).
- Rod power or rod integral power, is the length integrated linear power density in one rod (KW).
- Average rod power, is the total thermal power produced in the fuel rods divided by the number of fuel rods (assuming all rods have equal length).

The hot channel factors used in the discussion of power distribution in this section are defined as follows:

- FQ, heat flux hot channel factor is defined as the maximum local heat flux on the surface of a fuel rod divided by the average fuel rod heat flux, allowing for manufacturing tolerances on fuel pellets and rods.
- FQN, nuclear heat flux hot channel factor, is defined as the maximum local fuel rod linear power density divided by the average fuel rod linear power density, assuming nominal fuel pellet and rod parameters.
- FQE, engineering heat flux hot channel factor is the allowance on heat flux required for manufacturing tolerances. The engineering factor allows for local variations in enrichment, pellet density and diameter, surface area of the fuel rod and eccentricity of the gap between pellet and clad. Combined statistically, the net effect is a factor of 1.03 to be applied to fuel rod surface heat flux.
- F_{dH}^{N} , nuclear enthalpy rise hot channel factor is defined as the ratio of the integral of linear

- power along the rod with the highest integrated power to the average rod power
- F_N^U , is the uncertainty associated with the incore detector system. This factor is assumed to be equal to 1.05.

Manufacturing tolerances, hot channel power distribution and surrounding channel power distributions are treated in the calculation of the DNBR. Design limits are set in terms of the total peaking factor.

$$FQ = \text{Total peaking factor or heat flux hot-channel factor} = \frac{\text{Maximum KW/ft}}{\text{Average KW/ft}}$$

Without densification effects,

$$FQ = FQN \times FQE \times FNU$$

To include the allowances made for densification effect, which are height dependent, the following quantity is defined.

$H(Z)$ = the allowance made for densification effects at height Z in the core. This is called the power spike factor.

Then FQ ,

$$FQ = \max (H(Z) \times FQN \times FQE \times FNU)$$

For modern Westinghouse fuel, $H(Z) = 1.0$ everywhere (no densifications effects).

The envelope drawn over the calculated max ($FQ \times \text{Power}$) points in Figure A.12 represents an upper bound envelope on local power density versus elevation in the core. The calculated values have been increased by the nuclear uncertainty factor FNU for conservatism (1.05) and for the engineering factor FQE (1.03). This envelope is a conservative representation of the bounding values of local power density. Expected values are reported to be considerably smaller.

Allowing for fuel densification effects, the average linear power at a maximum analyzed power level of 3659 MWth is 5.84 KW/ft. Therefore, from Figure A.12, the conservative upper bound value of normalized local power density, including uncertainty allowances, is 2.50 corresponding to a peak linear power of 14.6 KW/ft at full power.

A.2.5.4.1 Radial Power Distributions

While radial power distributions in various axial planes of the core contribute to the axial FQ , the core radial enthalpy rise distribution as determined by the integral of power up each channel is generally of greater interest. The power shape is axially integrated to yield a two dimensional representation of assembly and pin powers (F_{dH}^N). Expected values are reported in Paragraph A.3.2.

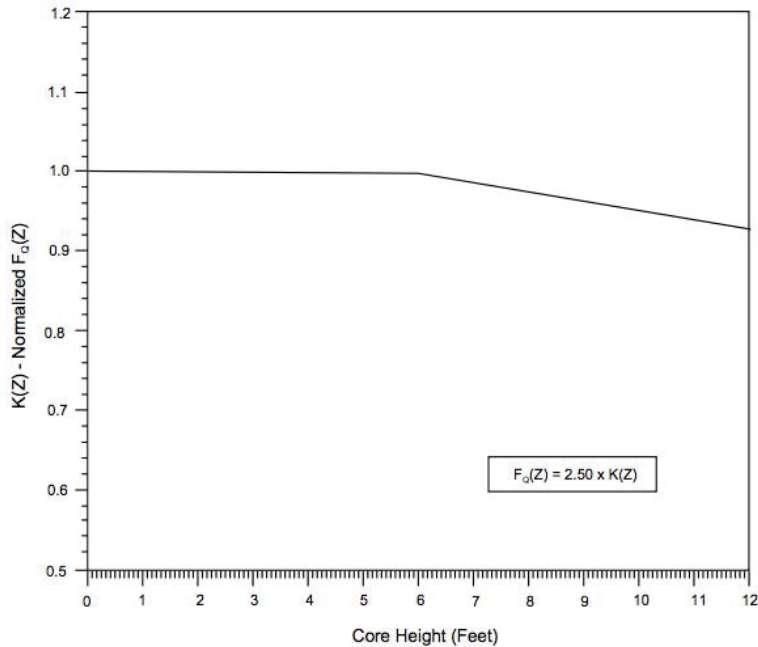


Figure A.12. Normalized F_Q versus Core Height.

A.2.5.4.2 Assembly Power Distributions

Expected assembly power distributions from the BOL and EOL conditions corresponding to a typical HE-LL core FA are reported in Paragraph A.3.4.

A.2.5.4.3 Axial Power Distribution

The shape of the power profile in the axial direction is largely under the control of the operator either through the manual operation of the full-length control rods or automatic motion of full-length rods responding to manual operation of the Chemical and Volume Control System (CVCS). Nuclear effects, which cause variations in the axial power shape, include moderator density, Doppler effect on resonance absorption, spatial xenon and burnup.

Automatically controlled variations in total power output and full-length rod motion are also important in determining the axial power shape at any time. Signals are available to the operator from the ex-core ion chambers, which are long ion chambers outside the reactor vessel running parallel to the axis of the core. Separate signals are taken from the top and bottom halves of the chambers. The difference between top and bottom signals from each of four pairs of detectors is displayed on the control panel and called the flux difference, I . Calculations of core average peaking factor for many plants and measurements from operating plants under many operating situations are associated with either I or axial offset in such a way that an upper bound can be placed on the peaking factor. For these correlations, axial offset I is defined as:

$$I = \frac{\varphi_t - \varphi_b}{\varphi_t + \varphi_b}$$

where ϕ_t and ϕ_b are the top and bottom detector readings, respectively.

Expected representative axial power shapes for typical BOL and EOL unrodded conditions are shown in Paragraph A.3.3.

A.2.5.5 Fuel Design Bases

The RFA fuel rod and fuel assembly design bases are established to satisfy some of the general performance and safety criteria presented hereafter. The fuel rods are designed for a peak rod burnup of approximately 60,000 MWd/tHM in the fuel cycle equilibrium condition. Peak rod burnups as high as 62,000 MWd/tHM can be licensed for Westinghouse fuel in individual fuel cycles using the Westinghouse Fuel Criteria Evaluation Process [A.3], [A.4].

Design values for the properties of the materials, which comprise the fuel rod, fuel assembly and incore control components, are given in [A.5] for ZIRLO™ clad fuel.

In the last years, a growing number of Westinghouse NPPs are making use of the Optimized-ZIRLO™ FAs [A.13], e.g. [A.14], [A.15]. Optimized-ZIRLO™ fuel clad provides improved corrosion resistance for high-duty fuel with a burnup up to 74,000 MWd/tHM.

A.2.5.5.1 Cladding

Material and Mechanical Properties

Zircaloy-4 and ZIRLO™ & Optimized ZIRLO™ combine neutron economy (low absorption cross section); high corrosion resistance to coolant, fuel, and fission products; and high strength and ductility at operating temperatures. Information on the material chemical and mechanical properties of the cladding with due consideration of temperature and irradiation effects are proprietary. Some information can be retrieved in publicly available documentation [A.7], [A.8], [A.9], [A.13]. Optimized-ZIRLO™ composition is given in Table A.11 below [A.17].

Table A.11. Optimized-ZIRLO™ Composition.

Element	Allowable Range (wt. %)
Niobium	0.8 – 1.2
Tin	0.6 – 0.79
Iron	0.09 – 0.13
Oxygen	0.09 – 0.16
Zirconium	Balance

Oxide Layer / Hydrogen Pick-up Limit.

Westinghouse states that Optimized ZIRLO™ is 40% less susceptible to water-side corrosion than ZIRLO™ [A.13]. The reduction of corrosion buildup has a beneficial effect on temperature feedback and ultimately on fuel rod internal pressure. The Optimized ZIRLO™ is expected to perform similarly to standard ZIRLO™ for all normal operating and accident scenarios, including both LOCA and non-LOCA scenarios (however license amendments requests are needed for using the 10 CFR 50 Appendix K / Baker-Just equation) [A.15].

The NRC has approved the use of Optimized-ZIRLO™ FA in 2013 with the following limitation and conditions [A.17], [A.18]:

1. The maximum Thermal Reaction Accumulated Duty (TRDs) are restricted to numbers corresponding to a cladding corrosion amount of **100 microns** for licensing applications. The corrosion formula is proprietary.
2. A (proprietary) waterside hydrogen pickup limit is prescribed for ZIRLO™ and Optimized ZIRLO™. Westinghouse is applying ZIRLO™ hydrogen pick-up limits to Optimized ZIRLO™. According to Pacific North-West National Laboratories (PNNL) this methodology is conservative, since the corrosion and the hydrogen levels appear to be significantly lower than for standard ZIRLO™ (-40% according to [A.13]). Westinghouse has also stated that ZIRLO™ and Zircaloy-4 have essentially the same relationship of hydrogen pickup at an equivalent level of oxidation (ZIRLO™ has a slightly smaller hydrogen pickup fraction compared to Zircaloy-4). Internal hydriding is limited by Westinghouse fuel design that imposes a fuel moisture content of less than 20 ppm.
3. The NRC disapproves the Westinghouse assertion that a single corrosion limit could ensure cladding integrity without a separate hydrogen pickup limit.

Stress-Strain Limits

Clad Stress

The von Mises criterion is used to calculate the effective stresses. The cladding stresses under Condition I and II events are less than the Zircaloy 0.2% offset yield stress, with due consideration of temperature and irradiation effects. While the cladding has some capability for accommodating plastic strain, the yield stress has been accepted as a conservative design basis.

Clad Tensile Strain

The total tensile creep strain is less than 1 % from the un-irradiated condition. The elastic tensile strain during a transient is less than 1 percent from the pre-transient value. These limits are consistent with proven practice.

A.2.5.5.2 Fuel Material/IFBA

Thermal-Physical Properties

The thermal-physical properties of UO₂ are described in [A.9] and [A.10].

Fuel pellet temperatures

The center temperature of the hottest pellet is to be below the melting temperature of the UO₂ (melting point of 5080 F un-irradiated and decreasing by 58114F per 10,000 MWd/tHM) [A.10]. While a limited amount of center melting can be tolerated, the design conservatively precludes center melting. A calculated fuel centerline temperature of 4700 F has been selected as an overpower limit to assure no fuel melting. This provides sufficient margin for uncertainties.

Fuel Densification and Fission Product Swelling

The design bases and models used for fuel densification and swelling are provided in [A.11] and [A.12].

A.3. EXPECTED CORE PARAMETERS

In the following paragraphs, it is reported data useful for validation of the computational model. This data could provide useful indications for the HE-LL core design and for the necessary iterations.

A.3.1. Excess Reactivity

Excess reactivity should be compensated by IFBA, RCCA, soluble boron and fission products accumulation. Table A.12 reports the excess reactivity for a single FA and for the core in cold, clean and un-borated conditions.

Table A.12. Excess Reactivity.

<u>Excessive Reactivity</u>	
Maximum fuel assembly k_{inf} (cold clean, unborated water)	1.430
Maximum core reactivity (cold, zero power, beginning of cycle, zero soluble boron)	1.210

A.3.2. Radial Power Distribution

Figure A.13 and Figure A.14 show the radial power distributions at BOL/ARO at HZP and HFP, Xenon Equilibrium. Figure A.15 and Figure A.16 show the radial power distribution at HFP/ARO for MOL and EOL, Xenon Equilibrium. Figure A.17 shows the $F_{\Delta H}$ for the Hot Channel, as function of the nominal reactor power and of cycle burnup. At HFP, the maximum $F_{\Delta H}$ is achieved before the MOL (~ 1.52).

	H	G	F	E	D	C	B	A
8	0.714	1.007	1.040	1.019	1.149	1.310	1.184	0.631
9	1.007	0.861	1.012	0.929	1.217	1.246	1.226	0.634
10	1.040	1.017	0.892	1.110	1.190	1.346	1.226	0.616
11	1.019	0.930	1.112	1.019	1.280	1.345	1.108	0.304
12	1.149	1.219	1.194	1.284	1.236	1.250	0.550	
13	1.310	1.252	1.352	1.349	1.250	0.942	0.273	
14	1.184	1.238	1.233	1.112	0.549	0.265		
15	0.631	0.640	0.621	0.306	Value Represents Assembly Relative Power			

Figure A.13. FA Relative Power – BOL, ARO, HZP, Equilibrium Xenon.

	H	G	F	E	D	C	B	A
8	0.858	1.162	1.160	1.100	1.165	1.255	1.123	0.629
9	1.162	1.001	1.136	1.007	1.228	1.199	1.164	0.631
10	1.160	1.141	0.992	1.171	1.182	1.268	1.156	0.615
11	1.100	1.008	1.172	1.051	1.248	1.256	1.046	0.314
12	1.165	1.230	1.185	1.250	1.181	1.177	0.551	
13	1.255	1.203	1.272	1.258	1.177	0.909	0.286	
14	1.123	1.173	1.160	1.048	0.550	0.277		
15	0.629	0.636	0.618	0.315	Value Represents Assembly Relative Power			

Figure A.14. FA Relative Power – BOL, ARO, HFP, Equilibrium Xenon.

	H	G	F	E	D	C	B	A
8	0.921	1.298	1.161	1.041	1.055	1.095	1.017	0.603
9	1.298	1.052	1.283	1.000	1.252	1.078	1.187	0.625
10	1.161	1.287	1.045	1.301	1.123	1.153	1.200	0.621
11	1.041	1.000	1.302	1.065	1.318	1.161	1.039	0.326
12	1.055	1.253	1.125	1.320	1.140	1.210	0.556	
13	1.095	1.080	1.155	1.161	1.209	0.951	0.307	
14	1.017	1.193	1.203	1.040	0.555	0.298		
15	0.603	0.628	0.623	0.326	Value Represents Assembly Relative Power			

Figure A.15. FA Relative Power – MOL, ARO, HFP, Equilibrium Xenon.

	H	G	F	E	D	C	B	A
8	0.908	1.235	1.108	1.019	1.034	1.083	1.043	0.682
9	1.235	1.019	1.234	0.984	1.216	1.063	1.214	0.701
10	1.108	1.236	1.018	1.248	1.080	1.123	1.219	0.696
11	1.019	0.984	1.248	1.030	1.256	1.129	1.075	0.389
12	1.034	1.215	1.080	1.257	1.100	1.208	0.620	
13	1.083	1.063	1.123	1.129	1.207	1.006	0.371	
14	1.043	1.217	1.220	1.074	0.619	0.361		
15	0.682	0.703	0.697	0.389	Value Represents Assembly Relative Power			

Figure A.16. FA Relative Power – EOL, ARO, HFP, Equilibrium Xenon.

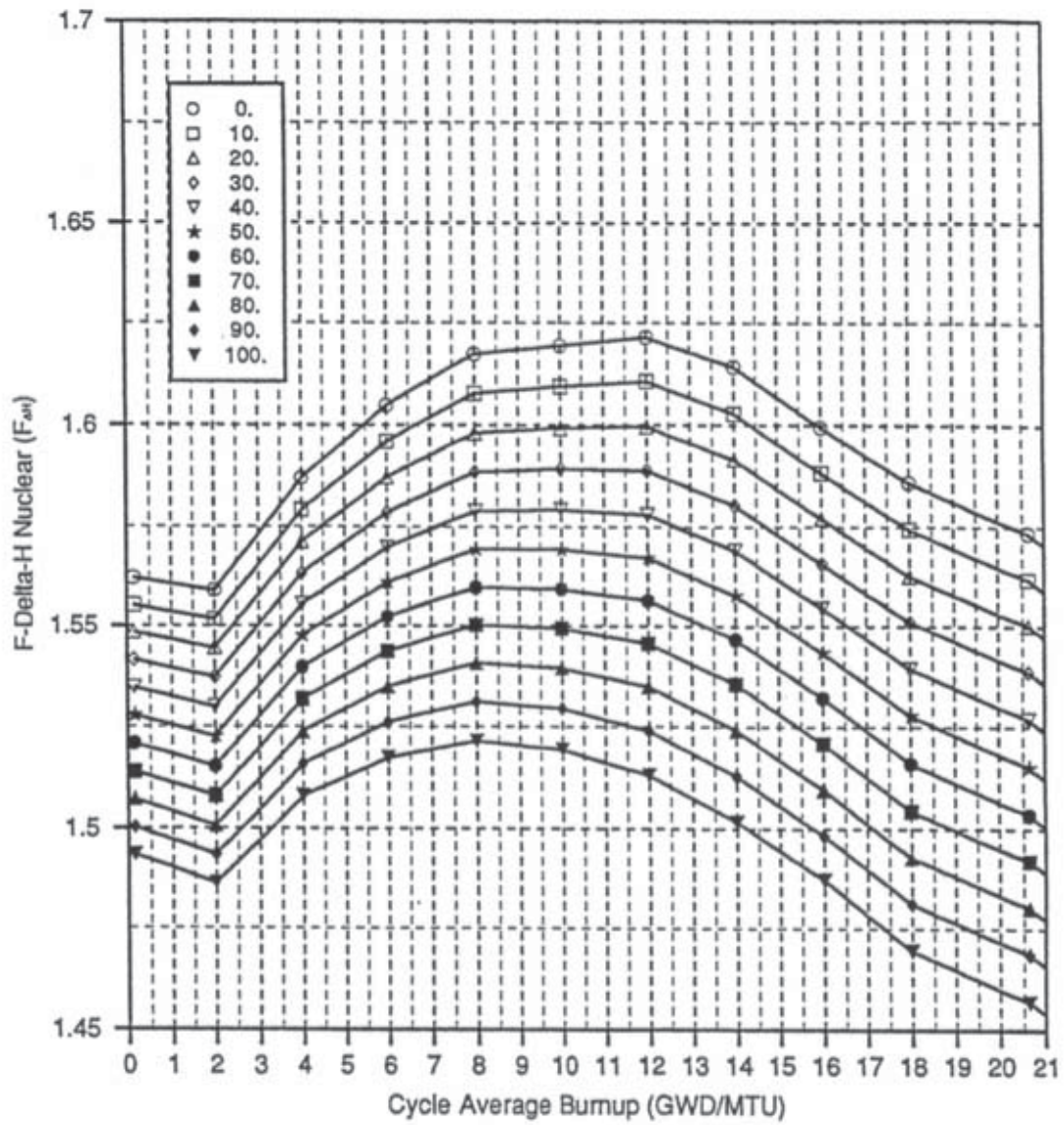


Figure A.17. Hot Channel $F_{\Delta H}$ vs. Normalized Reactor Power vs. Burnup – ARO, Equilibrium Xenon.

A.3.3. Axial Power Distribution

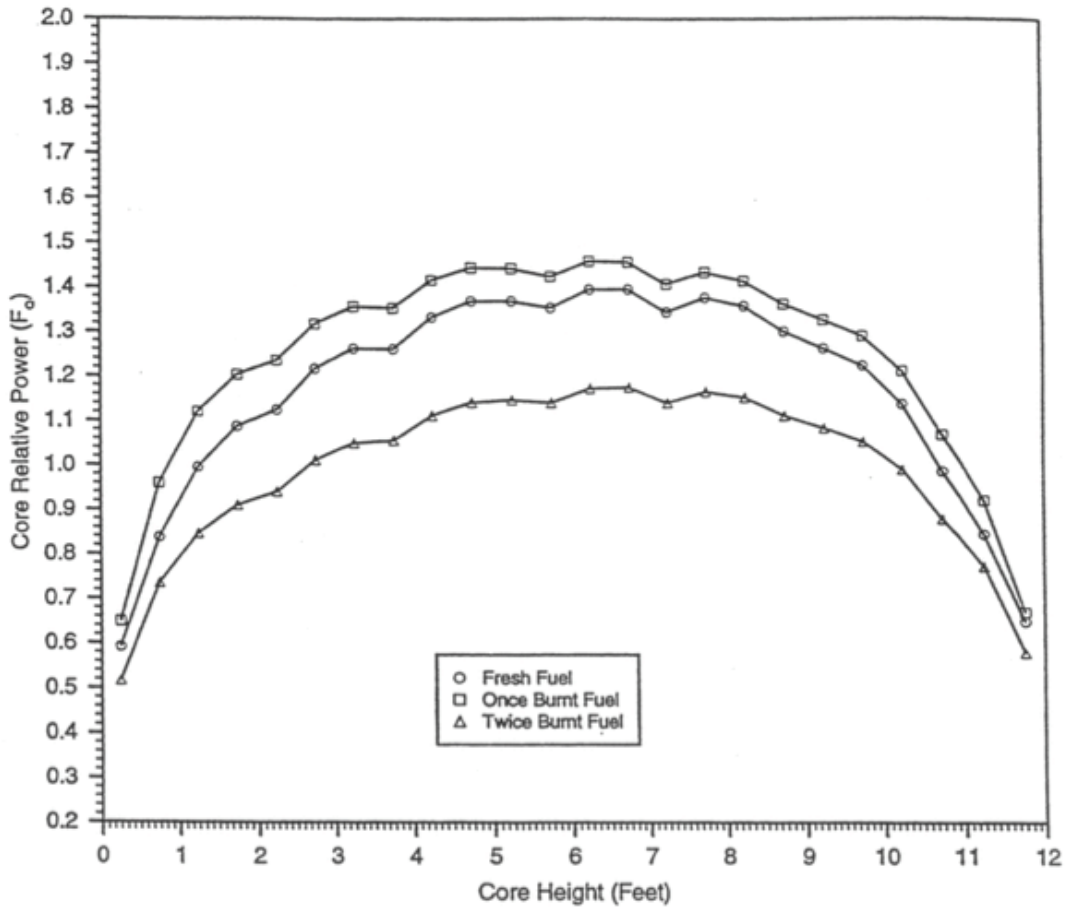


Figure A.18. Core Relative Axial Power – BOL, ARO, HFP, Equilibrium Xenon.

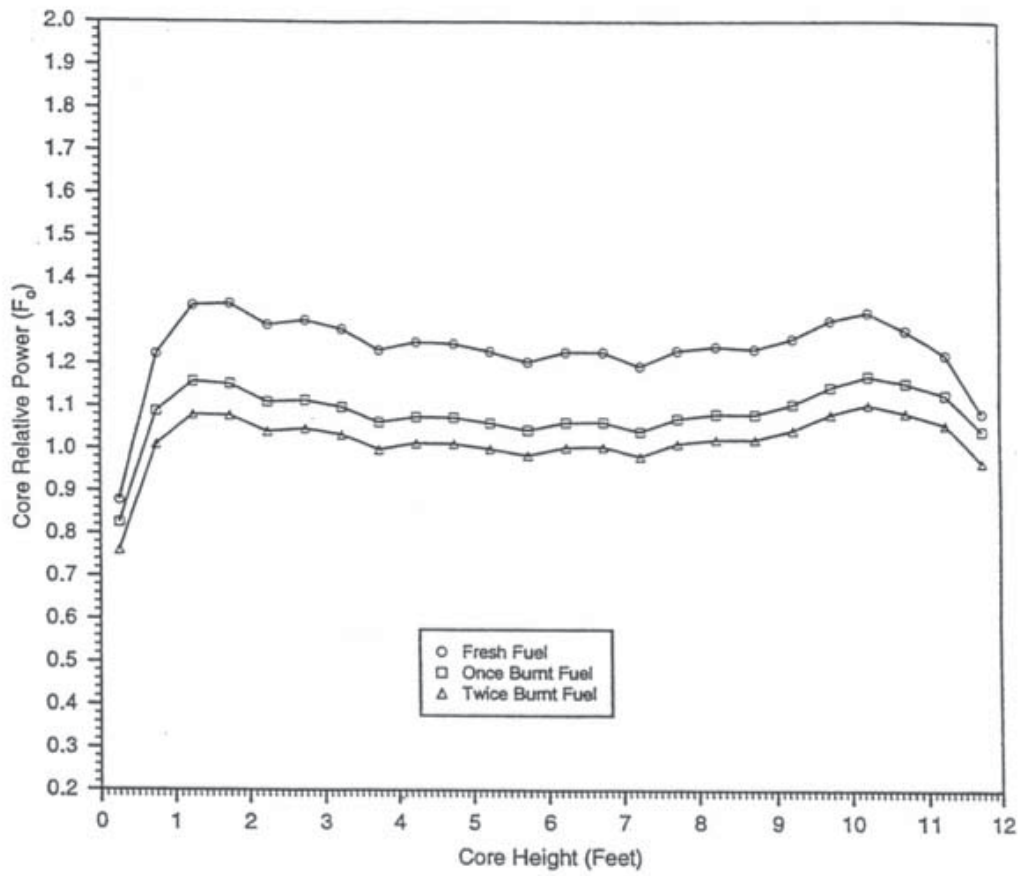


Figure A.19. Core Relative Axial Power – EOL, ARO, HFP, Equilibrium Xenon.

A.3.4. Typical FA Power Distribution

Figure A.20 and Figure A.21 represent the pin power distribution in a typical HE-LL core FA at BOL and EOL, ARO/HFP and Xenon Equilibrium.

1.054	1.112	1.124	1.140	1.163	1.177	1.191	1.201	1.200	1.207	1.206	1.200	1.194	1.177	1.166	1.157	1.094
1.101	1.095	1.052	1.080	1.161	1.157	1.194	1.209	1.181	1.217	1.211	1.182	1.195	1.119	1.096	1.143	1.143
1.100	1.041	1.070	1.185	1.166		1.174	1.240		1.248	1.192		1.204	1.232	1.119	1.091	1.146
1.106	1.058	1.174		1.234	1.176	1.189	1.153	1.235	1.162	1.209	1.206	1.276		1.232	1.114	1.157
1.119	1.129	1.145	1.223	1.159	1.231	1.147	1.193	1.177	1.203	1.168	1.264	1.201	1.297	1.205	1.192	1.176
1.124	1.116		1.156	1.221		1.229	1.176		1.187	1.252		1.267	1.212		1.182	1.185
1.131	1.144	1.135	1.161	1.130	1.220	1.144	1.190	1.174	1.201	1.165	1.255	1.174	1.217	1.200	1.214	1.195
1.134	1.152	1.192	1.118	1.167	1.160	1.182	1.147	1.230	1.158	1.205	1.194	1.213	1.173	1.261	1.224	1.199
1.130	1.121		1.192	1.144		1.159	1.223		1.233	1.181		1.190	1.251		1.190	1.195
1.134	1.152	1.191	1.117	1.166	1.158	1.181	1.146	1.228	1.156	1.203	1.192	1.211	1.171	1.259	1.222	1.198
1.130	1.143	1.134	1.159	1.128	1.218	1.141	1.187	1.170	1.197	1.161	1.251	1.170	1.213	1.196	1.210	1.191
1.122	1.114		1.154	1.217		1.224	1.171		1.180	1.244		1.260	1.205		1.176	1.179
1.117	1.126	1.141	1.210	1.154	1.224	1.141	1.185	1.168	1.194	1.158	1.253	1.191	1.268	1.196	1.184	1.168
1.104	1.055	1.170		1.227	1.168	1.180	1.143	1.224	1.150	1.196	1.193	1.262		1.219	1.103	1.147
1.098	1.037	1.065	1.179	1.158		1.162	1.226		1.233	1.176		1.187	1.215	1.104	1.077	1.133
1.098	1.091	1.046	1.072	1.152	1.145	1.180	1.193	1.164	1.198	1.191	1.162	1.174	1.099	1.077	1.125	1.126
1.052	1.108	1.116	1.131	1.151	1.162	1.175	1.182	1.179	1.185	1.182	1.174	1.168	1.152	1.141	1.135	1.075

Figure A.20. Typical Pin Power Distribution – BOL, ARO, HFP, Equilibrium Xenon.

1.171	1.173	1.180	1.190	1.201	1.210	1.213	1.215	1.220	1.219	1.219	1.220	1.215	1.208	1.201	1.197	1.192
1.170	1.164	1.167	1.183	1.218	1.234	1.228	1.231	1.240	1.234	1.234	1.244	1.233	1.202	1.189	1.187	1.188
1.171	1.162	1.191	1.240	1.256		1.253	1.264		1.266	1.259		1.272	1.260	1.215	1.186	1.190
1.176	1.173	1.234		1.280	1.266	1.255	1.247	1.273	1.249	1.261	1.277	1.296		1.260	1.199	1.196
1.181	1.202	1.245	1.274	1.259	1.280	1.251	1.262	1.271	1.265	1.257	1.291	1.276	1.297	1.272	1.230	1.204
1.186	1.213		1.255	1.274		1.283	1.276		1.278	1.289		1.292	1.279		1.243	1.211
1.185	1.203	1.233	1.241	1.242	1.279	1.255	1.268	1.275	1.270	1.262	1.291	1.260	1.265	1.263	1.234	1.211
1.185	1.204	1.241	1.230	1.251	1.269	1.265	1.259	1.285	1.262	1.272	1.281	1.270	1.255	1.272	1.236	1.212
1.187	1.211		1.255	1.259		1.272	1.284		1.286	1.278		1.276	1.279		1.243	1.213
1.184	1.203	1.241	1.229	1.250	1.268	1.264	1.258	1.284	1.260	1.270	1.279	1.268	1.252	1.270	1.234	1.210
1.184	1.202	1.232	1.239	1.241	1.277	1.253	1.266	1.273	1.268	1.259	1.288	1.258	1.262	1.260	1.232	1.208
1.185	1.212		1.254	1.273		1.280	1.273		1.274	1.285		1.288	1.275		1.239	1.207
1.180	1.200	1.243	1.272	1.256	1.276	1.247	1.258	1.266	1.260	1.252	1.286	1.271	1.292	1.267	1.225	1.199
1.175	1.171	1.232		1.276	1.262	1.250	1.241	1.267	1.242	1.254	1.270	1.289		1.253	1.193	1.190
1.170	1.160	1.189	1.237	1.252		1.248	1.257		1.259	1.251		1.263	1.252	1.207	1.178	1.183
1.169	1.163	1.165	1.180	1.214	1.229	1.222	1.224	1.232	1.225	1.225	1.235	1.223	1.193	1.180	1.178	1.180
1.171	1.173	1.178	1.187	1.197	1.204	1.206	1.208	1.212	1.211	1.211	1.211	1.206	1.199	1.193	1.188	1.184

Figure A.21. Typical Pin Power Distribution – EOL, ARO, HFP, Equilibrium Xenon.

A.4. REFERENCES

- [A.1] R. H. Szilard et al., "Industry Application – Emergency Core Cooling System Cladding Acceptance Criteria – Early Demonstration," INL/EXT-15-36541, September 2015.
- [A.2] NEXtera Energy Seabrook Station, Ultimate Final Safety Analysis Report, Chapter 4, Rev. 10.
- [A.3] Davidson, S. L., "Westinghouse Fuel Criteria Evaluation Process," WCAP-12488-A, October 1994. [Westinghouse Proprietary]
- [A.4] Letter from N. J. Liparolu (Westinghouse) to R. S. Jones (NRC), "Westinghouse Interpretation of Staff's Position on Extended Burnup," NTD-NRC-94-4275, August 29, 1994.
- [A.5] Davidson, S. L. and Ryan, T.L., "VANTAGE+ Fuel Assembly Reference Core Report," WCAP-12610-P-A and Appendices A through D. April 1995. [Westinghouse Proprietary]
- [A.6] Davidson, S. L., "Westinghouse Fuel Criteria Evaluation Process," WCAP-12488-A, October 1994. [Non-Proprietary]
- [A.7] K.J. Geelhood, W.G. Luscher, "FRAPCON-4.0: Integral Assessment," PNNL-19418, Vol. 2 Rev. 2, September 2015.
- [A.8] K.J. Geelhood, W.G. Luscher, "FRAPTRAN-1.5: Integral Assessment," NUREG/CR-7023, Vol. 2, Rev. 1, May 2014.
- [A.9] W.G. Luscher et al., "Material Property Correlations: Comparisons between FRAPCON-4.0, FRAPTRAN-2.0, and MATPRO", PNNL-19417 Rev. 2, September 2015.
- [A.10] Beaumont, M. D., and Iorii, J.A., "Properties of Fuel and Core Component Materials," WCAP-9179, Revision 1, July 1978. [Westinghouse Proprietary]
- [A.11] Hellman, J. M. (Ed.), "Fuel Densification Experimental Results and Model for Reactor Application," WCAP-8218-P-A [Westinghouse Proprietary] and WCAP-8219-A [Non-Proprietary], March 1975.
- [A.12] Weiner, R. A., et al., "Improved Fuel Performance Models for Westinghouse Fuel Rod Design and Safety Evaluations," WCAP-10851-P-A [Westinghouse Proprietary] and WCAP-11873-A [Non-Proprietary], August 1988.
- [A.13] <http://www.westinghousenuclear.com>
- [A.14] NEXtera Energy Seabrook Station, "License Amendment Request 13-04 & 10 CFR 50.12 Exemption Request Optimized ZIRLO Fuel Rod Cladding," NRC Docket No. 50-443, June 2013
- [A.15] Duke Energy, Catawba & McGuire Nuclear Station, Units No. 1 & 2, "License Amendment Request and 10 CFR 50.12 Exemption Request for Use of Optimized ZIRLO™ Fuel Rod Cladding," NRC Docket No. 50-413 & 50-414, 50-369 & 50-370, August 2015.
- [A.16] Westinghouse Electric Company, Addendum 1-A, "Optimized ZIRLO™," WCAP-1261 & CENPD-404-P-A, July 2006.
- [A.17] NRC, Safety Evaluation by the Office of Nuclear Reactor Regulation. Addendum 1 to WCAP-12610-P-A and CENPD-404-P-A, "Optimized ZIRLO™," June 2005.
- [A.18] NRC, Final Safety Evaluation by the Office of Nuclear Reactor Regulation. Topical Report WCAP-12610-P-A & CENPD-404-P-A, Addendum 2/WCAP-14342-A & CENPD-404-NP-A, Addendum 2, "Westinghouse Clad Corrosion Model for ZIRLO™ and Optimized ZIRLO™," July 2013.

